UNIVERSITA' DEGLI STUDI DI NAPOLI "FEDERICO II"

FACOLTA' DI FARMACIA

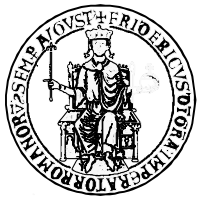

DOTTORATO DI RICERCA IN SCIENZA DEL FARMACO
XXI CICLO

Chitosan-based nanoparticles and microparticles

Coordinatori:

Ch.mo Prof. Enrico Abignente

Ch.mo Prof. Maria Valeria D'Auria

Tutor:
Ch.mo Prof. Maria Grazia Rimoli

Candidato:
Dott. Alessandro Nasti

Ch.mo Prof. Nicola Tirelli

Table of Content

List of Figures

List of Tables

List of Schemes

Abstract

Chitosan-Triphosphate Nanoparticles

There is a widespread interest in the use of nano-carriers for drug delivery and chitosan is one of the most sought-after components for designing biocompatible nanoparticles.

Here, using a rational experimental design, I have studied the influence of a number of variables (pH, concentrations, ratios of components, different methods of mixing) in the preparation of chitosan/triphosphate (CS/TPP) nanoparticles and in their coating with hyaluronic acid (HA). The aim was to minimise size polydispersity, maximise zeta potential and long-term stability, and control the average nanoparticle size. As a result, three kinds of optimised nanoparticles have been developed, two uncoated and one HA-coated. Their toxicity on fibroblasts and uptake by macrophages have been evaluated. Experiments showed the beneficial character of HA-coating in the reduction of toxicity (IC50 raised from 0.7-0.8 mg/mL to 1.8 mg/mL) and suggested that the uncoated chitosan/TPP nanoparticles had toxic effects following internalisation rather than membrane disruption. Uptake tests were performed after the conjugation of fluorescein isothiocyanate (fluorescent label) with chitosan. The nano-carrier can be produced in future for the delivery of short sequences of RNA (*e.g.* siRNA), be trackable and rather have the ability to specifically bind to target cells.

Chitosan-Triphosphate microparticles

Monodisperse microparticles were produced using the Inotech® encapsulator exploiting the gelation between chitosan and TPP. The target of 300 μm size was obtained through optimising several parameters (nozzle oscillation, nozzle diameter, pH, concentrations, flow rate, electrostatic charge). TPP was chosen for its non-toxicity and fast gelling ability. The method was mild and did not require organic solvents or toxic cross-linking reagents. These particles will be used in future experiments to embed hydrophobic actives, proteins or living cells.

Dedication

a Dio e alla mia famiglia

Acknowledgments

I show gratitude to my supervisor Prof. Maria Grazia Rimoli, for her guidance in this experience called *philosophiae doctor* and for supporting me along overall this time. I am genuinely grateful to my external tutor Prof. Nicola Tirelli for offering me the opportunity to work in his laboratory for most of the time of my PhD course, for his constant presence in every moment, for the heated discussions and the precious explanations. Moreover, I would want thank both my supervisors and the teaching staff of Naples, coordinated previously by Prof. Enrico Abignente and afterwards by Prof. Maria Valeria D'Auria, for the research independence received during my entire period of doctorate.

I am thankful for the gracious financial support provided to me by the *Università degli Studi di Napoli "Federico II"* and by Prof. Nicola Tirelli.

I would like to extend my thanks to Dr. Francesco Cellesi for his technical advices, Dr. Noha Zaki for her vast biological work done with my materials, and all the people in the group of Polymer and Biomaterial of Manchester and the ones in the group of Pharmaceutical Chemistry of Naples. A special thanks to Dr. Eman Abdeljaber for her constant support and advice.

Last but not least, many thanks to my family for the immense support and love, and numerous thanks to my friends constantly present in every circumstance.

Abbreviations

mg	10^{-3} gram
µl	10^{-6} liter
mmol	10^{-3} mol
µm	10^{-6} meter
nm	10^{-9} meter
M	mol·liter^{-1}
MW	Molecular Weight
PBS	Phosphate Buffered Saline
DMSO	Dimethyl sulfoxide
^{1}H NMR	Proton Nuclear Magnetic Resonance
Ex	Excitation
Em	Emission
UV-VIS	Ultra Violet-Visible (spectroscopy)
CS	Chitosan
TPP	Sodium Triphosphate
DD	Degree of deacetylation
siRNA	Small interfering ribonucleic acid
pK_a	Acid dissociation constant
TEER	Transepithelial electrical resistance
IL-1	Interleukin-1
CSNPs	Chitosan/TPP nanoparticles
IC50	Concentration inhibiting cell viability by 50%
TxR	Texas Red
DAPI	4',6-diamidino-2-phenylindole
RFU	Relative Fluorescence Units
HA	Hyaluronic acid
HA-CSNPs	Hyaluronic acid-coated Chitosan/TPP nanoparticles
Tween 20	Polyoxyethylene (20) sorbitan monolaurate
FITC-dextran	Fluorescein isothiocyanate-dextran
PTFE	Poly(tetrafluoroethylene)

Chapter 1

Introduction

1 Introduction. Background and scope of the thesis

1.1 What is chitosan?

Chitosan (a copolymer of β-(1→4)-linked D-glucose-2-amine and N-acetyl-D-glucose-2-amine) is a versatile biomaterial derived from chitin (essentially poly(β-1,4-N-acetyl-D-glucose-2-amine)) (Fig.1-1), which is one of the most abundant natural polysaccharides. Chitin is found in the cell walls of microorganisms such as yeasts or other fungi, in the exoskeletons of crustaceans and insects and in several other specialized organs such as the beaks of cephalopods.

In order to obtain chitosan, the removal of the acetyl groups is performed with a concentrated solution of NaOH avoiding depolymerization or production of undesired species. An alternative treatment was developed to avoid large use of NaOH, *i.e.* chitin is directly mixed with NaOH in powder at a weight ratio of 1 to 5, then at a temperature of 180°C the deacetylated chitosan is obtained by extrusion[1]; this procedure is eco-friendly due to the absence of waste water. The X-ray diffraction studies prove that chitosan has a orthorhombic crystallization form[2] with the three dimensions respectively of 0.828, 0.862 and 1.043 nm [3]. The degree of crystallization is related to the number of acetyl groups, these groups promote hydrogen bonds decreasing the chain mobility and modulating the sorption performance[4]. Chitosan is a biocompatible[5, 6] linear polymer that has low immunogenicity property, it has a ample range of applications[7-10]; the biocompatibility is directly proportional to the degree of deacetylation (DD), indeed the higher the content of amino groups in the backbone and the lower will be the toxicity of the resultant polymer[11]. The high percentage of nitrogen in chitosan (6.89%) gives a large number of groups that could be used for chemical modification; the physical properties depend on the type and the degree of substitution on primary amine.

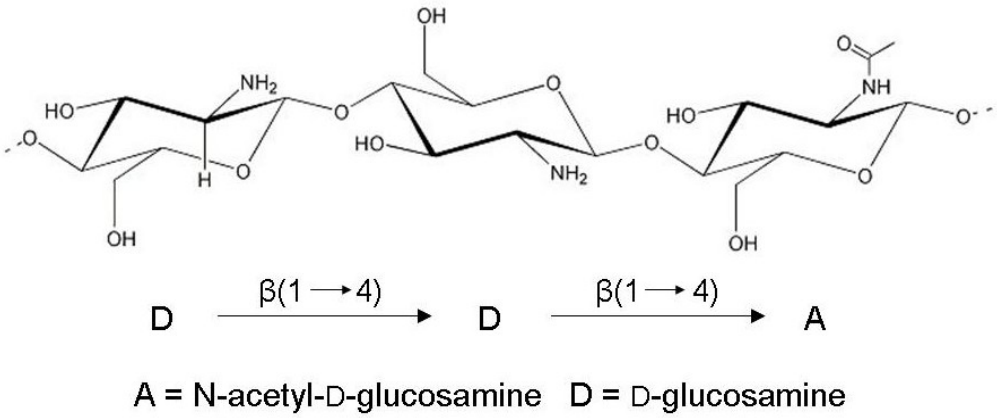

Figure 1-1. Chitosan, a copolymer of β-(1→4)-linked D-glucose-2-amine and N-acetyl-D-glucose-2-amine

The nitrogen contained in chitosan is in the form of primary aliphatic amino groups and therefore, it undergoes reactions typical of amines, the most important being N-acylation or alkylation and Schiff's reaction[12].

It is noteworthy that, although all characterized by the generic name of "chitosan", polymers with different properties are obtained through the deacetylation of chitin, which is often followed or accompanied by depolymerisation; different types of chitosan are obtained with varying the molecular weight (MW) and the charge density[13]. It is therefore essential to characterize chitosan samples at least in terms of average molecular weight and degree of deacetylation, in order to ensure reproducibility in the experimental results; the MW can be determined by viscosimetry or static light scattering, and the DD by infrared spectroscopy, by colloid titration or by ^{1}H-NMR. The deacetylation reaction can be performed as a heterogeneous[14] or homogeneous[15, 16] process, the first method gives chains with non uniform block copolymers of D-glucosamine and N-acetyl-D-glucosamine, the second method results in a homogeneous deacetylation of the chains; in the two cases the physicochemical properties appear to be different. It is preferable to have randomly distributed acetyl groups in order to compare easily chitosans with different MWs[16].

A few mammalian enzymes, such as α-amylase or lysozyme can degrade chitosan, therefore it can be generally regarded as a degradable material[17], its oligomers activate macrophages and moreover the hyaluronan synthesis is stimulated[12]. Tumor cells recognize the polycation; this gives a chance to have a selective vehicle. Chitosan has been extensively employed in the development of micro- or nano-carrier structures[18],

with a specific focus on the use of complex inclusive of active principles such as nucleic acids, e.g. small interfering RNA (siRNA)[19], or proteins[20] having enzymatic activity[21]. It is noteworthy that the activity of these nano-carrier systems towards a biological target may be affected by chitosan biological properties, for example its anticancer activity[12, 22].

The distribution charge in the polymer is highly positive, this allows the formation of complexes in presence of polyanions[12], moreover the adsorptive characteristic depends on the crystallinity and on the number of amines free to interact[23]. The safety and the non-toxicity is an advantage[24, 25] and the mucoadhesive property is another interesting characteristic of chitosan[26].

The chitosan mucoadhesion is strictly correlated with the degree of deacetylation, and this property change following the variation of pH[27] or of ionic strength values of the system[26]. Mucoadhesion and swelling properties could be improved by increasing the acid dissociation constant (pK_a) of the biopolymer[26], which can be modified by permanent substitution of the primary amines. The interaction of chitosan with mucosal surfaces is possible since the cells are negatively charged; this is due to the presence of sialic acid on the surface membrane, which with its negative charge permits binding and transport of positively charged molecules[28]. In addition, chitosan exhibits a permeation enhancing effect by opening the epithelial tight junctions; this was confirmed since the polymer is able to decrease in a reversible way the transepithelial electrical resistance (TEER) among cells without damaging them or lowering their functionality[29].

The purity of chitosan must be constantly checked, since the biopolymer is subject to several types of contamination during the food processing of chitin (*e.g.* protein contamination). Raw chitosan bought from different suppliers may differ in purity, due to its source, season, and conditions of the chemical deacetylation process[30].

Protein contamination must be avoided in formulations prepared for biomedical applications. Thus, a highly purified chitosan is desirable and various purification protocols were reported in literature[30, 31].

1.2 Chitosan applications

1.2.1 Chitosan potentiality

Chitosan has been studied extensively in industry for its enormous potentials as an ingredient for foods[8], porous beads for bioreactors, for hair care products, as a coagulant for waste-water treatment[10], in controlled release systems, wound healing[32], cell encapsulation, tissue engineering[33] (*e.g.* implants for the cartilage[34]) and as a drug carrier[35]. Chitosan serves as a successful candidate for various medical applications due to a number of reasons. It is a clotting agent and absorbs liquids, important aspects for wound healing; degradation products have no toxic effects and since it is depolymerised by lysozyme can be designated as a bioerodible system to deliver actives principles[36], through nasal[37], skin, intestinal, buccal and vaginal epithelia[38]; moreover higher is DD and more enhanced will be the absorption[37], this is due to the reduction of the rate of clearance, with a consequent prolonged contact time. In addition, the polymer possesses an antimicrobial activity[39], characteristic that was improved when the chlorhexidine, an antiseptic, was loaded[40] in chitosan microspheres. Chitosan induces the macrophage activation[41], this involves the production of interleukin-1 (IL-1) and nitric oxide, in addition to the chemotaxis response[42]. It was also demonstrate that chitosan influences the hydrogen peroxide generation[43].

1.2.2 Nanoparticles thought for gene delivery

Chitosan has a greater ability to complex DNA or RNA and form nano-complexes compared to other cationic polymers[44], the strength of complexation is influenced by salt concentration, pH, polymer charge density and molecular weight[45]. The biopolymer protects from nucleases activity[19, 45] and allows the cellular adhesion, the internalisation of the nano-carriers and escape from the lysosomes[46] in the cytoplasm. Lysosomotropic agents, *ie* chloroquine, were used in order to facilitate the nanoparticles escape and preserve DNA or RNA activity but they can bring undesirable side effects *in vivo*[44, 47, 48]. The transfection efficiency of chitosan-based nano-vehicles is cell-type dependent, there is no toxicity respect to other more toxic particles like Lipofectamine™, a cationic lipid; unluckily the transfection efficiency of chitosan nanoparticles is lower than Lipofectamine™ [44, 49, 50]. For an effective transfection, it is important not solely the internalization but successively as well the endo-lysosomal escape. Chitosan was

chosen since it can exploit its buffer capacity in a restricted interval of pH values (5-7), and promote after 72 hours the rupture of the endosomes with the consequent escape in the cytosol[51]. Moreover, for medical purposes, once produced the nanoparticles, they have to possess stability for long period of time, and so it is highlighted the importance of the lyophilization by freeze-drying. This procedure must not cause loss in activity and aggregation must me avoided, it is for these purposes that cryoprotective agents ought to be used (*ie* mannitol, sucrose)[52] during the process of drying.

1.2.3 Microparticles for proteins and cells delivery

The chitosan is used for microparticles production to overcome to problems of insolubility and hydrophobicity of several actives principles, adversely the polymer itself has not good stability under direct compression[12]. This problem was solved using excipients facilitating the compression[53] like magnesium stearate[54]. Chitosan is used as an efficient excipient in the gastrointestinal tract for delivery of proteins[55] that otherwise would have been destroyed by several enzymes, or would have not been intestinally absorbed[56].

1.3 Chitosan-Tripolyphosphate interactions

1.3.1 Complexation

An ionotropic gel is produced in a process of physical cross-linking between a polycationic (in this case a polyelectrolyte) and a polyanionic (in this case a multi-charged ion) component. The chosen polyanion is the sodium triphosphate (TPP), it is largely used in food industry, in detergents and biomedical applications for its non-toxicity[57] and fast gelling ability[30, 58].

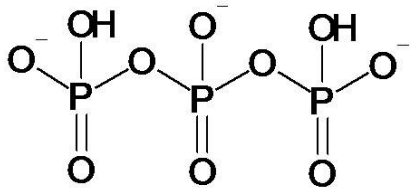

Figure 1-2. Triphosphate anion, it has three charges when the ph is between 3 and 5.5.

The interactions between chitosan and TPP depend on the ionic strength and pH of the solution. The complexation is most effective when the charge densities of the two combined partners reach a maximum, therefore, due to the above pH dependence, the pK_a values of both chitosan and TPP must be carefully taken into consideration. The pK_a of the chitosan amine groups ranges between 4.5 and 8. Therefore, it is fully positively charged below 4, and completely neutral above 9. The TPP pK_a values are pK_1=1, pK_2=2, pK_3=2.79, pK_4=6.47, pK_5=9.24.

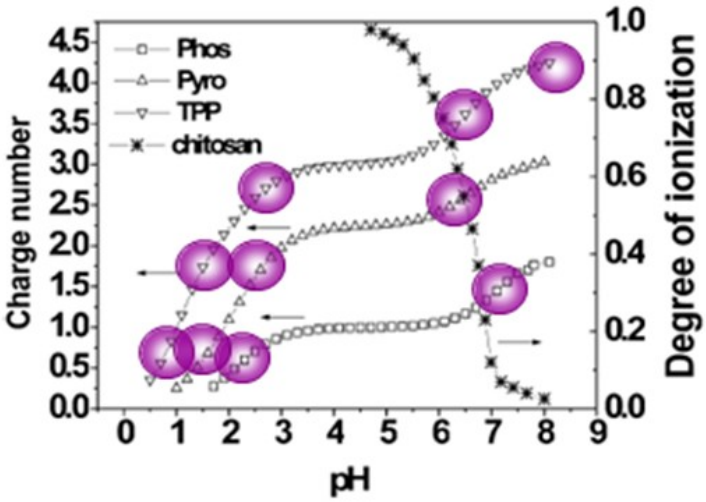

Figure 1-3. Chitosan and TPP behaviour at different pH values**.** pH affects the degree of ionization of chitosan and the charge number of TPP, pyrophosphate and phosphate. Each sphere shows where the degree of ionisation varies considerably for small variations of pH (buffer area); in these points, the pH corresponds to the pKa. Adapted from Shu *et al*, 2002[59]**.**

It is imperative to maintain a pH value lower than 5 in order to have a chitosan fully protonated, on the contrary pH of 3 is the minimum value for the TPP to possess three charges. Therefore, the complexation between chitosan and TPP and the resultant crosslinking density is pH dependent[60], since their charge density depend on pH values (see table 1-1); for an acceptable and stable complexation the values must range between 3 and 5.5 (Fig. 1-3).

Table 1-1. Varying the pH value, the percentage of protonation in the glucosamine units constantly change, and at the same fashion the TPP negative charges are range from 3 to 4 charges.

pH	4	5	5.5	6	7	8	9
Chitosan degree of ionization in %	0.995	0.953	0.863	0.666	0.166	0.020	0.002
TPP negative charges	3	3	3.1	3.9	4	4	4.9

Above pH 6, chitosan charge density is not sufficient to prevent falls and to provide good complexation behaviour; whereas below pH 4 the charge density of TPP is too low to keep at least 3 negative charges.

The linkage of chitosan amines with TPP molecules can be confirmed by infra-red spectroscopy; the ionotropic complexation is a mild method and does not require organic solvents or toxic cross-linking reagents (*e.g.* glutaraldehyde)[61].

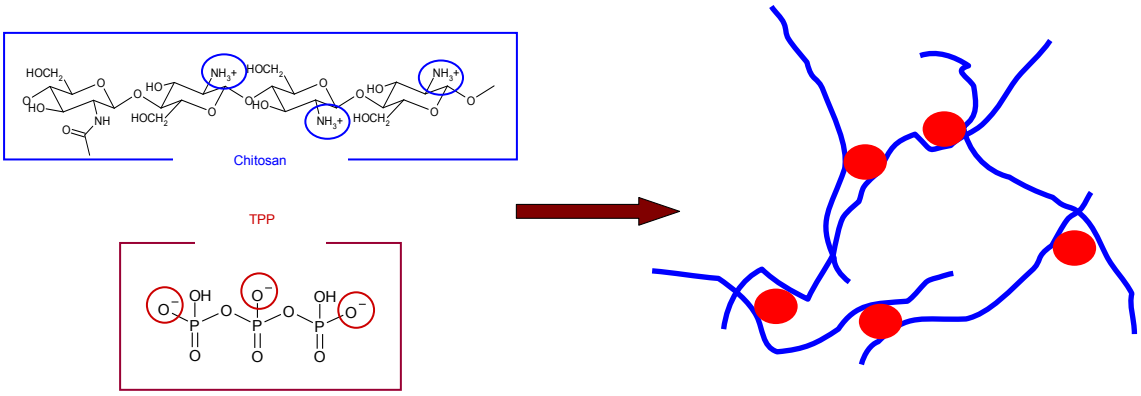

Figure 1-4. Ionotropic complexation between the free charged ammines and the three negative charges of the TPP.

At a pH lower than 4 pH, the chains of chitosan adopt a more extended conformation and form a complex with TPP in a ladder-shaped structure[62], which does not provide elastically active cross-links. Crosslink density is a key factor for stability, swelling behaviour and drug release. Generally, molecules entrapped in biopolymer matrices can be released by three mechanisms: desorption from the external particle surface; diffusion through the swollen matrix; or by erosion of the biopolymeric network[63]. Drugs with minute sizes can easily use the first two mechanisms, but macromolecules require the erosion mechanism once entrapped. Gan *et al*, furthermore

noticed that during the swelling behaviour (loss in particle density), there was no structural break in smaller particles but rather a swelling with loss in structure compactness and breaking of cross-linkage, followed by material degradation[63]. In the case of nanoparticles produced by ionotropic complexation, the MW strongly influences the particle size, indeed higher is this value and higher will be the dimensions of the nanoparticles[19].

1.3.2 Effect on the complexation and release of actives principles from a chitosan/TPP-based matrix

The release of actives principles from a gel matrix depends on chitosan MW and DD[62, 64], concentrations, chemical characteristics and charge density of the loaded molecules, viscosity, pH[65] and ionic strength of the solutions in which the matrix is immersed, chitosan/TPP ratios[30] and degree of crosslinking[66]. The increase in viscosity involves the formation of denser chitosan/TPP mesh, a higher crosslink density and a smaller ability of swelling with a consequent reduction in drug release. In addition, keeping constant the MW but increasing the DD will imply an increase in loading capacity, higher compactness and retardation in the release[64]. Moreover, it was demonstrated that a lower chitosan/TPP ratio could favour the entrapment of macromolecules[63]. In the study with microparticles, the high molecular weight (≅500g/mol) is selected in order to obtain high level of protein entrapment and burst effect reduction[30].

1.4 Scope of the thesis

During this project, chitosan was exploited in two different ways, which follow a similar preparative approach: the use of ionotropic gelation amid chitosan and TPP in order to form a) a nano-vehicle system and b) a micro-particulate system.

The aim of the first part of the project was the production of a bespoke nano-carrier for an effective gene delivery system. This delivery system had to be trackable and also must have the ability to specifically bind to target cells due to the presence of an external shell that recognizes unique cell-surface receptors thus enhancing the degree of therapeutic success by selective targeting.

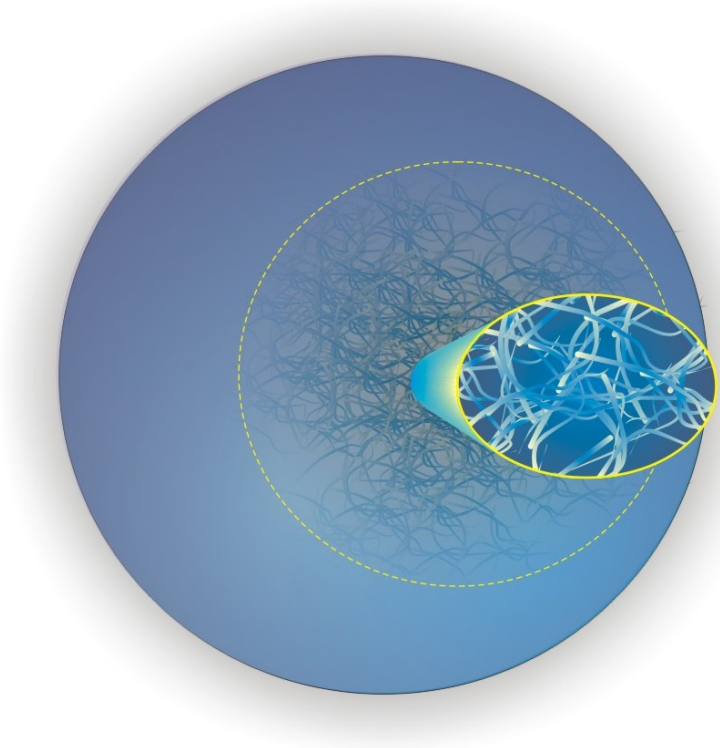

Figure 1-5. Hypothetical nanoparticle structure composed of inter/intra-connected linkages of chitosan.

The nano-carrier had to be capable of loading different types of actives during (embedding) or after (adsorption) the complexation between chitosan and TPP; some preparation will have fluorescently-labeled chitosan in order to monitor the fate of the nano-carriers *in vitro*. The actives principles would have been introduced and the effects of the delivery studied. Finally, the nanoparticles must increase the cellular uptake and protect the actives principles from intracellular degradation.

The study of the interactions between chitosan and sodium tripolyphosphate must aim to identify the most important parameters and to optimise them in view of improving the complexation and obtaining the most stable and reproducibly behaving nanoparticles.

The aim of the second part of the project was the production of chitosan-based microparticles using the encapsulator, medical device for active principles entrapment. The ionotropic gelation was used to form the particles and a number of variables were studied in order to obtain the most monodisperse microparticles. The target was to obtain particle size of 300 µm and to embed in these proteins or living cells.

References

1. Rogovina, S.Z.T.A. Akopova, **1994**, Modification of Polysaccharides under Shear Strain. *Vysokomolekulyarnye Soedineniya Seriya a & Seriya B*. 36(4): p. 593-600.
2. Clark, G.L.A.F. Smith, **1936**, X-ray diffraction studies of chitin, chitosan, and derivatives. *The Journal of Physical Chemistry*. 40(7).
3. Yui, T., K. Imada, K. Okuyama, Y. Obata, K. Suzuki, and K. Ogawa, **1994**, Molecular and Crystal-Structure of the Anhydrous Form of Chitosan. *Macromolecules*. 27(26): p. 7601-7605.
4. Guibal, E., **2004**, Interactions of metal ions with chitosan-based sorbents: a review. *Separation and Purification Technology*. 38(1): p. 43-74.
5. Rao, S.B.C.P. Sharma, **1997**, Use of chitosan as a biomaterial: Studies on its safety and hemostatic potential. *Journal of Biomedical Materials Research*. 34(1): p. 21-28.
6. Berscht, P.C., B. Nies, A. Liebendörfer, and J. Kreuter, **1995**, In vitro evaluation of biocompatibility of different wound dressing materials. *Journal of Materials Science: Materials in Medicine*. 6(4): p. 201-205.
7. Francis Suh, J.K.H.W.T. Matthew, **2000**, Application of chitosan-based polysaccharide biomaterials in cartilage tissue engineering: a review. *Biomaterials*. 21(24): p. 2589-2598.
8. Shahidi, F., J.K.V. Arachchi, and Y.-J. Jeon, **1999**, Food applications of chitin and chitosans. *Trends in Food Science & Technology*. 10(2): p. 37-51.
9. Piehler, J., A. Brecht, K.E. Geckeler, and G. Gauglitz, **1996**, Surface modification for direct immunoprobes. *Biosensors and Bioelectronics*. 11(6-7): p. 579-590.
10. Guibal, E., M. Janssoncharrier, I. Saucedo, and P. Lecloirec, **1995**, Enhancement of Metal-Ion Sorption Performances of Chitosan - Effect of the Structure on the Diffusion Properties. *Langmuir*. 11(2): p. 591-598.
11. Molinaro, G., J.C. Leroux, J. Damas, and A. Adam, **2002**, Biocompatibility of thermosensitive chitosan-based hydrogels: an in vivo experimental approach to injectable biomaterials. *Biomaterials*. 23(13): p. 2717-2722.
12. Ravi Kumar, M.N.V., **2000**, A review of chitin and chitosan applications. *Reactive and Functional Polymers*. 46: p. 1-27.

13. Illum, L., **1998**, Chitosan and its use as a pharmaceutical excipient. *Pharmaceutical Research*. 15(9): p. 1326-1331.
14. Tolaimate, A., J. Desbrières, M. Rhazi, A. Alagui, M. Vincendon, and P. Vottero, **2000**, On the influence of deacetylation process on the physicochemical characteristics of chitosan from squid chitin. *Polymer*. 41(7): p. 2463-2469.
15. Rinaudo, M., M. Milas, and P. Ledung, **1993**, Characterization of Chitosan - Influence of Ionic-Strength and Degree of Acetylation on Chain Expansion. *International Journal of Biological Macromolecules*. 15(5): p. 281-285.
16. Vårum, K.M., M.W. Anthonsen, H. Grasdalen, and O. Smidsrød, **1991**, 13C-N.m.r. studies of the acetylation sequences in partially N-deacetylated chitins (chitosans). *Carbohydrate Research*. 217: p. 19-27.
17. Etienne, O., A. Schneider, C. Taddei, L. Richert, P. Schaaf, J.C. Voegel, C. Egles, and C. Picart, **2005**, Degradability of polysaccharides multilayer films in the oral environment: an in vitro and in vivo study. *Biomacromolecules*. 6(2): p. 726-733.
18. Agnihotri, S.A., N.N. Mallikarjuna, and T.M. Aminabhavi, **2004**, Recent advances on chitosan-based micro- and nanoparticles in drug delivery. *Journal of Controlled Release*. 100(1): p. 5-28.
19. Katas, H.H.O. Alpar, **2006**, Development and characterisation of chitosan nanoparticles for siRNA delivery. *Journal of Controlled Release*. 115(2): p. 216-225.
20. Luangtana-anan, M., P. Opanasopit, T. Ngawhirunpat, J. Nunthanid, P. Sriamornsak, S. Limmatvapirat, and L.Y. Lim, **2005**, Effect of chitosan salts and molecular weight on a nanoparticulate carrier for therapeutic protein. *Pharmaceutical Development and Technology*. 10(2): p. 189-196.
21. Deng, Q.Y., C.R. Zhou, and B.H. Luo, **2006**, Preparation and characterization of chitosan nanoparticles containing lysozyme. *Pharmaceutical Biology*. 44(5): p. 336-342.
22. Dass, C.R.P.F.M. Choong, **2008**, The use of chitosan formulations in cancer therapy. *Journal of Microencapsulation*. 25(4): p. 275-279.
23. Keisuke Kurita, T.S.Y.I., **1979**, Studies on chitin. VI. Binding of metal cations. 23(2): p. 511-515.

24. Kanauchi, O., K. Deuchi, Y. Imasato, and E. Kobayashi, **1994**, Increasing Effect of a Chitosan and Ascorbic-Acid Mixture on Fecal Dietary-Fat Excretion. *Bioscience Biotechnology and Biochemistry*. 58(9): p. 1617-1620.
25. Harrison, T.A., **2002**, FDA regulation of labeling claims for nutraceuticals in the United States. *Agro Food Industry Hi-Tech*. 13(3): p. 8-11.
26. Lehr, C.M., J.A. Bouwstra, E.H. Schacht, and H.E. Junginger, **1992**, Invitro Evaluation of Mucoadhesive Properties of Chitosan and Some Other Natural Polymers. *International Journal of Pharmaceutics*. 78(1): p. 43-48.
27. Takayama, K., M. Hirata, Y. Machida, T. Masada, T. Sannan, and T. Nagai, **1990**, Effect of Interpolymer Complex-Formation on Bioadhesive Property and Drug Release Phenomenon of Compressed Tablet Consisting of Chitosan and Sodium Hyaluronate. *Chemical & Pharmaceutical Bulletin*. 38(7): p. 1993-1997.
28. Schauer, R., J.P. Kamerling, and J.F.G.V.a.H.S. J. Montreuil, **1997**, Chapter 11 Chemistry, Biochemistry and Biology of Sialic Acids. In, New Comprehensive Biochemistry. *Elsevier*. p. 243-402.
29. Borchard, G., H.L. Lueen, A.G. de Boer, J.C. Verhoef, C.-M. Lehr, and H.E. Junginger, **1996**, The potential of mucoadhesive polymers in enhancing intestinal peptide drug absorption. III: Effects of chitosan-glutamate and carbomer on epithelial tight junctions in vitro. *Journal of Controlled Release*. 39(2-3): p. 131-138.
30. Gan, Q., T. Wang, C. Cochrane, and P. McCarron, **2005**, Modulation of surface charge, particle size and morphological properties of chitosan-TPP nanoparticles intended for gene delivery. *Colloids and Surfaces B: Biointerfaces*. 44(2-3): p. 65-73.
31. Signini, R.S.P. Campana, **1999**, On the preparation and characterization of chitosan hydrochloride. *Polymer Bulletin*. 42(2): p. 159-166.
32. Muzzarelli, R.A.A., **1997**, Human enzymatic activities related to the therapeutic administration of chitin derivatives. *Cell. mol. life sci.* . 53: p. 131–140.
33. Durkut, S., Y.M. Elcin, and A.E. Elcin, **2006**, Biodegradation of chitosan-tripolyphosphate beads: in vitro and in vivo studies. *Artificial Cells, Blood Substitutes, & Immobilization Biotechnology*. 34(2): p. 263-76.

34. Vacanti, C.A., R. Langer, B. Schloo, and J.P. Vacanti, **1991**, Synthetic-Polymers Seeded with Chondrocytes Provide a Template for New Cartilage Formation. *Plastic and Reconstructive Surgery*. 88(5): p. 753-759.

35. Ko, J.A., H.J. Park, S.J. Hwang, J.B. Park, and J.S. Lee, **2002**, Preparation and characterization of chitosan microparticles intended for controlled drug delivery. *International Journal of Pharmaceutics*. 249(1-2): p. 165-174.

36. Sanford, P.A., **1984**, Chitosan: commercial uses and potential applications. In: G . Skjak-Braek, T. Anthonsen, and e. P. Sandford, Chitin and chitosan: sources, chemistry, biochemistry, physical properties and applications. *Elsevier Applied Science London and New York.* p. 51-69.

37. Schipper, N.G.M., K.M. Varum, and P. Artursson, **1996**, Chitosans as absorption enhancers for poorly absorbable drugs .1. Influence of molecular weight and degree of acetylation on drug transport across human intestinal epithelial (Caco-2) cells. *Pharmaceutical Research*. 13(11): p. 1686-1692.

38. Sandri, G., S. Rossi, F. Ferrari, M.C. Bonferoni, C. Muzzarelli, and C. Caramella, **2004**, Assessment of chitosan derivatives as buccal and vaginal penetration enhancers. *European Journal of Pharmaceutical Sciences*. 21(2-3): p. 351-359.

39. Zheng, L.-Y.J.-F. Zhu, **2003**, Study on antimicrobial activity of chitosan with different molecular weights. *Carbohydrate Polymers*. 54(4): p. 527-530.

40. Giunchedi, P., C. Juliano, E. Gavini, M. Cossu, and M. Sorrenti, **2002**, Formulation and in vivo evaluation of chlorhexidine buccal tablets prepared using drug-loaded chitosan microspheres. *European Journal of Pharmaceutics and Biopharmaceutics*. 53(2): p. 233-239.

41. Mori, T., M. Murakami, M. Okumura, T. Kadosawa, T. Uede, and T. Fujinaga, **2005**, Mechanism of macrophage activation by chitin derivatives. *Journal of Veterinary Medical Science*. 67(1): p. 51-56.

42. Peluso, G., O. Petillo, M. Ranieri, M. Santin, L. Ambrosic, D. Calabró, B. Avallone, and G. Balsamo, **1994**, Chitosan-mediated stimulation of macrophage function. *Biomaterials*. 15(15): p. 1215-1220.

43. Lip Yong Chung, R.J. Schmidt, P.F. Hamlyn, B.F. Sagar, A.M. Andrews, and T.D. Turner, **1998**, Biocompatibility of potential wound management products: Hydrogen peroxide generation by fungal chitin/chitosans and their effects on the proliferation of murine L929 fibroblasts in culture. 39(2): p. 300-307.

44. Mao, H.Q., K. Roy, V.L. Troung-Le, K.A. Janes, K.Y. Lin, Y. Wang, J.T. August, and K.W. Leong, **2001**, Chitosan-DNA nanoparticles as gene carriers: synthesis, characterization and transfection efficiency. *Journal of Controlled Release*. 70(3): p. 399-421.

45. Richardson, S.C.W., H.J.V. Kolbe, and R. Duncan, **1999**, Potential of low molecular mass chitosan as a DNA delivery system: biocompatibility, body distribution and ability to complex and protect DNA. *International Journal of Pharmaceutics*. 178(2): p. 231-243.

46. Behr, J.P., **1997**, The proton sponge: A trick to enter cells the viruses did not exploit. *Chimia*. 51(1-2): p. 34-36.

47. Ciftci, K.R.J. Levy, **2001**, Enhanced plasmid DNA transfection with lysosomotropic agents in cultured fibroblasts. *International Journal of Pharmaceutics*. 218(1-2): p. 81-92.

48. Leong, K.W., H.Q. Mao, V.L. Truong-Le, K. Roy, S.M. Walsh, and J.T. August, **1998**, DNA-polycation nanospheres as non-viral gene delivery vehicles. *Journal of Controlled Release*. 53(1-3): p. 183-193.

49. Corsi, K., F. Chellat, L. Yahia, and J.C. Fernandes, **2003**, Mesenchymal stem cells, MG63 and HEK293 transfection using chitosan-DNA nanoparticles. *Biomaterials*. 24(7): p. 1255-1264.

50. Dastan, T.K. Turan, **2004**, In vitro characterization and delivery of chitosan-DNA microparticles into mammalian cells. *Journal of Pharmacy and Pharmaceutical Sciences*. 7(2): p. 205-214.

51. Koping-Hoggard, M., I. Tubulekas, H. Guan, K. Edwards, M. Nilsson, K.M. Varum, and P. Artursson, **2001**, Chitosan as a nonviral gene delivery system. Structure-property relationships and characteristics compared with polyethylenimine in vitro and after lung administration in vivo. *Gene Therapy*. 8(14): p. 1108-1121.

52. Bozkir, A.O.M. Saka, **2004**, Chitosan-DNA nanoparticles: Effect on DNA integrity, bacterial transformation and transfection efficiency. *Journal of Drug Targeting*. 12(5): p. 281-288.

53. Knapczyk, J., **1993**, Excipient ability of chitosan for direct tableting. *International Journal of Pharmaceutics*. 89(1): p. 1-7.

54. Rege, P.R., D.J. Shukla, and L.H. Block, **1999**, Chitinosans as tableting excipients for modified release delivery systems. *International Journal of Pharmaceutics*. 181(1): p. 49-60.

55. Tozaki, H., T. Odoriba, N. Okada, T. Fujita, A. Terabe, T. Suzuki, S. Okabe, S. Muranishi, and A. Yamamoto, **2002**, Chitosan capsules for colon-specific drug delivery: enhanced localization of 5-aminosalicylic acid in the large intestine accelerates healing of TNBS-induced colitis in rats. *Journal of Controlled Release*. 82(1): p. 51-61.

56. Hejazi, R.M. Amiji, **2003**, Chitosan-based gastrointestinal delivery systems. *Journal of Controlled Release*. 89(2): p. 151-165.

57. Madsen, T., H. Buchardt Boyd, D. Nylén, A. Rathmann Pedersen, G.I. Petersen, and F. Simonsen, **2001**, Environmental and Health Assessment of Substances in Household Detergents and Cosmetic Detergent Products. *Environmental Project No. 615*. CETOX.

58. Kawashima, Y., T. Handa, A. Kasai, H. Takenaka, S.Y. Lin, and Y. Ando, **1985**, Novel Method for the Preparation of Controlled-Release Theophylline Granules Coated with a Poly-Electrolyte Complex of Sodium Polyphosphate Chitosan. *Journal of Pharmaceutical Sciences*. 74(3): p. 264-268.

59. Shu, X.Z.K.J. Zhu, **2002**, The influence of multivalent phosphate structure on the properties of ionically cross-linked chitosan films for controlled drug release. *European Journal of Pharmaceutics and Biopharmaceutics*. 54(2): p. 235-243.

60. Fwu-Long Mi, S.-S. Shyu, S.-T. Lee, and T.-B. Wong, **1999**, Kinetic study of chitosan-tripolyphosphate complex reaction and acid-resistive properties of the chitosan-tripolyphosphate gel beads prepared by in-liquid curing method. 37(14): p. 1551-1564.

61. Zeiger, E., B. Gollapudi, and P. Spencer, **2005**, Genetic toxicity and carcinogenicity studies of glutaraldehyde - a review. *Mutation Research-Reviews in Mutation Research*. 589(2): p. 136-151.

62. Fwu-Long Mi, S.-S. Shyu, C.-Y. Kuan, S.-T. Lee, K.-T. Lu, and S.-F. Jang, Chitosan-Polyelectrolyte complexation for the preparation of gel beads and controlled release of anticancer drug. I. Effect of phosphorous polyelectrolyte complex and enzymatic hydrolysis of polymer, J.o.A.P. Science, Editor. 1999. p. 1868-1879.

63. Gan, Q.T. Wang, **2007**, Chitosan nanoparticle as protein delivery carrier--Systematic examination of fabrication conditions for efficient loading and release. *Colloids and Surfaces B: Biointerfaces*. 59(1): p. 24-34.

64. Xu, Y.M.Y.M. Du, **2003**, Effect of molecular structure of chitosan on protein delivery properties of chitosan nanoparticles. *International Journal of Pharmaceutics*. 250(1): p. 215-226.

65. Acarturk, F., **1989**, Preparation of a Prolonged-Release Tablet Formulation of Diclofenac Sodium .1. Using Chitosan. *Pharmazie*. 44(8): p. 547-549.

66. Vrentas, J.S.J.L. Duda, **1976**, Diffusion of Small Molecules in Amorphous Polymers. *Macromolecules*. 9(5): p. 785-790.

Chapter 2

Chitosan/TPP and chitosan/TPP-hyaluronic acid nanoparticles

2 Chitosan/TPP and chitosan/TPP-hyaluronic acid nanoparticles

2.1 Summary

Gene medicine utilizes nucleic acids with the aim of restoring or shutting down a specific cellular function[1]. The formulation of negatively charged nucleic acids with various polycations into micro- or nanoparticulate structures (complexes) through electrostatic interactions has proven useful for creating non-viral delivery vehicles[2] where nucleic acids are physically condensed into small particles and should facilitate their cellular binding and uptake. In an ideal vehicle,

a) the nucleic acid is complexed in a reversible fashion,

b) the nature of the carrier does not depend strongly on the amount and nature of the nucleic acid,

c) the surface of the carrier is functionalisable with "stealth" groups and targeting groups can be added too.

Chitosan (CS) was selected as a building block, because

1) its complexation with poly/oligoanions is reversible (at acidic pH),

2) can form nanoparticles with a variety of polyanions, which can be used as a second building block to provide appropriate mechanical and transport properties to the nanoparticle (which therefore do not depend on the nature and concentration of the nucleic acid),

3) can impart a net charge to the particle surface, which allows its easy fictionalization via polyelectrolyte adsorption.

A rational study was performed for the optimisation of size, size dispersity and stability of nanoparticles formed by chitosan and sodium triphosphate (TPP), the anion used as a cross linking agent. After optimisation the nanoparticles were coated with hyaluronic acid.

Furthermore, a study of cytotoxicity and internalisation of the best nanoparticles on/in two model cell lines: non-phagocytic fibroblasts and phagocytic macrophages.

2.2 Introduction

The elastic, solid-like character of nanoparticles (→ morphological stability and control over diffusion kinetics of entrapped molecules) and the possibility of introducing appropriate surface functionalities (→ biological targeting) are at the basis of the widespread interest for this class of colloidal objects in the field of controlled and targeted release.

Nanoparticles can be rendered responsive, linking their performance to physico-chemical or biological stimuli[3], for example coupling morphological transitions and thus changes in release kinetics or in uptake by cells to changes in pH or temperature, to the presence of oxidants[4].

We will not discuss further the general applications of nanoparticles in biomedicine[5]; we will, on the other hand, specifically focus on a few key points that are essential for their structural design.

a) nanoparticle bulk: a colloidal drug carrier is generally internalized through endocytosis, ending up in endosomes characterized by an increasingly aggressive environment with time. In most cases, it is desired that the carrier escapes from these compartments; a commonly adopted strategy is based on the use of weakly basic groups that, due the acidity of endosomal compartments, can be protonated, thereby increasing the local osmotic pressure up to the collapse of the endosomal membrane.

b) nanoparticle surface: in the absence of a specific target, the surface composition should allow a prolonged circulation in the body fluid of choice, *i.e.* it should be "stealth" enough to allow the diffusion of the nanoparticles throughout the site[6]; to increase the stealthiness, the surface should be wettable by water in order to obtain a complete camouflage (*"if you want to be invisible, look like water"*)[7]. The evasion of the nanoparticles by macrophages is obtained avoiding the protein adsorption and eluding the opsonization and the complement activation[8]; indeed it was demonstrated that small neutral nano-vehicles have longer half-life circulation than the same type of particles with anionic surface[9]. Among the polymer structures that could be used for providing this protein-repellent character, besides the ubiquitous poly(ethylene glycol) (PEG), one could mention dextrans[10], poly(N-vinyl pirrolidone)[11], poly(glycerol methacrylate)[12] and glycosoaminoglycans, such as heparin[10] or hyaluronic acid (HA)[13].

c) degradability and biocompatibility: at the end of its life cycle, a carrier should be degraded to excretable or metabolisable products, showing negligible cytotoxicity

throughout the life cycle. It is noteworthy that in this process the interactions between cells and nanoparticles are mostly dependent on the nanoparticle surface composition, and specifically on charge, but also on their size[14-16].

We have here focused our attention of chitosan-based nanoparticles. Probably, the most popular way to produce chitosan-based nanoparticles is its ionotropic gelation with a small polyanion, sodium tripolyphosphate, which is characterized by a triple negative charge throughout the physiologically acceptable pH range[17, 18]. This form of polyelectrolyte complexation can be limited within a nano-size if one of the partners is present in large excess and if appropriately low concentrations are employed.

It has been initially found that concentrations below 2 mg/mL and 0.4 mg/mL respectively for TPP and chitosan, should be used, in order to avoid the formation of large aggregates, with chitosan/TPP mass ratios possibly not exceeding 15-20/1[17]; larger chitosan/TPP ratios yielded particles with larger size (but obviously lower cross-linking density) and zeta potential[17, 19, 20]. Kumacheva et al. have refined these initial studies, investigating the effect of chitosan fractional precipitation and deacetylation as means to increase its TPP-binding efficiency[21].

We have here expanded the findings of Kumacheva, using a highly deacetylated chitosan and focusing on the different variables that may affect the chitosan – TPP complexation: not only the chitosan/TPP mass ratio, but also the pH, which determines chitosan protonation degree and therefore both its binding ability and its self-association, and the volume ratio between the solutions. The latter parameter is of often neglected significance: if the complexation kinetics is of the same order of magnitude as or quicker than the mixing of the two solutions, it is likely to have a kinetic control over the properties of the final nanoparticles.

The main method to vary the size and modulate the reaction kinetics is to vary the NH_3^+/O^- charge ratio (free chitosan amines/TPP oxygen negatively charged), the ratio can range from 6 to 0.5[17, 20, 22-24]; this modulation has a consequent effect on the ζ-potential (range +20/+60mV), on the loading capacity[17] and on cellular transfection[24].

The scope of this part of our study was the development of chitosan/TPP nanoparticles optimized against the following parameters:

a) reasonably narrow size dispersity and size control, possibly producing <200 nm (“small”) and 200-400 nm (“large”) nanoparticles, in order to later study the effect of size in the interactions with cells,

b) high zeta potential, possibly with a narrow distribution, in order to obtain both a good electrostatic stabilisation and the possibility of a surface functionalisation through polyelectrolyte deposition,

c) stability of both size and zeta potential in water and/or buffer, in order to ensure long-term storage

d) stability of pH when the nanoparticles are stored in unbuffered water solutions. Drifts in pH would signal ongoing complexation (or de-complexation) phenomena: the basicity of chitosan primary amines can indeed be influenced by the density of immobilized negative charges present nearby, and correspondingly we expect an increase in pH for increasing complexation.

Having therefore optimised the design of these nanoparticles, we have studied the conditions for the adsorption of hyaluronic acid on their surface, with the aim to produce HA-coated nanoparticles; these colloidal carriers could at the same time present "stealth" character and allow targeting of HA receptors[25].

These coated nanoparticles would present a bulk mostly composed of TPP-cross-linked chitosan and a surface where HA would concentrate, thus providing a negative zeta potential (Figure 2-1), and possibly a "stealth" character and the possibility to target HA receptors.

Finally, both uncoated and coated nanoparticles have been characterized not only in terms of their physical properties, but also for their cytotoxic effects on two model cell lines: non-phagocytic fibroblasts and phagocytic macrophages. Specifically, we have investigated their effects on cell viability and on the integrity of cell membrane.

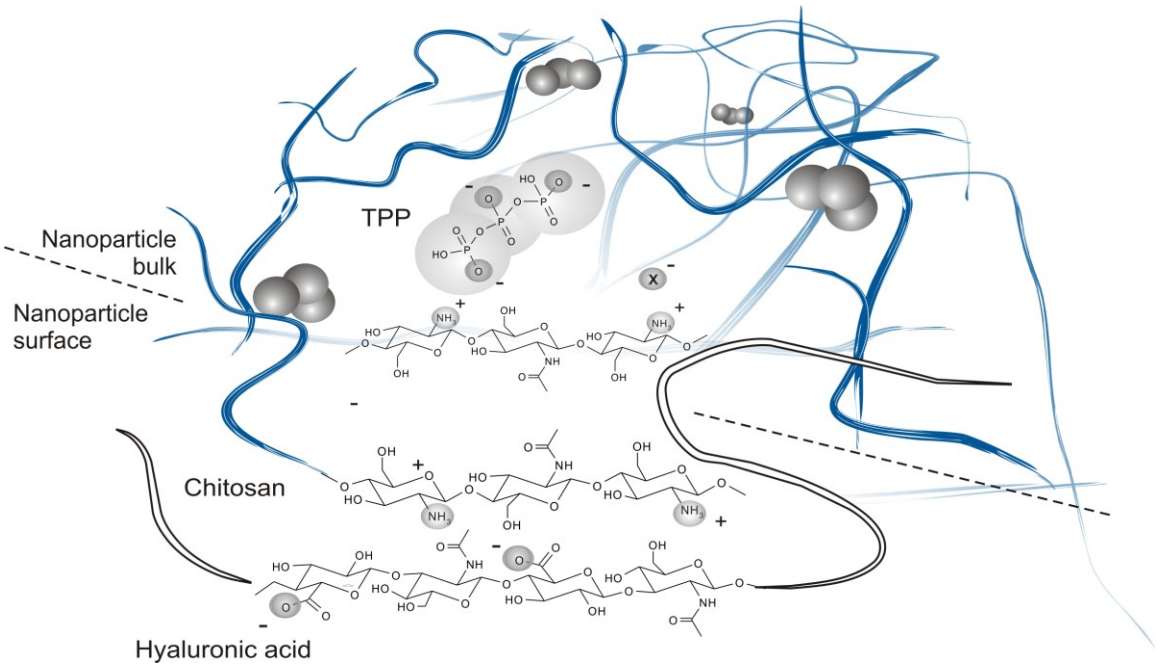

Figure 2-1. Graphical view of the structure of HA-coated chitosan/TPP nanoparticles, where TPP is present in low concentrations in the bulk of the nanoparticles, acting as a cross-linker and bridging between positive charges on the chitosan chains. The negatively charged HA complexes chitosan on the external part (the surface) of the nanoparticles, although a certain degree of diffusion in the bulk is possible.

2.3 Experimental section

2.3.1 Materials

Pentasodium triphosphate (Fluka), 1N hydrochloric acid, DMSO, 1N sodium hydroxide (Aldrich), fluorescein isothiocyanate (FITC) (Sigma), glacial acetic acid and sodium acetate (VWR BDH Chemicals, Poole, UK) were used as received. 10 mM Phosphate buffered saline (PBS) was prepared from appropriate tablets (Oxoid, Basingtoke, UK). Chitosan ("low MW": Cat. No. 448869, Aldrich) was used after purification as described hereafter. Hyaluronic acid with average viscosimetric molecular weight of $15*10^3$ g/mol and $360*10^3$ g/mol was obtained from Medipol (Lausanne, Switzerland). The two single strand DNAs (Metabion, Martinsried, DE) were used as received, 5'-CGG TGT GTC TGT CGG TTG-3' (MW=5569 g/mol) and 5'-GGA TCC TAA TAC GAC TCA CTA TAG GCA GTA ACT ATA ACG GTC CTA AGG TAG-3' (MW=16004 g/mol).

The QuantiPro BCA assay kit was supplied from Sigma, Gillingham, UK: QuantiPro Reagent QA (M3810) was a solution consisting of sodium carbonate, sodium tartrate, and sodium bicarbonate in 0.2 M NaOH, pH 11.25. QuantiPro BCA QB (M3685) was a 4% (w/v) bicinchoninic acid solution, pH 8.5. Copper (II) sulfate, Pentahydrate 4% Solution (C2284) (Reagent QC) was a 4% (w/v) copper (II) sulfate, pentahydrate solution.

Protein Standard Solution (P0914) was supplied in 10 flame-sealed glass ampoules, each containing 1.0 ml of a solution consisting of 1.0 mg/ml bovine serum albumin in 0.15 M NaCl with 0.05% sodium azide as a preservative.

Double distilled Milli-Q water was produced using in series an ELGA Docking Vessels DV35 and a Milli-Q Gradient A10 System.

2.3.2 Physico-chemical characterisation

Dynamic Light Scattering (DLS) and zeta potential measurements were performed on a Zetasizer Nanoseries ZEN3600 (Malvern Instruments) equipped with a solid state HeNe laser (λ = 633 nm). All the samples were analyzed at an angle of 114° and a temperature of 25°C. AFM measurements were performed on nanoparticles deposited on a mica surface from dispersions in deionised water using a MPF-3D instrument (Asylum Research). Viscosity measurements were performed on a 0.25 M acetic acid/0.25 M sodium acetate solution using a falling ball automated microviscometer (Anton Parr) at 25°C equipped with a 1.6 mm internal diameter capillary tube at an inclination angle of 30 degrees. The visosimetric average molecular weight was calculated assuming the parameters of the Mark-Houwink equation to be equal to $K = 1.57 \times 10^{-5}$ L.g^{-1} and $a = 0.79$ [26].

^{1}H-NMR spectra were recorded on JEOL EX270 270 MHz NMR spectrometer (Bruker Avance 270, Coventry, UK). Infrared spectra were recorded on a Tensor 27 in ATR mode. UV-Vis spectra were recorded on a Perkin Elmer Lambda 850 spectrometer.

Fluorescence measurements were performed using a Perkin Elmer LS55 luminescence spectrometer equipped with a xenon discharge lamp; the cuvette used was made of quartz glass.

2.3.3 Purification of chitosan

5 g of chitosan (MW 495, DD 90%) were dissolved in 400 mL of a 2% w/v acetic acid solution in double distilled water. Complete dissolution was achieved after 16 hours of stirring. The solution was then boiled for 15 minutes in order to denature and precipitate any proteic contaminant.

The mixture was then centrifuged for 10 minutes at 4500 rpm; the supernatant was removed then and filtered through 1 μm pore size filters. The pH of the solution was then corrected to 9 with 1N sodium hydroxide, in order to precipitate chitosan from the aqueous phase. After centrifugation, the precipitate was redispersed and again sedimented via centrifugation twice, always using water at pH = 9 as a dispersing medium. The procedure was repeated with Millipore water until the pH and conductivity values reached the values of pure water. The sample was freeze-dried (yield of the overall procedure = 86%) and stored at 4°C.

^{1}H-NMR (2%w/w HCl/D_2O): δ = 2.3 – 2.4 (acetamide CH_3), 3.4 – 3.6 (C**H**-NH_2), 3.8 – 4.4 (two broad peaks comprising C**H**-$NHCOCH_3$ and all other non-anomeric protons), 5.15 - 5.3 (anomeric protons) ppm.

ATR-IR (thin film): 3500-3000 (ν OH and NH_2), 2875 (ν CH), 1647 (amide I), 1588 (amide II) 1380, 1320, 1063, 1030 cm^{-1}.

Colloid titration was performed in a 0.02 M acetate buffer/0.1 M NaCl at pH 4.5, which was used as the solvent for chitosan and poly(styrene sulfonate) (PSS) and toluidine blue (a cationic metachromatic indicator). 2 ml of $5*10^{-3}$ mg/ml chitosan solution were added of 20 μl of 0.03% toluidine blue O solution and then titrated with a PSS solution $1*10^{-3}$ M in sulfonate groups, recording the ratio of the absorbance values at 635 and 600 nm.

Degree of deacetylation: before purification 91.01 mol % (^{1}H-NMR: ratio between acetamide protons and anomeric protons, Fig. 2-23), 87.50 mol % (IR: ratio between the absorbance values at 1655 and at 2875 cm^{-1}), 91.20 mol % (colloid titration); after purification: 92.02 mol % (^{1}H-NMR, Fig. 2-24), 85.4 mol% (IR), 89.70 mol % (colloid titration).

Intrinsic viscosity and viscosimetric average molecular weight: before purification [η] = 0.493 L/g, Mv = $492*10^3$ g/mol; after purification [η] = 0.481 L/g, Mv = $477*10^3$ g/mol.

Table 2-1. Degree of deacetylation, MW, intrinsic viscosity before and after purification.

	Degree of deacetylation (mol %)				
	^{1}H-NMR	IR(1655/2875)	Colloid titration	Intrinsic viscosity (L/g)	MW (g/mol)
Commercial chitosan Aldrich®	91.01	87.50	91.20 ± 0.49	0.493	$492.41*10^3$
Purified chitosan	92.02	85.40	89.70 0.89	0.481	$477.73*10^3$

Assessment of protein content: The assay consists of mixing 1 part of a protein sample with 1 part of the prepared QuantiPro Working Reagent. The protein sample is a blank, a protein standard, or an unknown sample. The blank consists of a buffer solution with no protein, a protein standard of a known concentration of protein, and an unknown sample is the solution to be quantified.

The QuantiPro Working Reagent was prepared by mixing 25 parts of Reagent QA with 25 parts of Reagent QB. After Reagents QA and QB had been combined, 1 part of Reagent QC (copper (II) sulfate) was added and mixed until it was uniform in color.

Two chitosan solutions were prepared, one with the Aldrich commercial chitosan and the other one with the purified chitosan. In both cases the chitosan was dissolved in a 0.1M HCl solution in order to obtain a 2% w/v concentration (10 mL in volume for each solution). The solutions are left under stirring until complete dissolution. Then the pH is increased with 1 mL of 1M NaOH provoking complete precipitation. Both the samples were centrifuged at 4500rpm for 50 minutes and supernatant collected (at this point the concentrations of HCl and NaOH were of both 0.09M) and analysed with a QuantiPro kit in a Biotek© Synergy multiplate reader: 100 µL of the supernatant or of albumin solutions of different concentration were added of 100 µL of QuantiPro Working Reagent. In the same well plate, eleven wells were filled with the standard protein solution; the concentrations were several in order to obtain a standard curve to use as a reference. The ratio of the volumes of the protein or unknown sample and QuantiPro Working Reagent was fixed to 1:1. The 96 well-plate was placed in incubation at 37°C for 2 hours, after this step the absorbance was read at 562 nm.

The concentration of proteins in the unpurified and purified samples were measured to be, respectively, 19.0 µg/mL and 10.2 µg/mL, which correspond to 1.056 mg and 0.561 mg of protein per gram of dry chitosan.

2.3.4 Chitosan fluorescein isothiocyanate-labeling

100 mg of purified chitosan is dissolved in 0.10 M acetic acid solution, the pH is corrected to 4 with sodium hydroxide. The final volume has to be 18 mL and placed in a round bottom flask (capacity of 50 mL). 10 mg of FITC are dissolved in 2 mL of DMSO and they are slowly added to the chitosan solution using a dropping funnel. The final ratio of FITC respect to the D-glucosamine residue is 1:23.5. The reaction is left in stirring for 12 hours. Precipitation could occur at the beginning of the reaction but after one hour it disappears. FITC-labelled chitosan solution must be completely clear; in case of presence of precipitation, the pH was corrected to 3.5 using 1 N HCl. The solution is left under stirring for 40 min. Once had a clear solution, the volume of the solution is doubled with distilled water in order to reduce the risk of damage for the ultrafiltration membrane during the purification, this could happen due to the presence of DMSO. The solution is placed in the ultrafiltration chamber in order to start the purification with an ultrafiltration membrane of 10000 Da cut-off; solutes of high molecular weight are retained, while water, DMSO, non-reacted FITC and salts pass through the membrane. During the process, conductivity, pH and fluorescence of the filtrate were checked. The solution is washed extensively with distilled water until there is a complete absence of free FITC and absence of salts. Once the pH of the solution has the same value of distilled water, it is lyophilized by freeze-drying. The yield of reaction was evaluated; 10.5 mg of FITC-chitosan was dissolved in 49.6 mL of 0.1 M acetic acid solution, the fluorescence intensity was read with the luminescence spectrometer (λ_{ex}=494 λ_{em}=518) and compared with a fitted calibration line of FITC, the yield of reaction was calculated to be 25.4%.

2.3.5 Preparation of chitosan-TPP nanoparticles

Chitosan was dissolved in 4.6 mM HCl at concentrations 0.038, 0.054, 0.069, 0.085 and 0.1% wt. adjusting the pH of the different solutions to 3, 4, 4.5 or 5 by the addition of appropriate volumes of NaOH. All solutions were sonicated for 40 minutes.

TPP was always prepared as a 0.1% (w/w) solution at pH = 3, 4, 4.5, 5 or 8, the pH value was corrected with HCl 1 N.

Both solutions were filtered through a 0.22 μm pore size filter and, in order to remove any large aggregate possibly present. The complexation was then carried out at 25°C and under magnetic agitation (750 rpm) for a duration of 30 minutes, followed by

sonication for 40 minutes, leaving then the dispersion undisturbed for additional 16 hours prior to any purification (ultrafiltration through 500 kDa molecular weight cut-off polyethersulphone (PES) membranes) or analysis. Dispersions with different nanoparticle content could be obtained by concentrating the dispersions during ultrafiltration and assessing their concentration by measuring the dry content after freeze drying.

Method A: variable chitosan concentration, constant volumes of solution.

2.786 mg of a chitosan solution with concentration 0.038, 0.054, 0.069, 0.085 or 0.1% wt. and pH = 3, 4, 4.5 or 5 were mixed with 214 mg of a 0.1% wt. TPP solution at the same pH; in alternative a chitosan solution with one of the above concentrations and pH = 4 was mixed with a 0.1% wt. TPP solution at pH = 8.

In the final dispersion the chitosan and TPP concentrations were therefore 0.035, 0.050, 0.064, 0.079 or 0.093% wt. and 0.0071% wt., respectively, corresponding to 5/1, 7/1, 9/1, 11/1 or 13/1 mass ratios between the two components.

Method B: constant chitosan concentration, variables volumes of solution.

A 0.1% wt. chitosan solution at pH = 3, 4, 4.5 or 5 was mixed with a 0.1% wt. TPP solution at the same pH, or, in alternative, the chitosan solution at pH = 4 was mixed with the TPP solution at pH = 8, according to the following mass ratios and for a total mass of 3g: 2786/214, 2750/250, 2700/300, 2625/375 and 2500/500.

In the final dispersion the chitosan and TPP concentrations were therefore 0.083, 0.088, 0.090, 0.092 and 0.093% wt. and 0.0071, 0.0083, 0.0100, 0.0125, 0.0167% wt., respectively, corresponding to 5/1, 7/1, 9/1, 11/1 or 13/1 mass ratios between the two components.

Characterisation: the nanoparticles were characterised by measuring size, zeta potential and morphology (AFM). Due to TPP low concentration, IR analysis did not reveal any peak typical of phosphate groups; it is therefore generally assumed the chitosan/TPP ratio to be the same as in the feed.

Preparation of fluorescent CS-TPP nanoparticles (FITC-CSNPs).

The fluorescent nanoparticles were prepared with the FITC-labelled chitosan in the same fashion of the non fluorescent nanoparticles, the FITC-chitosan was used in place of the plain chitosan. The fluorescent nanoparticles reproduced were the type “large” and “small”.

NOTE: the breadths of both the distributions of size and that of zeta potential were expressed in reference to the width at half height of the distribution. When evaluating the dispersity in size, we have divided the width at half height of the distribution by the peak value, providing the aspect ratio of the distribution: in this way distributions peaked sometimes at largely different sizes and correspondingly present largely different widths half height. We have followed the same approach for multimodal distributions, using the size corresponding to the highest peak and the overall width of the distribution.

The same approach cannot be used for the evaluation of zeta potential data, since their peak values are sometimes too close to zero to provide meaningful figures; therefore the breadth of the zeta potential distributions was evaluated just on the basis of the width at half height of the peaks.

2.3.6 Coating of chitosan-TPP nanoparticles with hyaluronic acid

Chitosan/TPP nanoparticles ("small" nanoparticles, method A, pH5-pH5, CS/TPP 9:1, Z av. size 240 nm, Zeta potential = 43.9 mV) were dispersed in a 100 mM acetic acid/acetate buffer at pH = 5 at a concentration of 0.05 or 0.1 wt.%. 2 mL of these dispersions were slowly added under vigorous stirring (30 minutes, 1200 rpm) to an equal amount of acetate buffer of equal strength containing hyaluronic acid of molecular weight $15*10^3$ g/mol and $360*10^3$ g/mol at a concentration of 0.05, 0.10, 0.15, 0.20 or 0.50 wt.%. The dispersions were then purified via ultrafiltration using a 500kDa cut off membrane, and concentrated up to 0.30% w/w.

2.3.7 ssDNA loading tests

Two different MW of single strand DNAs (ssDNAs) and the "small" nanoparticles were used for the loading tests; the concentrations of the ssDNAs used for the two experiments were fixed to 420 μg/mL (before loading). The ssDNA solution (35 μL, conc. 420 μg/mL) was added in the TPP solution (214 μL, conc. 0.1% wt.). In the same time a chitosan solution (2751 μL, 0.070 %wt.) was placed under stirring in a glass vial (10.5mL in volume). The ssDNA/TPP solution was pipetted in the chitosan solution and the complexation was left in stirring for 30 minutes, following the sonication for 40 minutes. The two types of DNA were undergone in two different samples; moreover

two blank experiments with the two ssDNAs in TPP solution, without chitosan, were prepared. Three blanks of nanoparticles without the loading of ssDNAs were prepared. Z-average and z-potential were verified after complexation and sonication; each sample was precipitated with NaOH (final pH 7.4), centrifuged and filtered through a 0.22 μm pore size filter, and the absorbance was read with the UV/VIS spectrometer in order to quantify the amount of ssDNA left in the supernatant; the difference between the absorbance value of the supernatants and the value of absorbance in the blanks of ssDNA (maximum absorbance that corresponds to a concentration of 4.9 μg/mL of ssDNA) gives the percentage yield of loading. The purity/stability of the ssDNAs in each passage was confirmed by the ratio between the absorbance read at 260 nm and the absorbance read at 280 nm (Abs_{260}/Abs_{280}), this value must be between 1.3 and 2.0 [27].

2.3.8 Cell culture and cytotoxicity assays

Murine fibroblasts L929 and macrophages J774.2 (ECACC, UK) were maintained as, respectively, adherent and semi-adherent cell culture at 37°C in humidified atmosphere (5% CO_2) in Dulbecco modified Eagle's minimal essential medium (DMEM, 25 mM glucose) supplemented with 2 mM glutamine (Gibco), 10% heat inactivated fetal calf serum (FCS) (Invitrogen, UK), 100 IU/ml penicillin and 100 IU/ml streptomycin (Gibco). For fibroblasts L929 cells splitting, trypsin-EDTA (Invitrogen, UK) consisting of 2.5% (w/v) of trypsin and 0.2% (w/v) EDTA in PBS was used while macrophages J774.2 cells were detached by scraping. For experiments, both cell lines were adjusted to the required concentration of viable cells, by counting in a haemocytometer in the presence of 0.4% trypan blue.

The nanoparticles used for cytotoxicity experiments were purified by dialysis in PBS (10mM, pH 6). Once reached the equilibrium in conductivity between filtrate and PBS solution the samples were concentrated to the appropriate concentration in an ultrafiltration cell. In each step the size and z-potential was checked by DLS.

The MTT assay measures the cell metabolic activity whereby the mitochondrial dehydrogenase enzyme of viable cells reduces the yellow tetrazolium salt, 3-[4,5-dimethylthiazol-2-yl]-2,5-diphenyl tetrazolium bromide dye (MTT), to a purple formazan crystals[28-30] (Scheme 2-1).

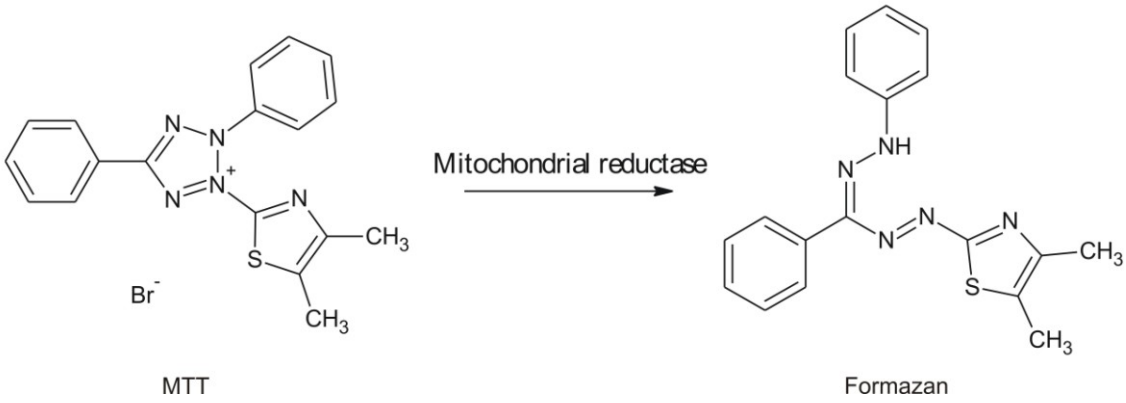

Scheme 2-1. The MTT assay is a colorimetric test that measures the activity of the mitochondrial enzymes. The enzymes reduce the MTT in formazan, the absence of this reduction means that the cellular activity is diminished, either the cells are dying or they are already dead.

Macrophages J774.2 and fibroblasts L929 cells were seeded in 96-well plates at 10,000 cells per well in complete medium containing 10% FCS. The cytotoxicity of the nanoparticles was evaluated using the MTT assay by determining the cells viability after for 24h-incubation with different concentrations of hyaluronic acid-coated or uncoated chitosan nanoparticles; 4h incubation was used for the tests run at 4°C and for their controls at 37°C, since longer incubation times at low temperature cause a drastic decrease in cell viability also in the absence of nanoparticles. At the end of the incubation period in the presence of nanoparticles, cells were washed three times with PBS pH 7.4 and incubated with 100 μl of a MTT solution (0.5 mg/ml in DMEM) for 4 h at 37°C. One hundred microliters of dimethyl sulfoxide (DMSO) were then added to dissolve the formazan crystals. The UV absorbance of the solubilized formazan crystals was measured spectrophotometrically (Microplate reader, TECAN, Safire, Austria) at 550 nm. Cell viability was expressed as the ratio between the absorbance reading for cells treated with the different nanoparticles and for control non-treated cells. The concentration inhibiting cell viability by 50% (IC50) was obtained by interpolation of the cell viability curves[31, 32].

The LIVE/DEAD double staining kit (Sigma, St Louis, MO, USA), which allows the simultaneous fluorescence staining of viable (Calcein-AM, excitation 495 nm, emission 515 nm) and dead (Propidium iodide, PI, excitation: 535 nm, emission: 617 nm) cells[33, 34], was used. Macrophages J774.2 were seeded in a 96-well plate at a count 8,000 cells/well and incubated for 24h with 0.1 mg/ml of coated or uncoated chitosan/TPP nanoparticles (CSNPs). After removal of the two treatments, cells were washed with

PBS, incubated with solution of both stains for 15 min at 37^{o}C and then observed under fluorescent microscope (Leica DMI5000,) at 20-fold magnification. Both Calcein-AM and PI-DNA were excited with 490 nm, allowing simultaneous monitoring of viable and dead cells while with 545 nm excitation, only dead cells were observed. In order to quantitatively assess the data obtained from the fluorescent images, the total number of cells and number of dead cells in 3 microscopic fields were counted (ImageJ 1.4d, USA) such that each microscopic filed contains around 300-360 cells. Each NPs formulation was assayed at least in triplicate wells.

All experimental results are expressed as mean ± SD. Statistical tests of significance were performed using one-way ANOVA followed by Bonferroni test for multiple comparisons at $P < 0.05$ (Origin® 7SR1, Northampton MA, USA).

2.3.9 Cellular Uptake of FITC-CSNPs and FITC-HA-CSNPs

Cellular Uptake of CSNPs and HA-coated CSNPs by Microscopy techniques. Macrophages J774.2 and Fibroblasts L929 cells were grown on cover slips, FITC-CSNPs or FITC-HA-CSNPs were suspended in DMEM (serum-free medium) or PBS. The cells were incubated separately with HA-coated and uncoated nanoparticles for 30 minutes at 37°C. Extracellular fluorescence was quenched with a trypan blue solution[35]. The cells were washed with PBS, followed by the fixation with 4% methanol-free formaldehyde and permeabilization with 0.1% Triton-X100. The Texas Red Phalloidin (TxR-phalloidin, Ex_{max}/Em_{max} 591/608 nm) was used to label the actin filaments, the 4',6-diamidino-2-phenylindole (DAPI, Abs_{max}/Em_{max} 358/461 nm[36]) was used to label the nucleus. The problem of overlapping in the emission of fluorescence between the DAPI, TxR-phalloidin and FITC is avoided taking images of the same cells sequentially. The confocal or fluorescent microscopes were used for taking the images.

Cellular uptake of HA-coated and uncoated CSNPs by Micro-fluorimetric Assay. Macrophages J774.2 cells were seeded in black 96-well plate-transparent bottom. The HA-coated and uncoated nanoparticles were placed in incubation with the cells subjected to different variables like nanoparticles concentrations, incubation times and presence of several effectors. At the end of the incubation period, the cells were washed with a PBS solution and then the lysis of the cells was performed with 0.5% Triton-X 100 in 0.2 N NaOH. The quantitation of nanoparticles uptake was expressed as micrograms of nanoparticles internalized divided milligrams of cellular proteins.

Calibration curve was plotted in order to relate the amount of nanoparticles with the fluorescence intensity (RFU), the fluorescence intensity was measured with a microplate reader (TECAN, Safire, Austria); the protein content was quantified with the QuantiPro Micro BCA assay kit.

2.4 Results and discussion

2.4.1 Preamble

In this study we have used chitosan with high degree of deacetylation (≈90%), employing a precipitation-redissolution procedure for removing contaminants, which are supposedly, but not necessarily, of proteic nature. The process did not modify the degree of deacetylation, which was evaluated through ^{1}H-NMR, IR and colloid titration, nor the intrinsic viscosity of the polymer, but removed a significant amount of contaminants in form of soluble proteins or colloidal impurities, which are capable of significantly affect both the process of nanoparticle formation and the interactions with cells.

As a qualitative measure of the efficacy of the purification procedure, the amount of base-soluble proteins is reduced to about 0.05 wt. % of the chitosan mass (roughly 50% of the initial base-soluble protein content): this would correspond to a protein content of 0.5 ppm for a 0.1% chitosan concentration, a protein level that was deemed acceptable for further use.

2.4.2 Preparation of chitosan/TPP nanoparticles

Variables and observables. We have investigated the influence of chitosan/TPP mass ratio, of pH and of the mixing procedure on the phenomenon of nanoparticle formation, monitoring the effects of these variables on the average value and the dispersity of size and zeta potential, and on the stability of these values and of pH at two different time points: 16 hours after complexation and then 30 days, in order to highlight possible stability issues.

- Since an excess of chitosan has always been used, the chitosan/TPP mass ratio is inversely related to the cross-link density of the material; larger ratios therefore correspond to lower cross-linking densities and thus to softer materials, but also

possibly to a slower kinetics of formation (both nucleation and growth), which may mean a more "thermodynamically" controlled process of formation. Specifically, we have varied the mass ratio between 5:1 and 13:1.

- The environmental pH can be varied only within a restricted range, since very acidic pH will lower the charge of TPP, decreasing its cross-linking capability, while pH larger than 6 would lower the charge density of chitosan, decreasing not only its capability to be cross-linked, but also its solubility, promoting its self-association. We have therefore performed most complexation experiments mixing TPP and chitosan solutions with an identical pH, with values ranging between 3 and 5. Additionally, we have explored an alternative procedure by mixing an acidic (pH = 4) chitosan solution in combination with a slightly basic (pH = 8) TPP solution. The transient exposure of chitosan to region of higher pH may induce some aggregation, increasing its local concentration: this may increase the number of nuclei available for nanoparticle growth (higher nucleation rate → smaller particles) larger nanoparticles, but it is also possible the aggregates to cluster in a TPP-mediated fashion (hence larger particles).

- We have mixed chitosan and TPP solutions according to two different methods: A) constant volume ratio between the two solutions, but different concentrations. Since all solutions are very dilute, we do not expect them to significantly differ in viscosity; therefore the mixing dynamics should be substantially identical for all samples. Any difference recorded in the nanoparticle properties should be ascribed simply on the thermodynamic and kinetic features of the complexation process. B) Solutions with constant concentrations of TPP and chitosan (0.1% for both), but mixed in different volume ratios. Differences between the results of this set of experiments and those of method A would signal that the fluidodynamics of mixing of the two solutions and/or local concentration of the polyelectrolytes have important effects on nanoparticle formation.

Effects on nanoparticles properties. The graphs in Figure 2-2 and 2-3 three-dimensionally show the influence of the above variables on the average size of chitosan/TPP nanoparticles (the darker the colour, the smaller the nanoparticle size) and on the aspect ratio of their size distribution (the larger the circles, the more "monodisperse" the distribution), or on the zeta potential (the darker, the more positive) and of the width at half height (again, the larger the circles, the narrower the distribution). Only experiments with a reliable scattering intensity were reported, thus excluding all the combinations that provided soluble, very small or extremely

polydisperse materials; therefore, when at a certain time point an experimental point is not reported, the values at the same position in different graphs must be taken as purely indicative, due to the impossibility of a quantitative comparison. Figure 2-4 presents the pH variation of the dispersions between the two time points of 16 hours and 30 days.
The following considerations apply:
- it is apparent that method B generally provides largely different results from method A, showing that the nature of the mixing process has a profound influence on the nanoparticle properties. Additionally, a number of samples prepared through method B at one or the other time point are not analysable (too low scattering intensity and/or too large polydispersity).
- the use of two solutions with different pH has a marked effect and leads to significantly larger nanoparticles. Firstly, this indicates that a higher pH in the TPP solution induces some form of chitosan aggregation: if not, no effect would be recorded. The final nanoparticles, however, are not simply formed by chitosan aggregates, because they would re-dissolve at the equilibrium pH (5.5-6); therefore, these nanoparticles are likely to be formed through the association of chitosan clusters.

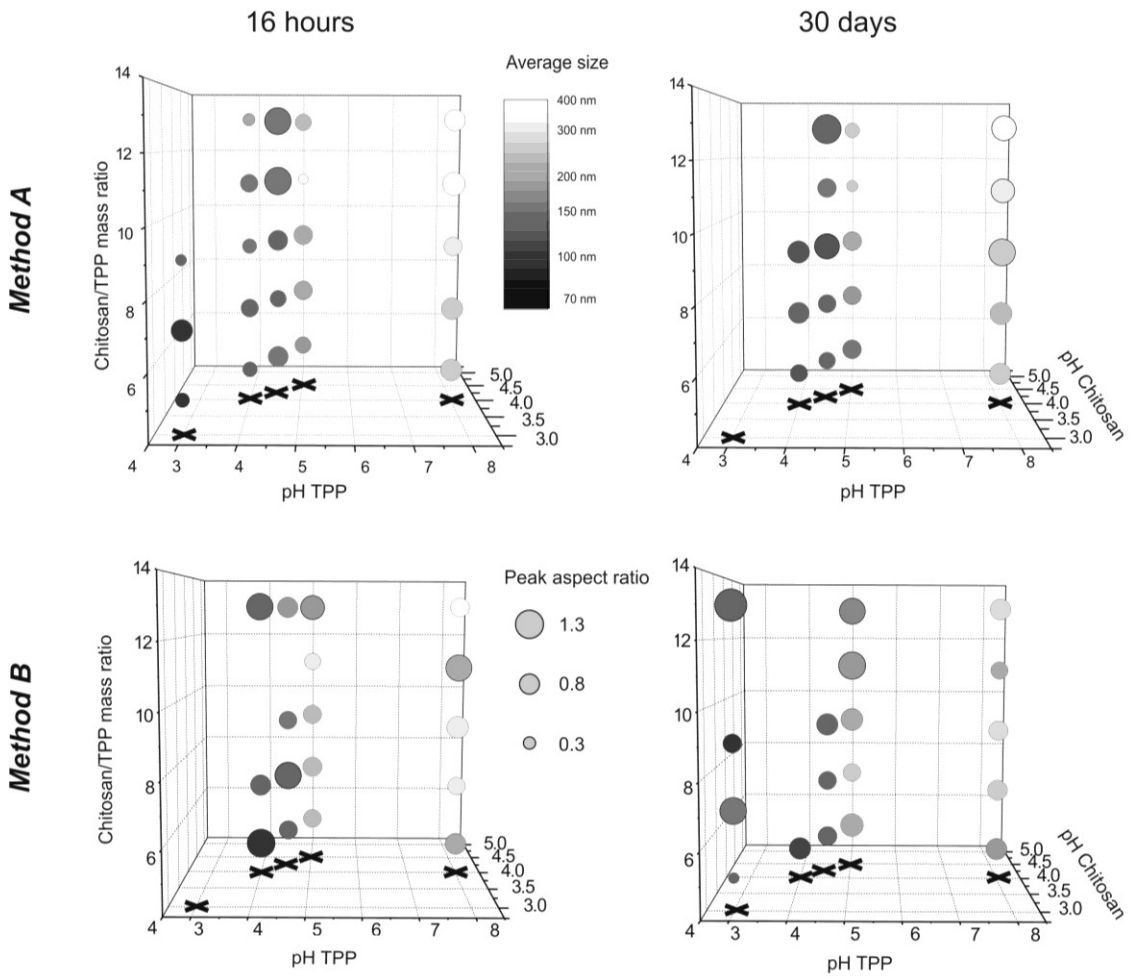

Figure 2-2. Average size and aspect ratio of the size distributions (average over three different preparations) as a function of chitosan/TPP mass ratio and pH of both solutions, using two mixing methods and recorded at two different times. For an easier reading, the pH values are highlighted with black crosses at the bottom of graphs. In some positions symbols are absent, due to very low values of the scattered intensity of the corresponding samples. A representative size distribution curve is shown in Figure 2-27.

- the use of solutions at pH = 3, on the contrary, generally provides very low amounts of nanoparticles, close to the detection limit of dynamic light scattering. This is likely due to the decreasing charge density of TPP with decreasing pH (TPP's pKa_3 = 2.3, therefore at pH =3 slightly less than 20% of its molecules are only double charged). A very high chitosan/TPP ratio seems a detrimental factor too (low cross-linking density),
- particles evolve with time, in some cases their size increases (aggregation), but more frequently it decreases; in general, the variation is more pronounced for particles obtained through method B than for method A. We are inclined to ascribe this effect to

the formation of a more compact matrix, i.e. new cross-links could be formed, releasing couples of counterions, and the slow kinetics is likely due to the fact that this process happens in an already cross-linked matrix. We expect a tighter complexation with chitosan and TPP to increase the basicity of amines: TPP is not a mobile counterion and has a multiple charge; therefore it can shield the positive charge of a protonated amine more effectively than *e.g.* a chloride or an acetate. Hence a neighbouring amine can be easier deprotonated due to the lower electrostatic repulsion; correspondingly we assume that a sound increase in cross-linking density may lead to an increase in pH. The pH of the particles obtained through method A is substantially stable, with a slight acid drift for those with higher size stability, while a clear increase up to one pH unit is seen for method B particles, which would confirm the possibility of a slow-running complexation.

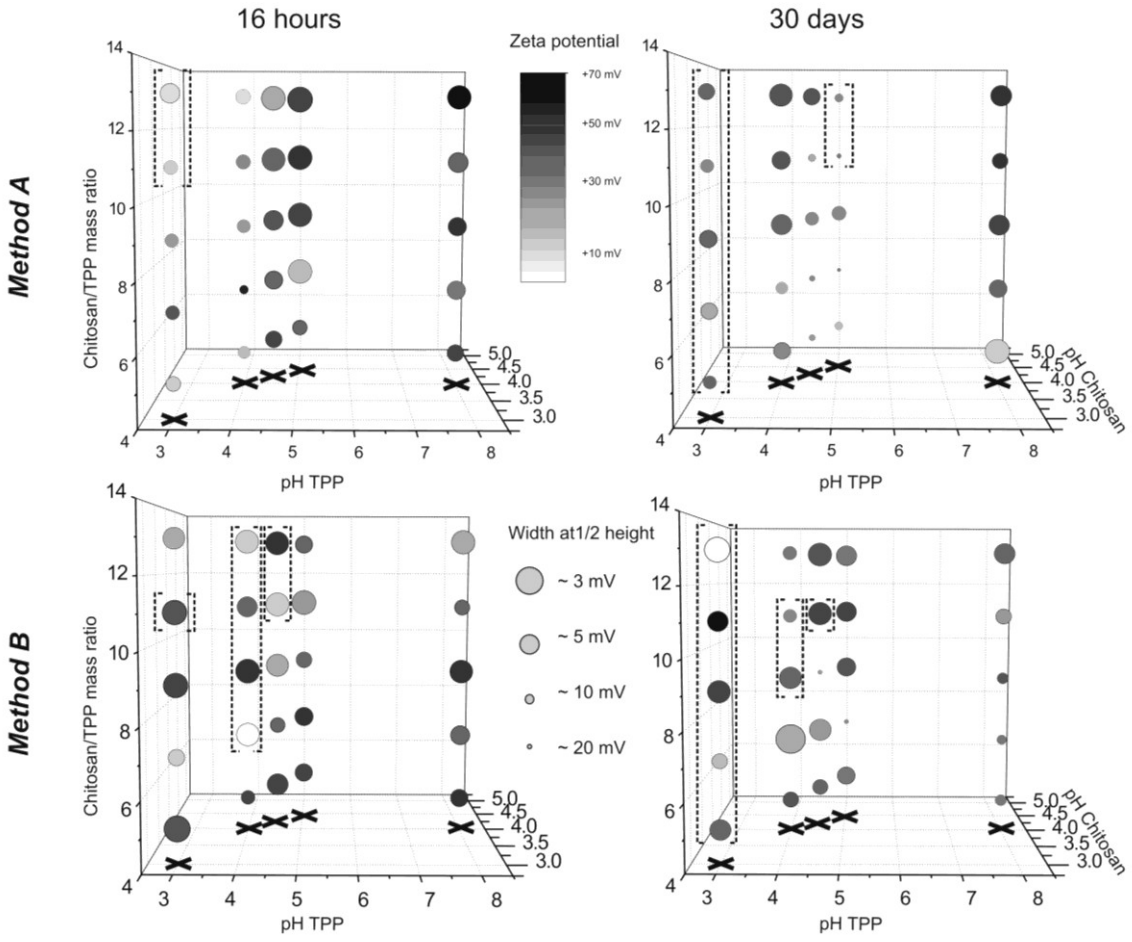

Figure 2-3. Average Zeta potential and width at half height for the Zeta potential distribution (average over three different preparations) as a function of chitosan/TPP mass ratio and pH of both solutions, using two mixing methods and recorded at two different times. For an easier reading, the pH values are highlighted with black crosses at the bottom of graphs. Where brackets are used, the samples showed

very low scattered intensity in DLS analysis and the values of Zeta potential have to be considered just qualitative. A representative Zeta potential distribution curve is shown in Figure 2-27.

- The average Zeta potential of all samples is largely positive, with reasonably narrow distributions fully comprised within the positive potential region. These data do not appear to have any dependence on the studied variables for method B particles; for method A particles it seems lower pH samples to show the broadest dispersity immediately after preparation and the narrowest after ageing; the variability of these data is, however, fairly large and it is difficult to conclusively ascribe this effect to a specific phenomenon. It is noteworthy that within the pH range used for the production of stable particles (between 4 and 6), the Zeta potential did not show any sound dependence on pH.

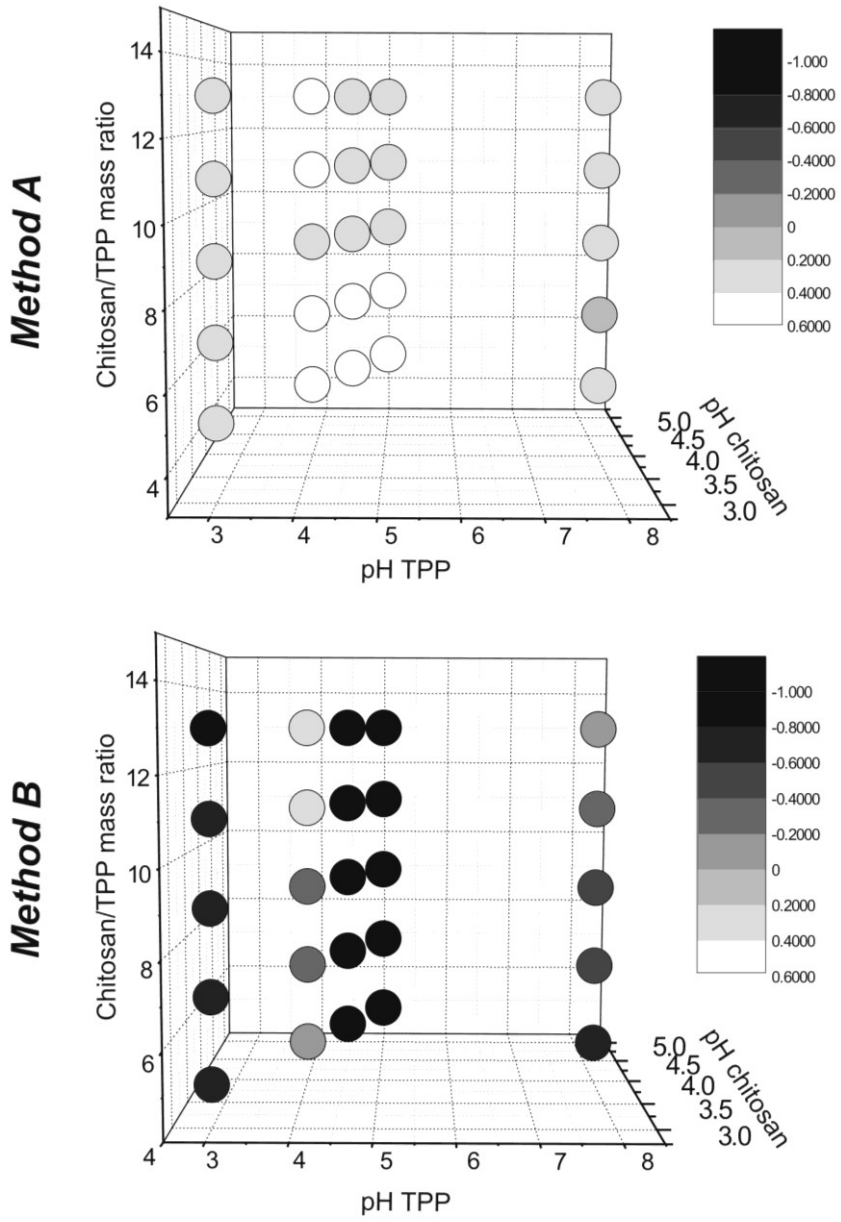

Figure 2-4. pH stability of the dispersions presented in Figures 2-2 and 2-3, expressed as the difference between the pH values at 16 hours and 30 days.

Selection of optimised nanoparticles. For further investigations we have selected two kinds of nanoparticles, which show the best combination of stability of size, Zeta potential and pH, high value of the average Zeta potential and narrow size dispersity, and are characterized by a "small" (200-300 nm in deionised water) or a "large" (300-400 nm) size. Our aim is to employ the "small" nanoparticles for further coating with hyaluronic acid: this process is very likely not only to modify their surface, but also to

increase their size; therefore we have chosen to target also "large" nanoparticles as a reference system that will exhibit similar size and bulk composition to the coated ones. The above features could be obtained by using method A, moderate chitosan/TPP ratios and pH = 4.5-5 for a lower average size, and pH = 4 and 8 for a larger size. Specifically, the following conditions were chosen:

"small" nanoparticles, pH5 for both solutions, chitosan/TPP 9:1, Z-average size 240 nm, Zeta potential = 43.9 mV.

"large" nanoparticles, pH4-pH8, CS/TPP 13:1, Z-average size 360 nm, Zeta potential = 47.0 mV

2.4.3 Environmental effects on chitosan/TPP nanoparticles

Chitosan/TPP nanoparticles are kept together by electrostatic forces, which clearly depend on the protonation extent and on the concentration of the ionic species.

Effect of pH. As suggested by the nanoparticle formation experiments conducted using pH = 3 solutions, an acidic environment is detrimental for the nanoparticle stability, because the protonation of TPP lowers its charge. Chitosan neutralization should set the upper stability limit. Indeed it can be seen (Figure 2-5) that under acidic conditions, at pH = 3 the scattering intensity is already low enough to hardly allow a reliable zeta potential determination and below it drops further. It is worth mentioning that DLS does not show any variation in dimensions (swelling), but just a decrease in the number of scattering particles. At pH > 6, on the other hand, the Zeta potential approaches neutrality and, instead of dissolution, the nanoparticles undergo agglomeration and macroscopic flocculation.

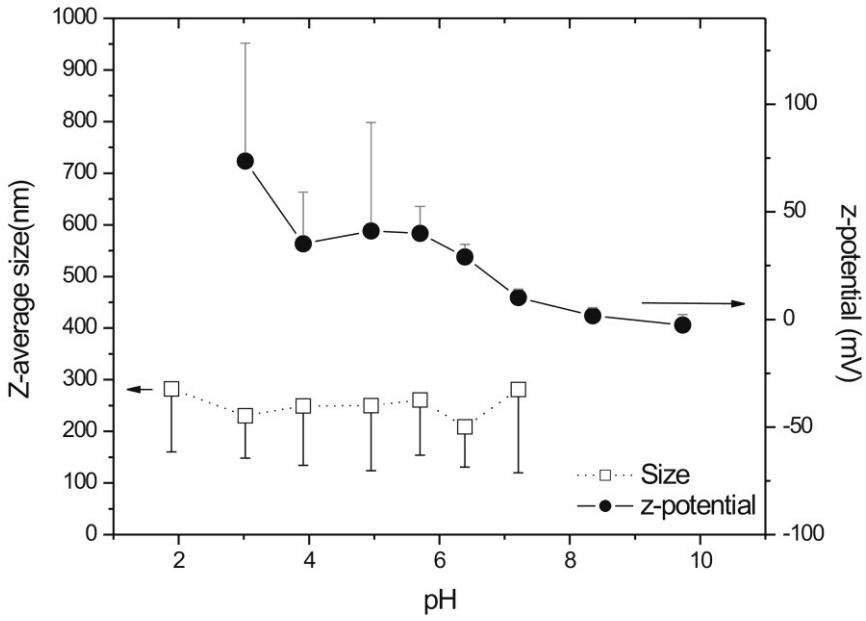

Figure 2-5. Dependence of the z-average size and of the Zeta potential on the pH for the "large" nanoparticles. A similar trend is recorded for the "small" nanoparticles. It is worth mentioning that the data were obtained by adding appropriate quantities of HCl or NaOH to the nanoparticles originally at pH = 5.5, without the use of any buffer.

Presence of ionic species. Due to the existence of a "stability window" in the pH region between 4 and 6, the use of buffers for the long-term storage of the dispersions appears to be the most logical solution. Since, however, the nanoparticles are held together and stabilised by electrostatic forces, it is of the essence to understand whether the presence of ionic species may influence their morphology and/or stability. Indeed upon exposure to moderate or high ionic strength buffers, the nanoparticles show a sound reduction in size to 62-68% the original average diameter, corresponding to a shrinkage to roughly one third of the initial volume. The extent of the shrinkage was substantially analogous in 10 mM PBS at pH = 6 (Figure 2-6) and in 100 mM acetate at pH = 5, with a negligible influence on the Zeta potential in both cases.

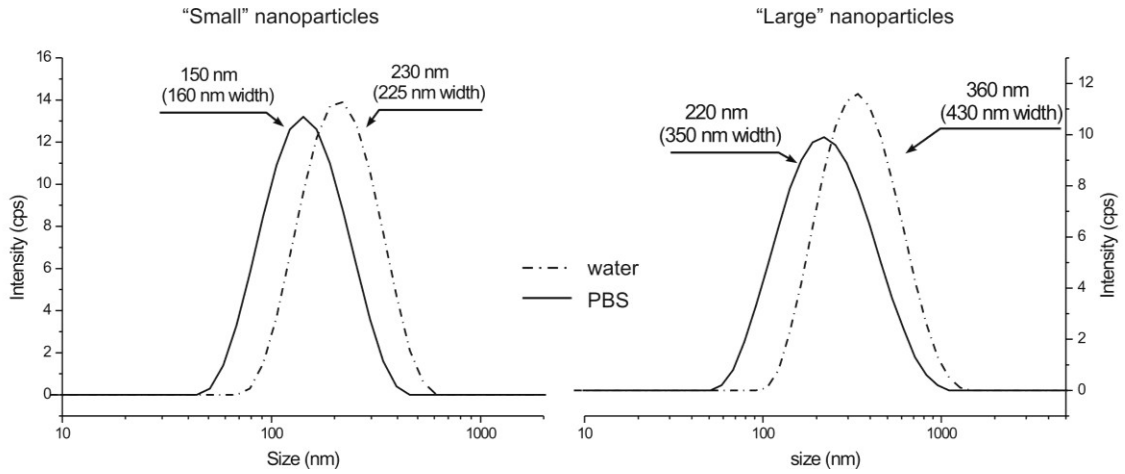

Figure 2-6. Changes in the size distribution of "small" and "large" chitosan/TPP nanoparticles as a consequence of the exchange of the medium from deionised water to 10 mM PBS.

2.4.4 Hyaluronic acid-coated nanoparticles

Due to the surface charge reversal, the adsorption of a polyanion on positively charged nanoparticles can result in agglomeration and possibly flocculation, either because of the interactions between positively and negatively charged patches on different nanoparticles, or because of the absence of electrostatic stabilization during the intermediate states of the adsorption.

The final outcome, i.e. surface functionalisation vs. agglomeration, depends on concentration and size of both nanoparticles and polyanion and on the strength of their interactions. Since the last parameter is automatically set by the choice of the materials (interactions between protonated amines and carboxylates) and pH (5 to ensure both stability of the initial chitosan nanoparticles and sufficient deprotonation to HA), we have studied the influence of the other parameters, limiting our investigation to dilute systems, in order to minimize the chance of aggregation, to "small" nanoparticles and to two HA molecular weights ($15*10^3$ g/mol and $360*10^3$ g/mol).

We have coated only "small" nanoparticles because the deposition of HA is likely to increase their size up to a few tens of nanometers: therefore coated "small" nanoparticles are likely to be analogous in size and bulk composition to the uncoated "large" nanoparticles, which therefore would be an ideal reference system to highlight effects arising only from surface composition. On the other hand, no similar reference system would be available for the coated "large" nanoparticles.

Very high molecular weight HA was excluded, on the grounds that the high viscosity of its solutions could result in scarcely reproducible experiments.

Our experiments have shown that a low molecular weight of HA, on the other hand, appeared to be detrimental to the stability of the nanoparticles (Figure 2-7). Low polydispersity and reasonably low size increase was on the contrary recorded with HA of MW=360*10^3 g/mol at concentrations comprised between 0.1 and 0.2 wt.%.

The lowest polydispersity and the smallest size increase (average size = 260 nm in acetate buffer, compared to 160 nm before adsorption) were recorded for the combination of "small" nanoparticles at 0.05 wt.% and HA at 0.15 wt.%. These conditions suggest a very moderate agglomeration, with the volume of a final particle corresponding to that of 3-4 parent ones, and were therefore adopted for any further investigation.

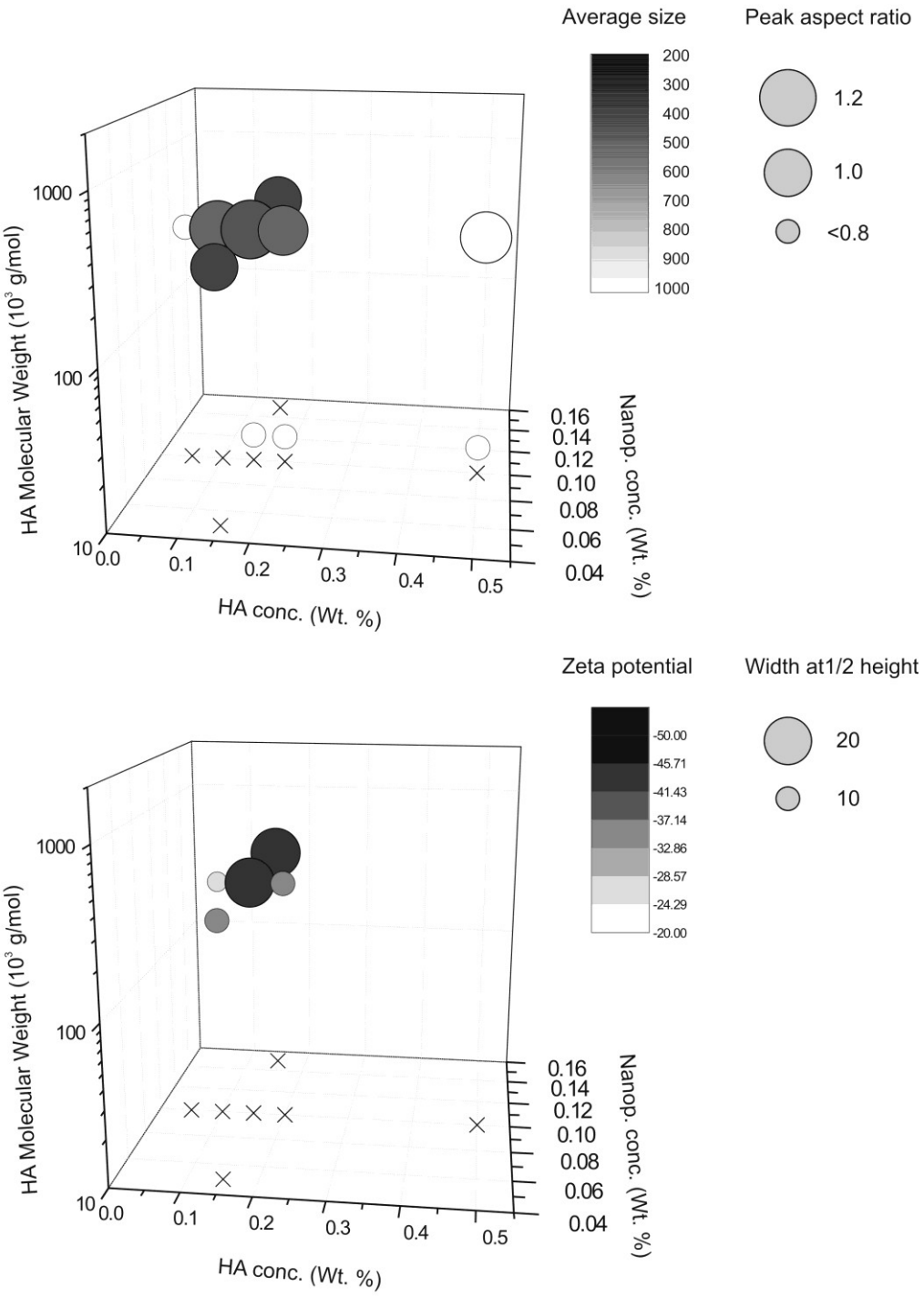

Figure 2-7. Average size and aspect ratio of the size distributions (top), average Zeta potential and width at half height for the Zeta potential distribution (bottom) as a function of nanoparticle and HA concentration. For an easier reading, the concentration values are highlighted with black crosses at the bottom of graphs

A morphological comparison of the three different kinds of nanoparticles through Atomic Force Microscopy (Figure 2-8) highlights a few important points:

- the dimensional difference between "large", "small" and HA- nanoparticles is real and not an artifact of the DLS analysis. It is noteworthy that the HA-coated nanoparticles, although each likely obtained through the agglomeration of few "small" ones, do not appear as clusters.
- all nanoparticles are soft and flatten when deposited on a solid surface. This is likely due to the low cross-link density.
- "Large" and HA-coated nanoparticles generally show some fracture lines as a consequence of drying, which suggests them to display a harder surface. "Small" nanoparticles appear to be always surrounded by a halo, which is barely visible in height images but more clear in phase images (not shown), indicating it to be very soft and thin; we interpret it as a "fuzzy" corona composed by tethered chitosan chains. Consistently with this hypothesis, the halo disappears after coating,

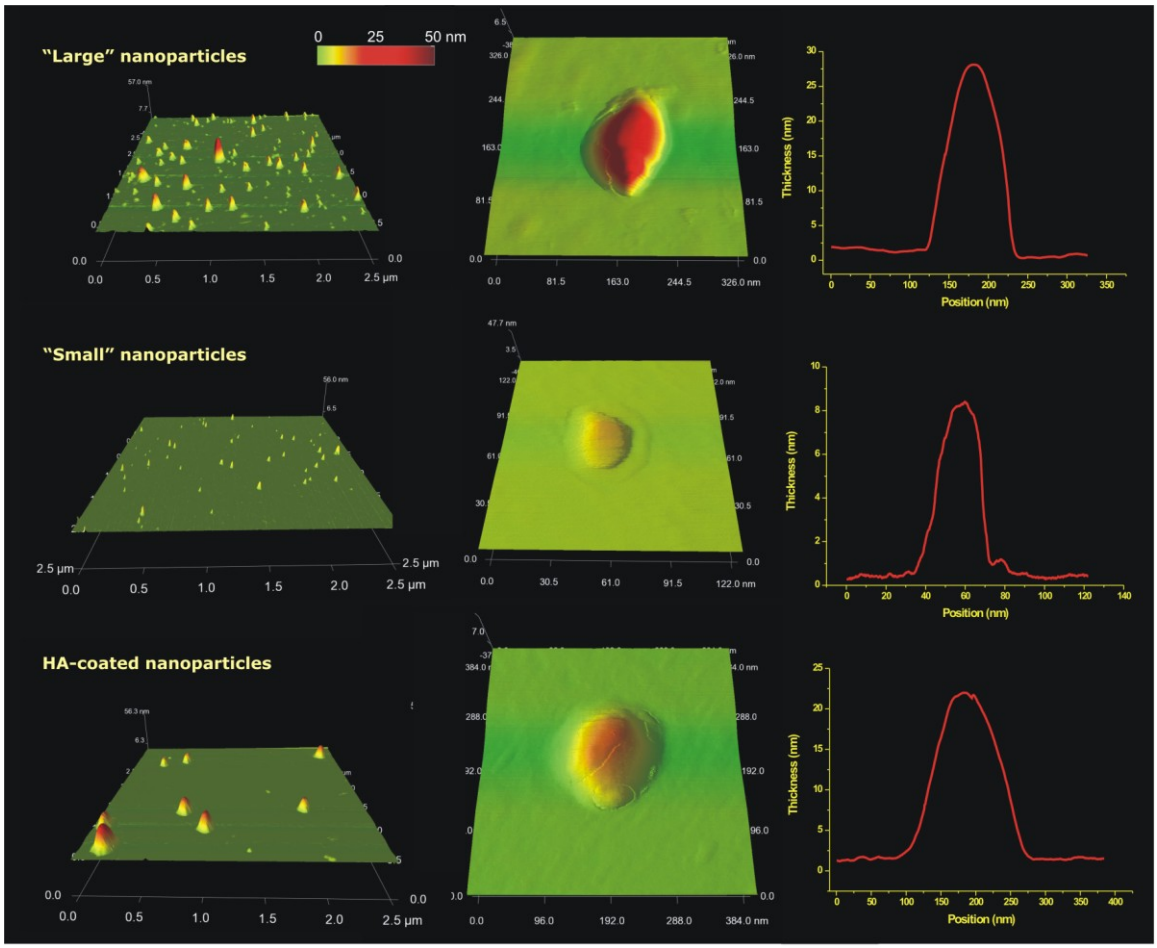

Figure 2-8. AFM analysis of the three different kinds of nanoparticles deposited on mica surfaces from dispersions in deionised water. The lower (left) or higher (centre) magnification pictures and the height scans along the median point of particles (right) highlight the larger dimensions of "large" and HA-coated nanoparticles compared to the "small" ones.

2.4.5 ssDNA loading tests

The nanoparticles with embedded ssDNAs did not show significant difference in sizes and zeta potentials compared with the blanks of plain nanoparticles (Table 2-2).

Table 2-2. DLS measurements, 1A = nanoparticles with ssDNA (MW = 5569 g/mol), 1B = nanoparticles with ssDNA (MW = 16004 g/mol), 1C1 = 1C2 = 1C3 = plain nanoparticles without ssDNA.

Sample name		Z-average	Z-potential	ssDNA MW (g/mol)
1A		323	+51.7	5569
1B		374	+48.5	16004
1C1 (blank)	1C	312	+53.3	=
1C2 (blank)		322	+43.2	=
1C3 (blank)		317	+49.9	=

The Figure 2-9 shows the UV/VIS spectra of the nanoparticles supernatants and of the ssDNAs blanks. There is no presence of absorbance of ssDNAs in the range of wavelength 240-290 nm in the supernatant of the sample of nanoparticles 1A and 1B, this imply that all the DNA, complexed with the chitosan nanoparticles, was removed with the precipitation of the nanoparticles; therefore it is presumed the 100% of loading. Furthermore, it was notice, from the spectra of the DNA blanks, a decrease in purity/integrity of the fragments after 24 hours of storage, especially in the ones that were besides sonicated; the major damage was in the fragments with high MW.

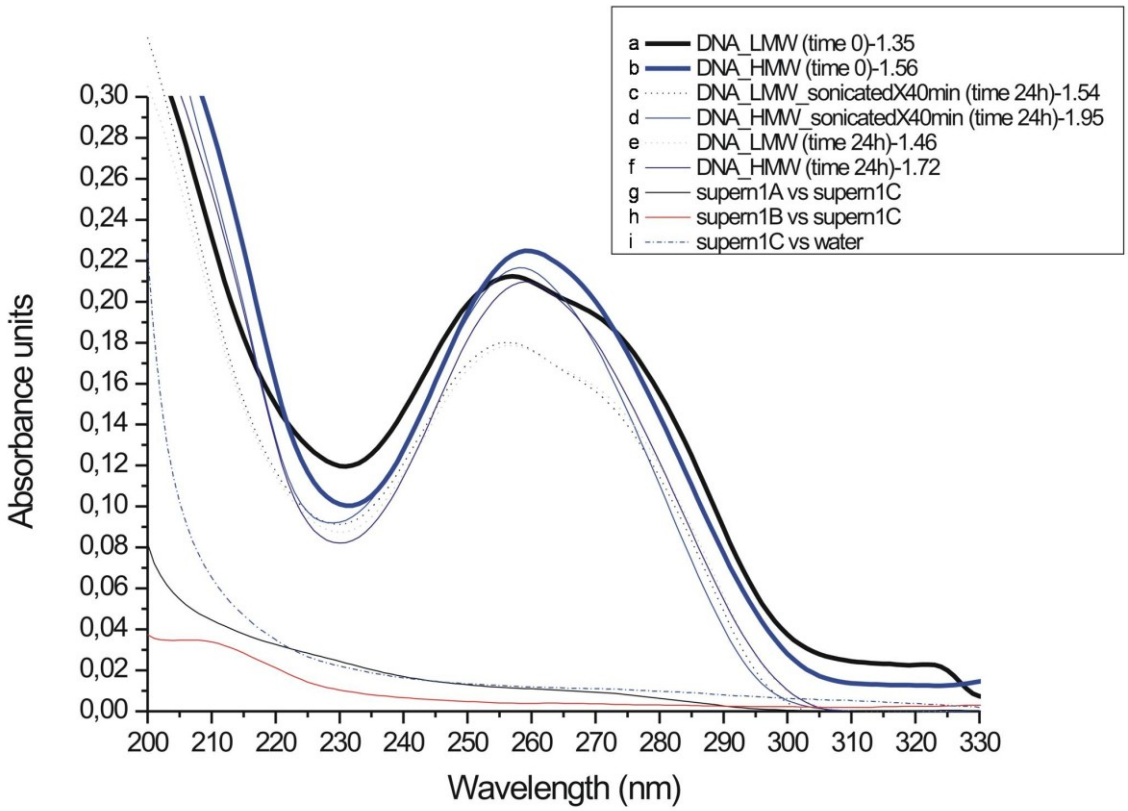

Figure 2-9. UV/VIS spectra (from the top to the bottom of the legend): "a" is the ssDNA spectra with MW 5569 g/mol in TPP solution at time 0; "b" is the ssDNA spectra with MW 16004 g/mol in TPP solution at time 0; "c" is the spectra of "a" sonicated for 40 minutes at time 0 and then checked after 24h; "d" is the spectra of "b" sonicated for 40 minutes at time 0 and then checked after 24h; "e" is the spectra of "a" after 24h; "f" is the spectra of "b" after 24h; "g" is the supernatant spectra of the sample 1A against 1C (blank without ssDNA); "h" is the supernatant spectra of the sample 1B against 1C (blank without ssDNA); "i" is the supernatant spectra of the sample 1C against double distilled water.
The numbers that are after the name in the legend (lines "a" to "f"), identify the grade of purity of the single strand DNAs (the value Abs_{260}/Abs_{280} must be in the range 1.3-1.5, however varying pH and ionic strength this value can increase till 2.0)[27].

In the future, a more reliable quantitation of DNA or RNA concentrations will be the use of fluorescent tags bound with the nucleic acids, and proceed with the detection of the fluorescence intensity; this method is much more accurate and cases of contaminants absorbing in the range 240-280 nm are efficiently avoided. The use of nuclease-free water during the experiments decreases the damage of DNA or RNA by the activity of the free nucleases in the environment.

2.4.6 Evaluation of nanoparticle cytotoxicity

Cytotoxicity was evaluated on two murine cell lines: J774 macrophages as a model for professional phagocytes[37-39] and L929 fibroblasts as a non-phagocytic and widely recommended reference cell line[40, 41]. Two methods were employed: the MTT (3-(4,5-dimethylthiazol-2-yl)-2,5-diphenyl tetrazolium bromide) assay to evaluate the effects that nanoparticles may have intracellularly on mitochondria and metabolic activity and determine IC50 values for the above nanoparticles, and a Live/Dead fluorimetric assay (calcein/propidium bromide) to assess not only cell death, but also possible non-lethal cell membrane damage, since the first site of interaction of nanoparticles is likely to be the cell membrane[31, 42]. The combination of these two different methods can provide hints about the *modus operandi* of the nanoparticle toxicity, since effects may appear at lower concentrations or shorter times than those recorded through the measurement of mitochondrial activity.

The results of the MTT assay (Figure 2-10) clearly show that

- for all nanoparticles and at any concentration, cytotoxicity was always higher for macrophages than for fibroblasts. Specifically, the decrease in viability recorded on fibroblasts is still small also at concentrations as high as to 2 mg/ml.

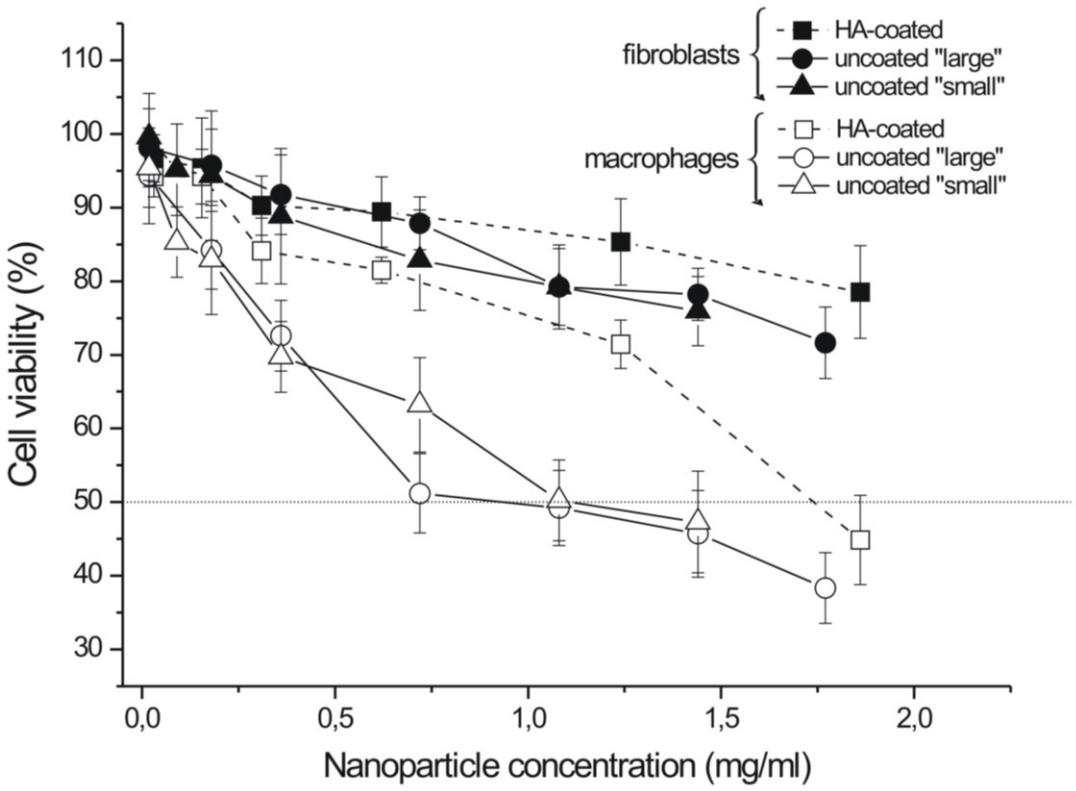

Figure 2-10. Cell viability (MTT assay) for L929 fibroblasts and J774 macrophages as a function of nanoparticle concentration at 37°C after 24 h exposure. Provided by Dr Noha Zaki.

- Using macrophages as a more sensitive model, it is also apparent that the uncoated, positively charged nanoparticles have higher cytotoxicity than the HA-coated ones. "Large" and "small" nanoparticles show IC50 values in between 0.7 - 1.0 mg/ml; although "small" nanoparticles often show higher cell viability than the "large" ones, the data offer no statistically significant difference. The HA-coated nanoparticles show a higher IC50 of about 1.8 mg/ml.

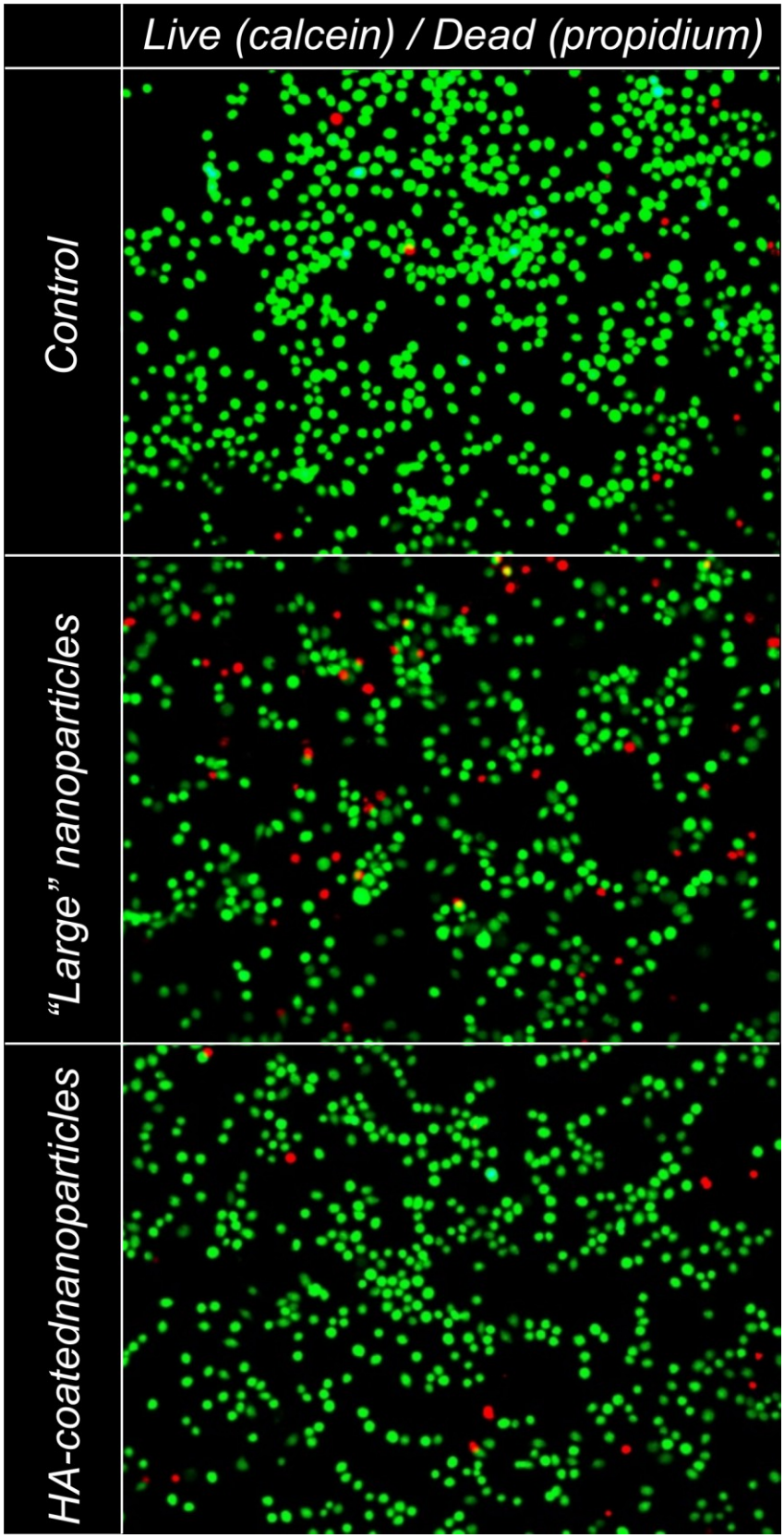

Figure 2-11. Fluorescence microscopy pictures (overlaid) of metabolically active (green) and membrane-damaged (red) cells. It is apparent that while pure culture media and 0.1 mg/mL HA-coated nanoparticles show both negligible toxic effects, a 0.1 mg/mL dispersion of the uncoated and positively charged "large" nanoparticles has a detrimental effect on the cell viability; interestingly, there is large number of

cells with reduced green fluorescence, but substantially no overlap between red and green-emitting cells. Provided by Dr Noha Zaki.

- The more benign character of the HA-coated nanoparticles is also revealed by the Live/Dead assay at concentrations where the MTT assay still indicates no significant decrease of viability (0.1 mg/mL). "Large" nanoparticles have a fraction of membrane-damaged cells which is considerably higher than for the HA-coated ones, which on its turn is almost undistinguishable from the control (Figure 2-11). It is noteworthy those red and green emissions are not co-localised and that there are a considerable number of cells with low green emission, but no red one. This is likely an indication that membrane damage, i.e. penetration of the red-emitting propidium iodide in the cell, takes place only after a sound decrease of the cell metabolic activity. Therefore, even when the nanoparticles are positively charged, they appear to have a toxic effect directly on metabolism rather than on membrane properties; a logical conclusion is that their cytotoxicity is mediated by their intracellular uptake, a finding corroborated by several literature reports[43, 44].

- The higher sensitivity of macrophages could therefore be due to their higher internalisation activity. This hypothesis is confirmed by conducting the experiments at 4°C, i.e. at a temperature where active endocytosis is substantially inhibited (Figure 2-12): the decrease in temperature increased the viability of macrophages at surely cytotoxic concentrations at 37°C.

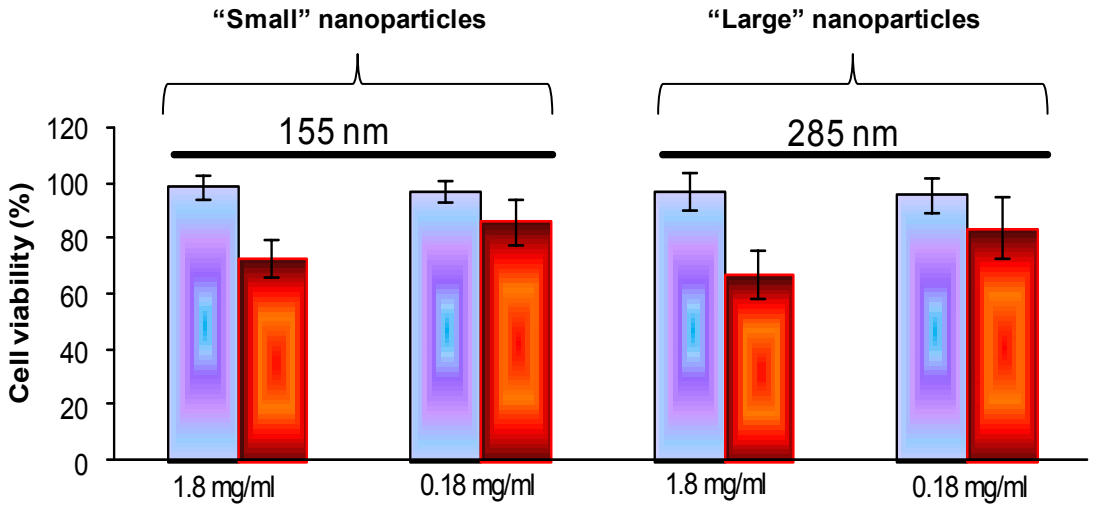

Figure 2-12. Comparison of the viability (MTT assay) of J774.2 macrophages after 4h exposure to uncoated chitosan/TPP nanoparticles at 4 (blue bars) and 37°C (red bars). It is apparent that, above all at

higher nanoparticle concentrations, toxic effects disappear at low temperature. Chitosan nanoparticles concentration were 1.8 mg/ml and 0.18 mg/ml (mean±sd, n=8)). Provided by Dr Noha Zaki.

Our data therefore suggest that the cytotoxicity of chitosan nanoparticles appears to be mostly dependent on their internalisation, which on its turn seems to be scarcely dependent on size and clearly dominated by surface composition/charge: indeed it is well known that positively charged nanoparticles are more quickly internalised than negatively charged ones, possibly utilising clathrin-mediated mechanisms[45], where, however, interactions with membrane-linked negatively charged GAGs may play a role too[46].

2.4.7 Nanoparticles uptake

The uptake was evaluated using Macrophages J774.2 and Fibroblasts L929 cells for both uncoated CSNPs and HA-coated CSNPs. Two methods were employed: the use of microscopy techniques by using confocal or fluorescent microscope and have qualitative data, and the micro-fluorimetric assay to obtain quantitative data.

Chitosan nanoparticles uptake. The cells were incubated with the nanoparticles for 30 minutes, and after several washings, the trypan blue was used to quench the signal of fluorescence outside the cellular membrane[35]. This was performed in order to distinguish between CS-NPs internalized and those adhering to the cellular membrane. The localization of CSNPs appears to be mainly in the cytoplasm (Fig. 2-13), this means that there is a potential for cytosolic delivery.

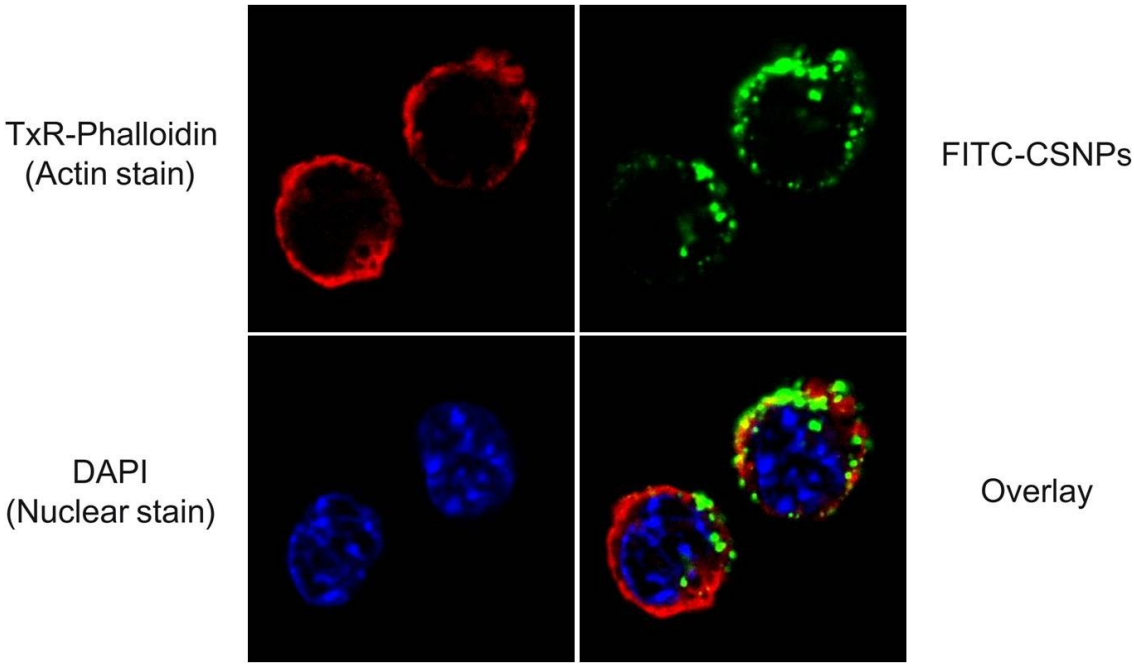

Figure 2-13. Localization of CS-NPs in the Macrophages J774.2. Images of the same cells taken sequentially with different value of excitations: on the top left the actin staining, on the top right the fluorescent nanoparticles, on the bottom left the nucleus staining and on the bottom right the overlay of all the three images. Provided by Dr Noha Zaki.

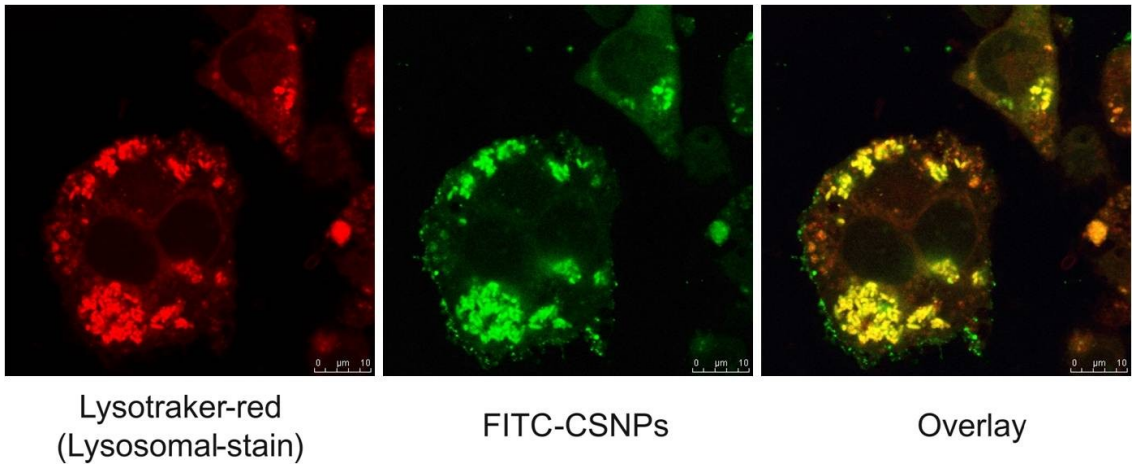

Figure 2-14. Effect of Bafilomycin A1. The Bafilomycin A1 is an inhibitor of vacuolar ATPase endosomal proton pumps and inhibits the acidification of vacuoles. The use of this inhibitor highlights the co-localization of the CSNPs in the endosomes and in the lysosomes preventing their endo-lysosomal escape. Provided by Dr Noha Zaki.

CS-NPs were internalized by Macrophages J774.2 in an energy-dependent endocytic process. This was indeed demonstrated when the cells, under effect of energy depletion by sodium azide or treated at a lower temperature, showed a diminution in uptake (Fig

2-15), and more exactly the decrease in internalization went down to 58% and 70% respect to the cells control.

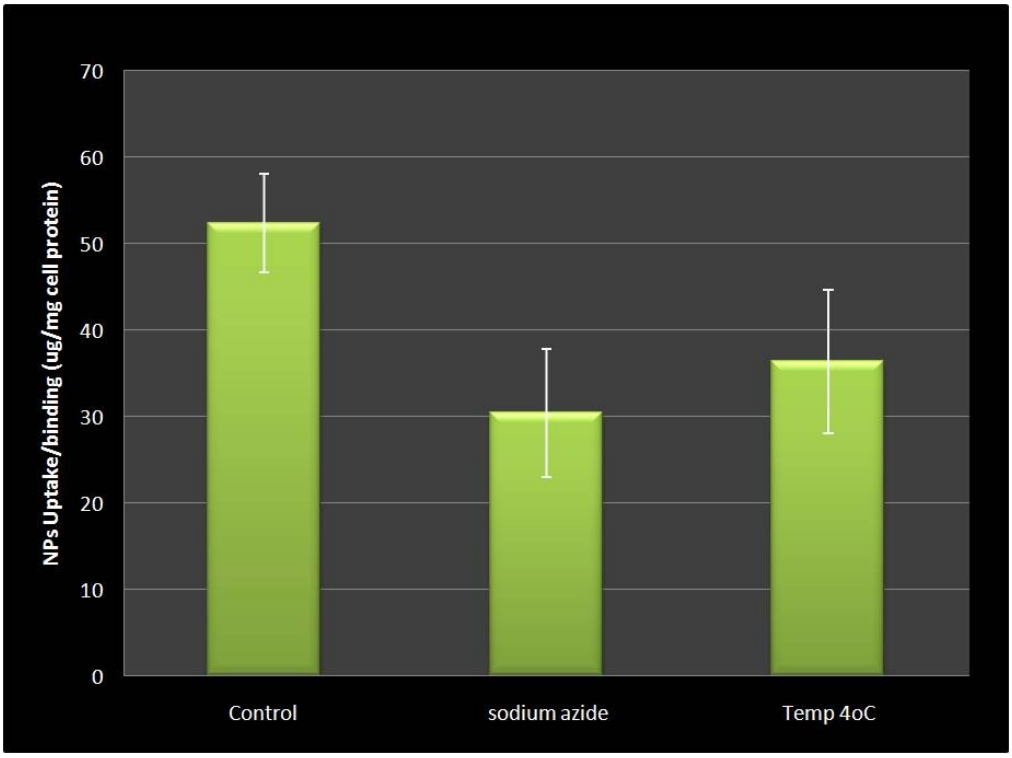

Figure 2-15. Effect of metabolic inhibitors on CS-NPs uptake by Macrophages J774.2. Provided by Dr Noha Zaki.

The mechanism of CSNPs uptake by Macrophages J774.2 was highlighted with a test that use several endocytosis effectors, objective is to discover, by exclusion, which system rules the internalization. The results were the followings (Fig. 2-16): the inhibition of endocytosis by caveola-coated pit by using filipin did not affect soundly the CSNPs uptake (+27% in comparison with the control); as well the use of Bafilomycin A1, a specific inhibitor of proton pumps in the endosomes, did not alter deeply the degree of internalization (+20%). Nocodazole and Cytochalasin D, respectively inhibitors of microtubules formation and of actin polymerization, slightly affect the internalization (-25% and -26%); moreover, a K^+ free buffer imply a diminution in cellular excitability with a decrease in nanoparticles uptake (-26%). Only the hypertonic growth medium reduces the cellular uptake drastically (-47%), consequently, it is evinced that the activity of the clathrin-coated pit has a central role in the CSNPs internalization.

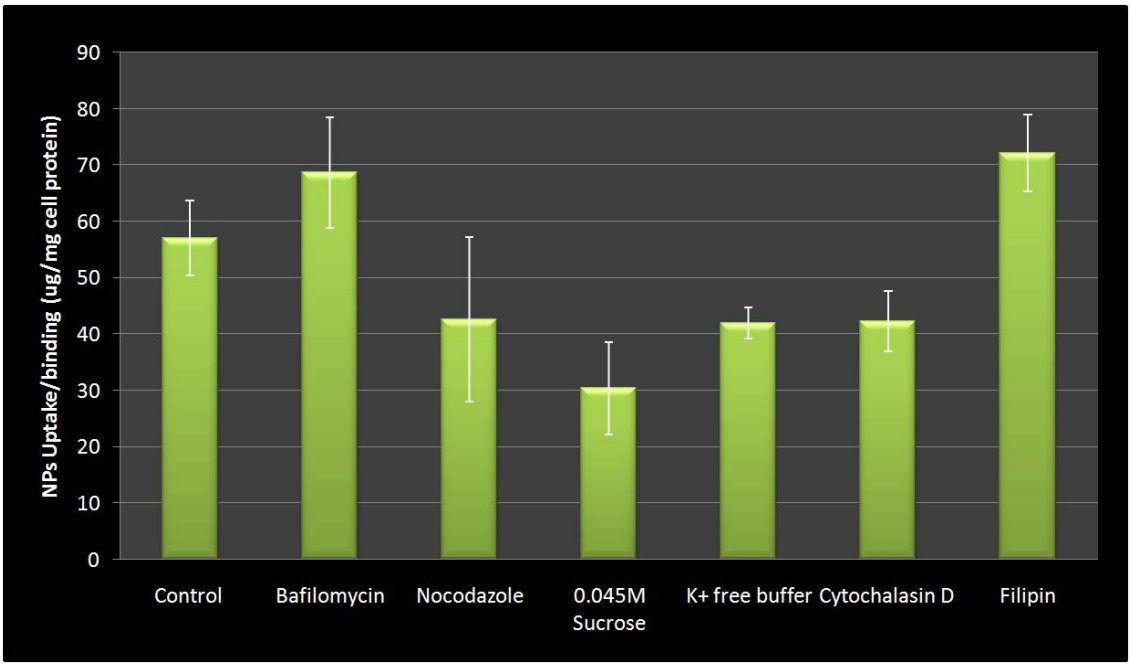

Figure 2-16. The uptake of uncoated CSNPs by Macrophages J774.2 was tested under different endocytosis effectors. Provided by Dr Noha Zaki.

HA-coated chitosan nanoparticles. The cells were incubated with the nanoparticles for 30 minutes, after the washings there was non need of trypan blue since the HA-CSNPs did not interact so strongly with the cellular membranes like the uncoated ones did. The images at the microscopes confirmed the localization of the nanoparticles in the cytoplasm (Fig. 2-17). The kinetic of HA-CSNPs uptake was evaluated taking images of Macrophages J774.2 cells in incubation at different time, it was observed that the HA-CSNPs uptake starts after 2 hours of incubation and appear to be biphasic (Fig. 2-18, 2-19, 2-20).

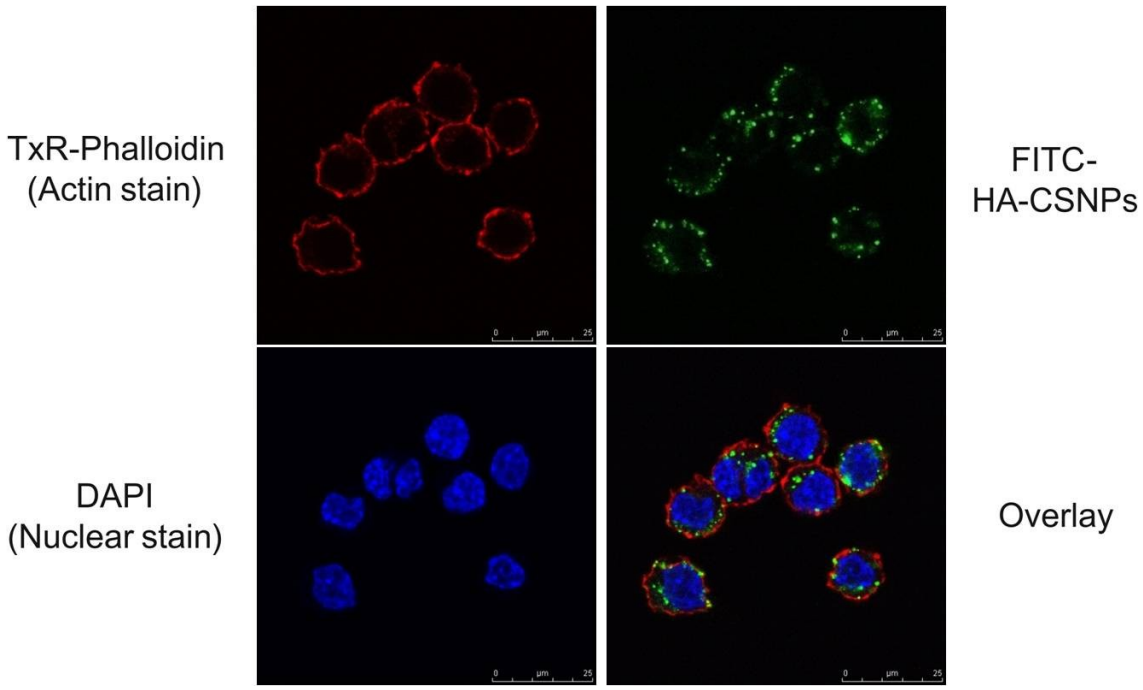

Figure 2-17. Localization of HA-coated CS-NPs in the Macrophages J774.2. Images of the same cells taken sequentially: on the top left the actin staining, on the top right the fluorescent nanoparticles, on the bottom left the nucleus staining and on the bottom right the overlay of all the three images. Provided by Dr Noha Zaki.

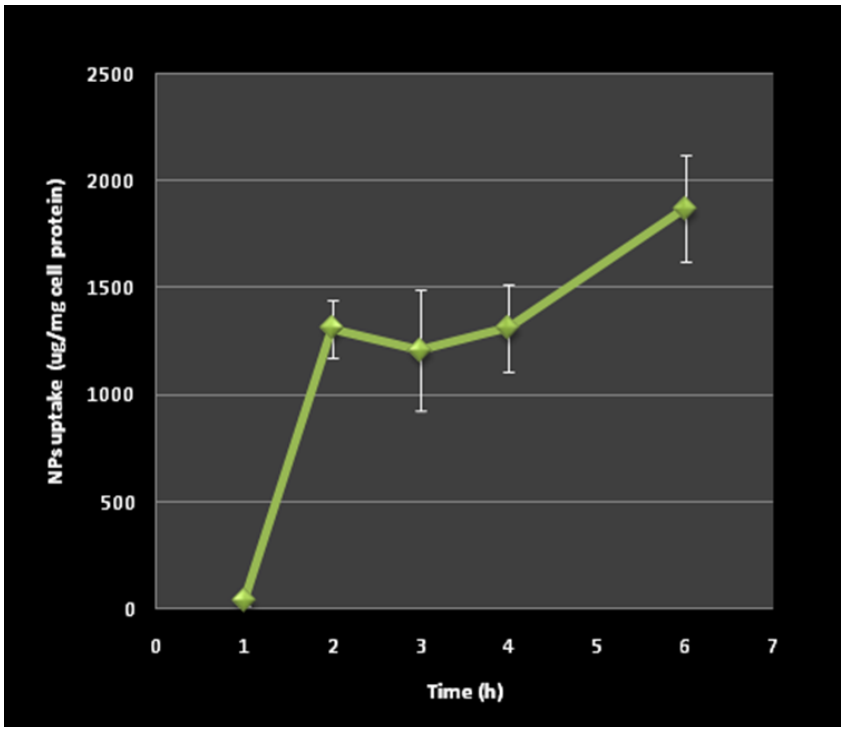

Figure 2-18. Time course of HA-coated CSNPs uptake (0.05mg/ml) by Macrophages J774.2 at 37°C. The HA-NPs were taken up after a lag period of 2h incubation. The type of uptake is biphasic. Provided by Dr Noha Zaki.

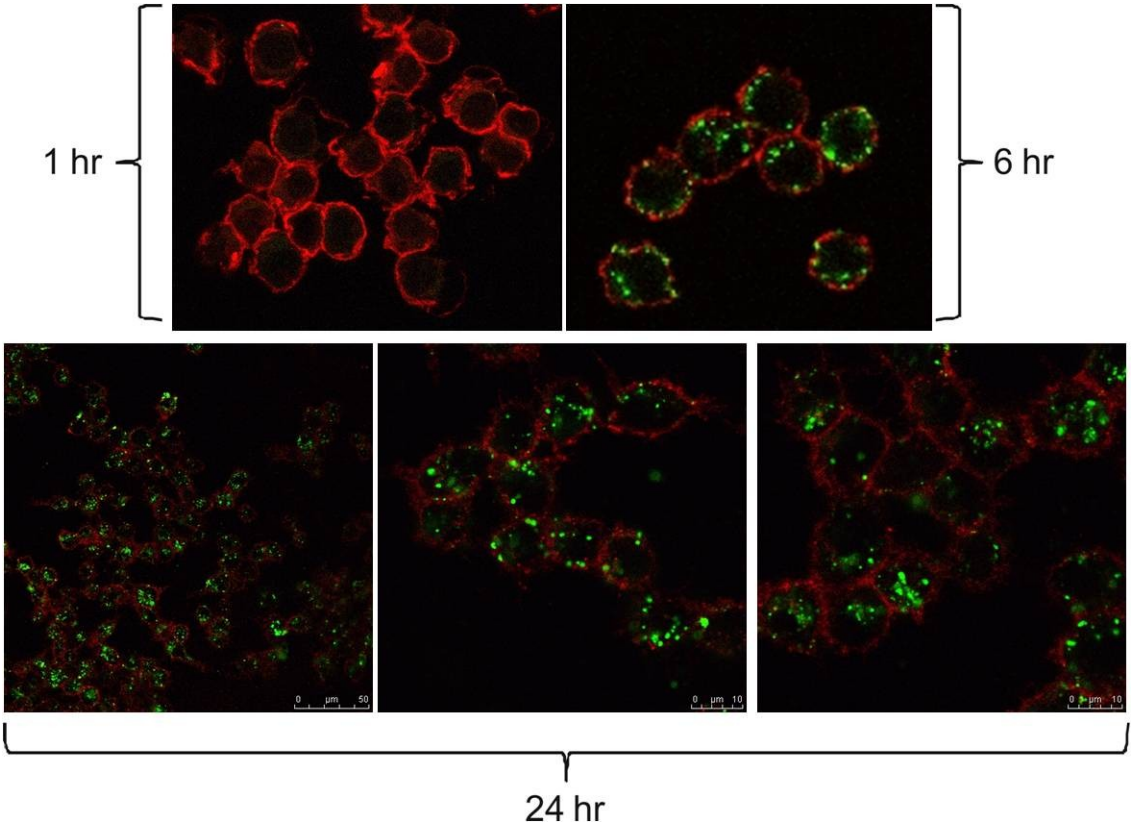

Figure 2-19. Kinetic of internalization of HA-coated CS-NPs in Macrophages J774.2. Provided by Dr Noha Zaki.

The mechanism of HA-CSNPs internalization was clarified, different endocytosis effectors were used for this purpose, thus to discover also in this case, like with the uncoated nanoparticles, which is the system that regulates the internalization (Fig. 2-21). The results showed that: the inhibition of microtubules formation by Nocodazole provoked a higher increase in nanoparticles uptake (+48%). The use a Filipin and Cytochalasin D did not bring sound differences (+5% and -24%), the caveola-coated pits were not involved and the blockage of actin polymerization did not hinder greatly the internalization.

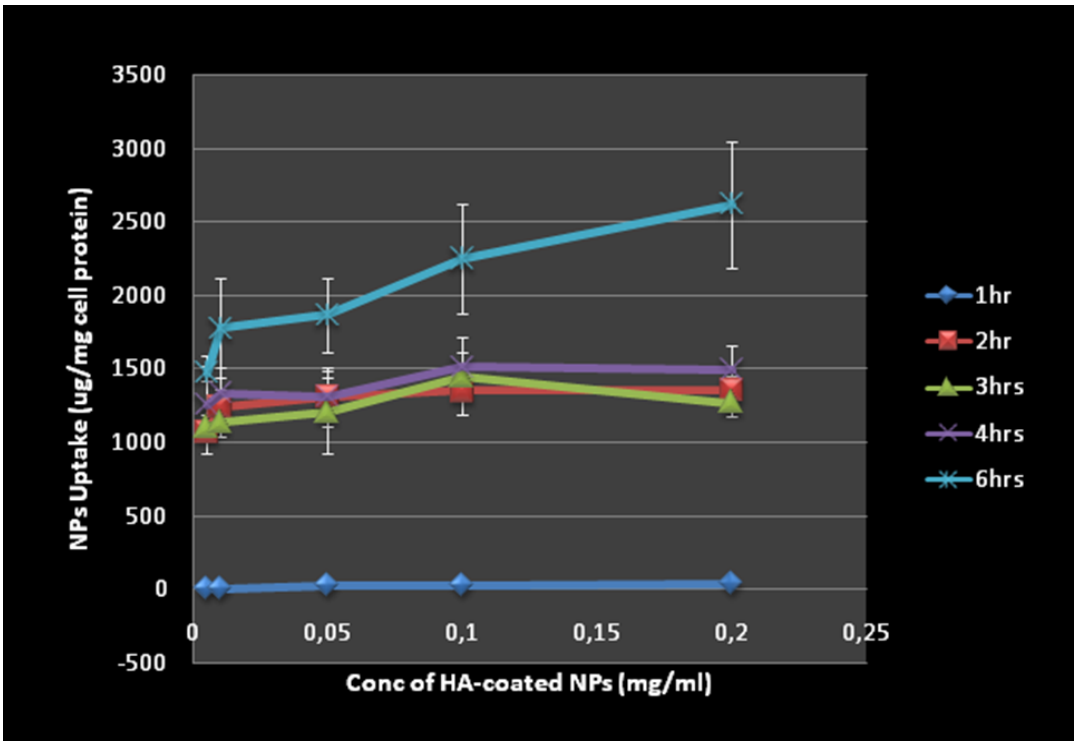

Figure 2-20. Effects in the uptake of HA-coated NPs. The sampling was performed at different concentrations and different time of incubation. The cellular uptake is carried out by Macrophages J774.2 at 37°C. It is noted that the uptake is time and concentration dependent; the differences in terms of concentration were highlighted after 6 hours of incubation. Provided by Dr Noha Zaki.

There was a strong decrease in the internalization (-41%) in the cells treated with Bafilomycin A1, the HA-coated nanoparticles had much difficulties in the escaping from the endosomes with the blockage of the proton pumps, the buffer effect of the nanoparticles was not implying the break out of the in the cytosol; possibly the low internalization it was justified because of the endosomes recycling and so the excretion of the nanoparticles from the cells. Similar to the uptake mechanism of the uncoated CSNPs, the main decrease in uptake (-46%), for the HA-coated nanoparticles, was due to the higher concentration of sucrose, the endocytosis is clathrin-dependent in this case too.

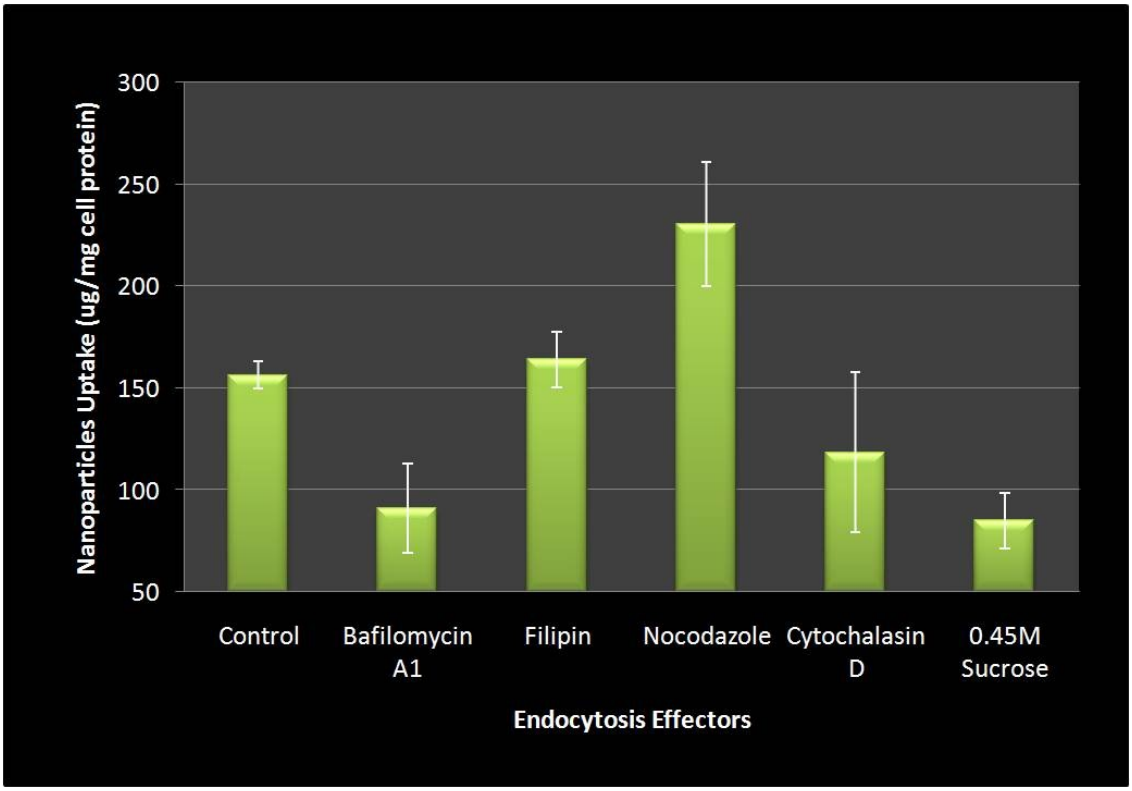

Figure 2-21. The uptake of HA-coated CSNPs by Macrophages J774.2 was tested under different endocytosis effectors. Provided by Dr Noha Zaki.

2.5 Conclusions

As a result of the application of a robust approach for the optimization of the method for the chitosan/TPP nanoparticle preparation, we have focused on "small" nanoparticles with a size ≤200 nm, which were later coated with hyaluronic acid (HA), and on "large" nanoparticles with a size 200-400 nm, which can be used as a control for the HA-coated ones, featuring analogous dimensions but different surface properties. The HA-coating markedly reduces the nanoparticle toxicity and increases the colloidal stability; the internalization of the HA-coated CSNPs is delayed respect to the uncoated ones (no cellular uptake before 2 hours), it is important to note that the lower cytotoxicity due to polysaccharidic coatings, demonstrated in the past for a number of nano-carriers, e.g. also dextran-coated nanoparticles[47], often corresponds to longer circulation times *in vivo*[48, 49].

2.6 Supporting information

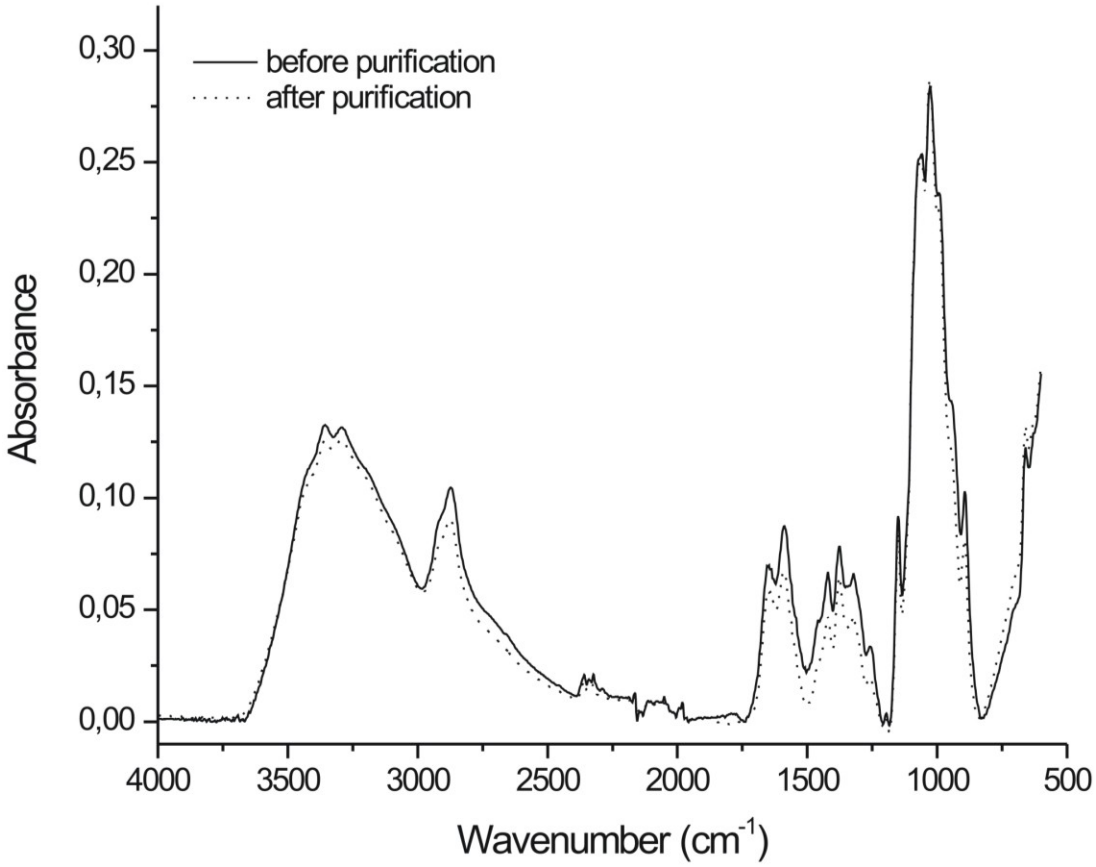

Figure 2-22. The IR spectra of chitosan before and after purification show a substantial overlap.

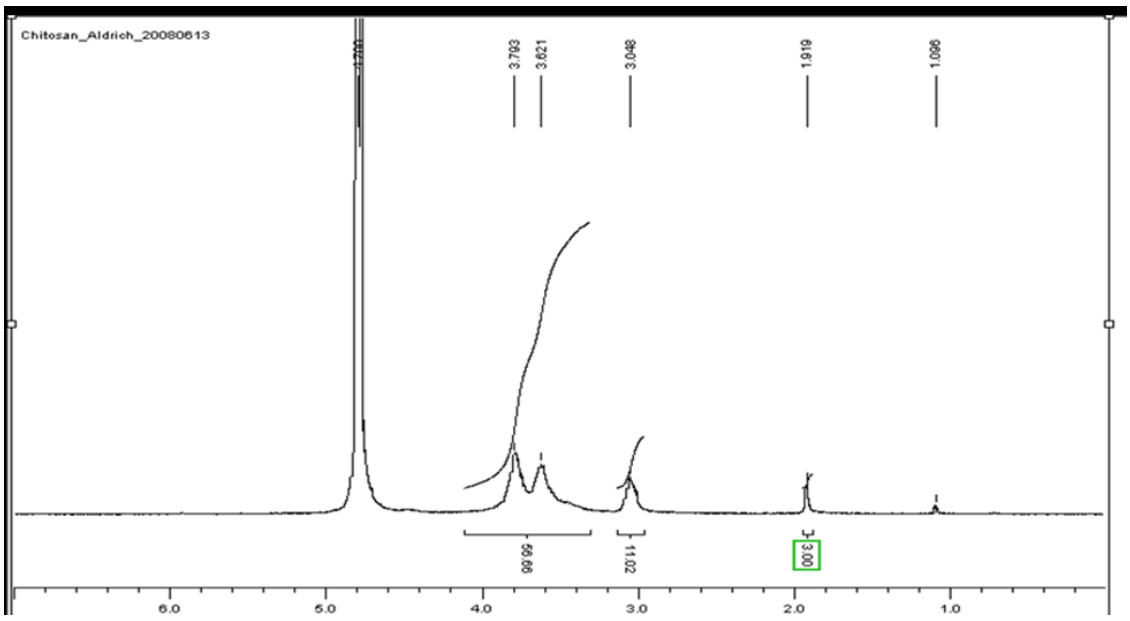

Figure 2-23. ^{1}H-NMR of chitosan (Aldrich) in 0.5 M DCl/D_2O before purification, %DD = 91.01%

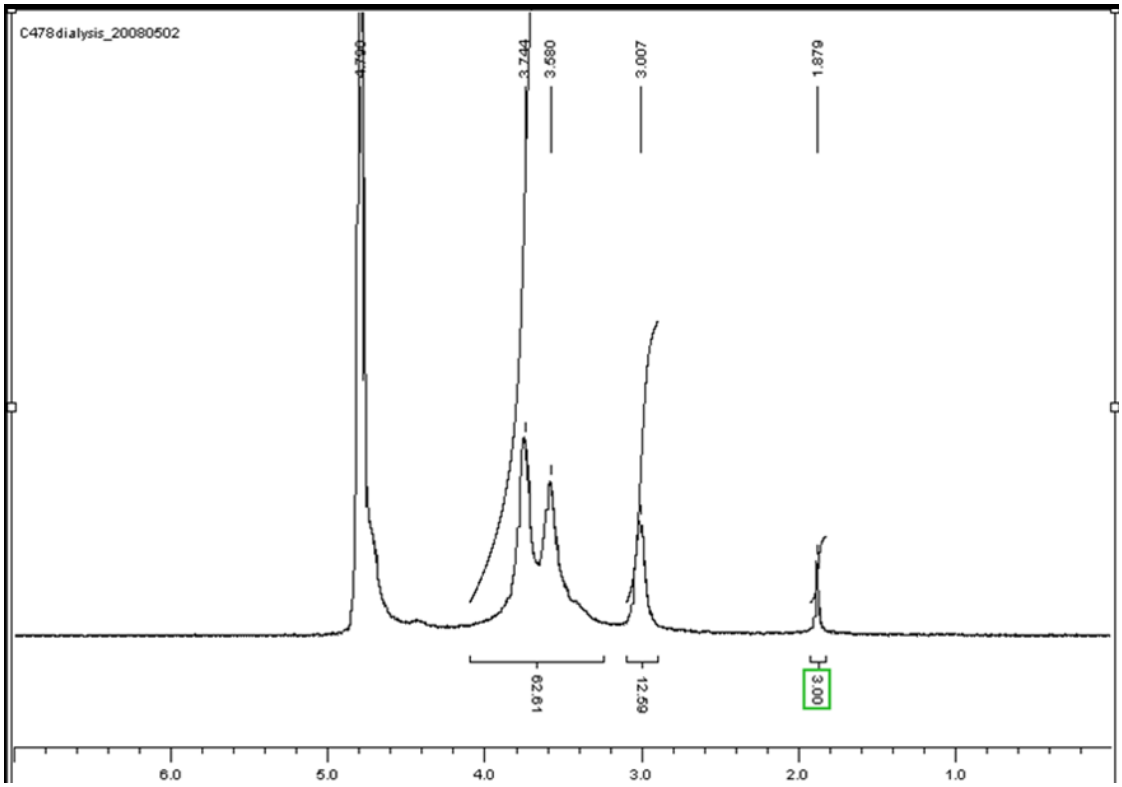

Figure 2-24. ^{1}H-NMR of purified chitosan in 0.5 M DCl/D_2O before purification, %DD = 92.02 %

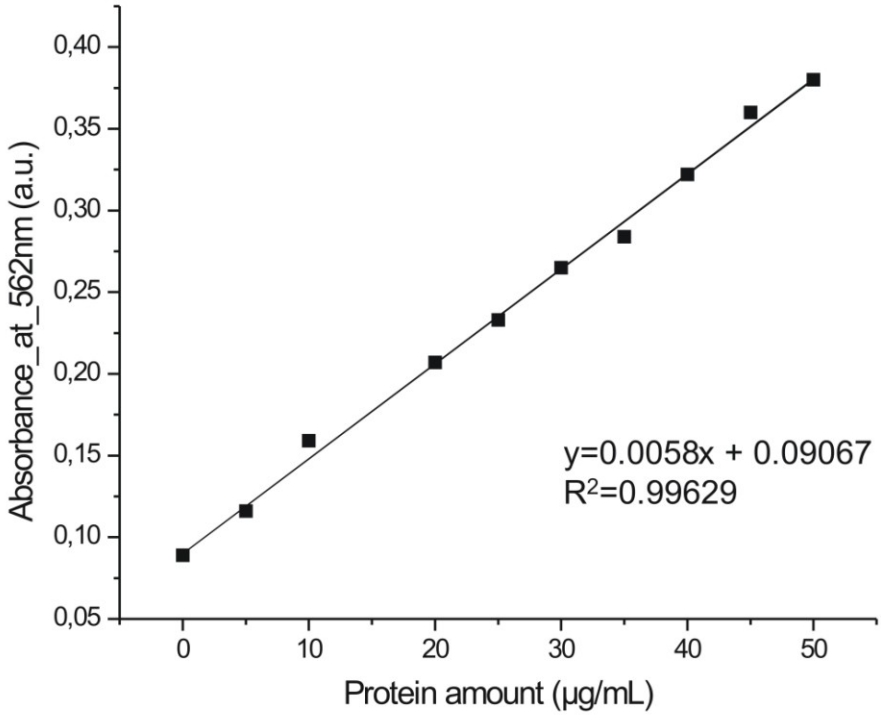

Figure 2-25. Standard curve for the protein determination assay.

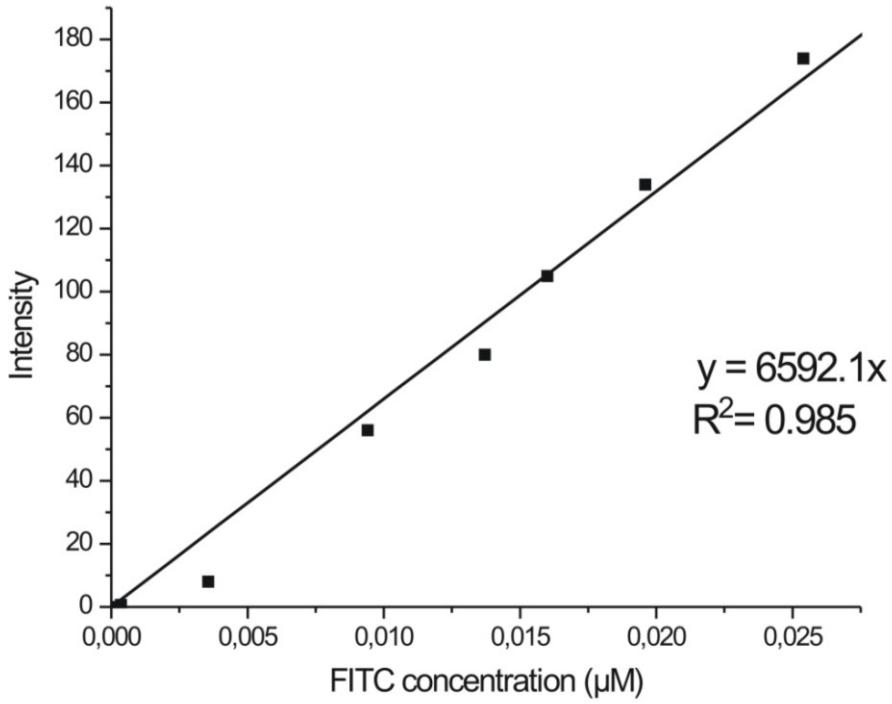

Figure 2-26. FITC calibration line. The dilutions were executed with 0.1M acetic acid.

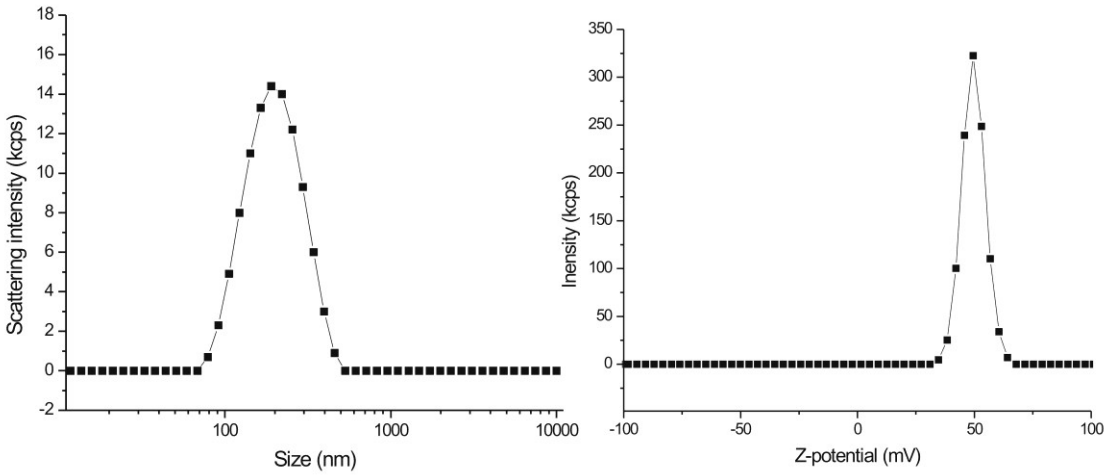

Figure 2-27. Size and Zeta potential distributions for "small" nanoparticles.

Table 2-3. Live/dead results for macrophages J77.4 cells

	Control	HA-coated NPs	"large" uncoated NPs
No. of damaged cells	10±4	13±5	48±6
Total No. of cells	342±12	330±11	320±14
Damaged cell fraction	0.036± 0.003	0.045±0.005	0.14±0.02**

References

1. Opalinska, J.B.A.M. Gewirtz, **2002**, Nucleic-acid therapeutics: Basic principles and recent applications. *Nature Reviews Drug Discovery*. 1(7): p. 503-514.
2. Leong, K.W., H.Q. Mao, V.L. Truong-Le, K. Roy, S.M. Walsh, and J.T. August, **1998**, DNA-polycation nanospheres as non-viral gene delivery vehicles. *Journal of Controlled Release*. 53(1-3): p. 183-193.
3. Tirelli, N., **2006**, (Bio)Responsive nanoparticles. *Current Opinion in Colloid & Interface Science*. 11(4): p. 210-216.
4. Rehor, A., J.A. Hubbell, and N. Tirelli, **2005**, Oxidation-sensitive polymeric nanoparticles. *Langmuir*. 21(1): p. 411-417.
5. Brannon-Peppas, L.J.O. Blanchette, **2004**, Nanoparticle and targeted systems for cancer therapy. *Advanced Drug Delivery Reviews*. 56(11): p. 1649-1659.
6. Vonarbourg, A., C. Passirani, P. Saulnier, and J.P. Benoit, **2006**, Parameters influencing the stealthiness of colloidal drug delivery systems. *Biomaterials*. 27(24): p. 4356-4373.
7. Allen, T.M., **1994**, The Use of Glycolipids and Hydrophilic Polymers in Avoiding Rapid Uptake of Liposomes by the Mononuclear Phagocyte System. *Advanced Drug Delivery Reviews*. 13(3): p. 285-309.
8. Moghimi, S.M., A.C. Hunter, and J.C. Murray, **2001**, Long-Circulating and Target-Specific Nanoparticles: Theory to Practice. 53(2): p. 283-318.
9. Senior, J.G. Gregoriadis, **1982**, Stability of Small Unilamellar Liposomes in Serum and Clearance from the Circulation - the Effect of the Phospholipid and Cholesterol Components. *Life Sciences*. 30(24): p. 2123-2136.
10. Passirani, C., G. Barratt, J.P. Devissaguet, and D. Labarre, **1998**, Long-circulating nanoparticles bearing heparin or dextran covalently bound to poly(methyl methacrylate). *Pharmaceutical Research*. 15(7): p. 1046-1050.
11. Higuchi, A., K. Shirano, M. Harashima, B.O. Yoon, M. Hara, M. Hattori, and K. Imamura, **2002**, Chemically modified polysulfone hollow fibers with

vinylpyrrolidone having improved blood compatibility. *Biomaterials*. 23(13): p. 2659-2666.

12. Mequanint, K., A. Patel, and D. Bezuidenhout, **2006**, Synthesis, swelling behavior, and biocompatibility of novel physically cross-linked polyurethane-block-poly(glycerol methacrylate) hydrogels. *Biomacromolecules*. 7(3): p. 883-891.
13. Lee, J.Y.A.P. Spicer, **2000**, Hyaluronan: a multifunctional, megaDalton, stealth molecule. *Current Opinion in Cell Biology*. 12(5): p. 581-586.
14. Zhang, Y., M. Yang, N.G. Portney, D. Cui, G. Budak, E. Ozbay, M. Ozkan, and C.S. Ozkan, **2008**, Zeta potential: a surface electrical characteristic to probe the interaction of nanoparticles with normal and cancer human breast epithelial cells. *Biomed Microdevices*. 10(2): p. 321-8.
15. Basarkar, A., D. Devineni, R. Palaniappan, and J. Singh, **2007**, Preparation, characterization, cytotoxicity and transfection efficiency of poly(dl-lactide-co-glycolide) and poly(dl-lactic acid) cationic nanoparticles for controlled delivery of plasmid DNA. *International Journal of Pharmaceutics*. 343(1-2): p. 247-254.
16. Rehor, A., H. Schmoekel, N. Tirelli, and J.A. Hubbell, **2008**, Functionalization of polysulfide nanoparticles and their performance as circulating carriers. *Biomaterials*. 29(12): p. 1958-1966.
17. Calvo, P., C. RemunanLopez, J.L. VilaJato, and M.J. Alonso, **1997**, Novel hydrophilic chitosan-polyethylene oxide nanoparticles as protein carriers. *Journal of Applied Polymer Science*. 63(1): p. 125-132.
18. Gan, Q.T. Wang, Chitosan nanoparticle as protein delivery carrier--Systematic examination of fabrication conditions for efficient loading and release. *Colloids and Surfaces B: Biointerfaces*. In Press, Corrected Proof.
19. Janes, K.A.M.J. Alonso, **2003**, Depolymerized chitosan nanoparticles for protein delivery: Preparation and characterization. *Journal of Applied Polymer Science*. 88(12): p. 2769-2776.
20. Katas, H.H.O. Alpar, **2006**, Development and characterisation of chitosan nanoparticles for siRNA delivery. *Journal of Controlled Release*. 115(2): p. 216-225.
21. Zhang, H., M. Oh, C. Allen, and E. Kumacheva, **2004**, Monodisperse chitosan nanoparticles for mucosal drug delivery. *Biomacromolecules*. 5(6): p. 2461-2468.

22. Xu, Y.M.Y.M. Du, **2003**, Effect of molecular structure of chitosan on protein delivery properties of chitosan nanoparticles. *International Journal of Pharmaceutics*. 250(1): p. 215-226.
23. Janes, K.A., M.P. Fresneau, A. Marazuela, A. Fabra, and M.J. Alonso, **2001**, Chitosan nanoparticles as delivery systems for doxorubicin. *Journal of Controlled Release*. 73(2-3): p. 255-267.
24. Gan, Q., T. Wang, C. Cochrane, and P. McCarron, **2005**, Modulation of surface charge, particle size and morphological properties of chitosan-TPP nanoparticles intended for gene delivery. *Colloids and Surfaces B: Biointerfaces*. 44(2-3): p. 65-73.
25. Lee, J.Y.A.P. Spicer, **2000**, Hyaluronan: a multifunctional, megaDalton, stealth molecule. *Current Opinion in Cell Biology*. 12: p. 581-586.
26. Kasaai, M.R., J. Arul, and C. Charlet, **2000**, Intrinsic viscosity-molecular weight relationship for chitosan. *Journal of Polymer Science Part B-Polymer Physics*. 38(19): p. 2591-2598.
27. Wilfinger, W.W., K. Mackey, and P. Chomczynski, **1997**, Effect of pH and ionic strength on the spectro-photometric assessment of nucleic acid purity. *Biotechniques*. 22(3): p. 474-&.
28. Mosmann, T., **1983**, Rapid colorimetric assay for cellular growth and survival: application to proliferation and cytotoxicity assays. *J Immunol Methods*. 65(1-2): p. 55-63.
29. Zange, R., Y. Li, and T. Kissel, **1998**, Biocompatibility testing of ABA triblock copolymers consisting of poly(-lactic-co-glycolic acid) A blocks attached to a central poly(ethylene oxide) B block under in vitro conditions using different L929 mouse fibroblasts cell culture models. *Journal of Controlled Release*. 56(1-3): p. 249-258.
30. He, X., J. Ma, A.E. Mercado, W. Xu, and E. Jabbari, **2008**, Cytotoxicity of Paclitaxel in Biodegradable Self-Assembled Core-Shell Poly(Lactide-Co-Glycolide Ethylene Oxide Fumarate) Nanoparticles. *Pharm Res*.
31. Fischer, D., Y. Li, B. Ahlemeyer, J. Krieglstein, and T. Kissel, **2003**, In vitro cytotoxicity testing of polycations: influence of polymer structure on cell viability and hemolysis. *Biomaterials*. 24(7): p. 1121-1131.

32. Zhang, Z., S. Huey Lee, and S.S. Feng, **2007**, Folate-decorated poly(lactide-co-glycolide)-vitamin E TPGS nanoparticles for targeted drug delivery. *Biomaterials*. 28(10): p. 1889-99.
33. Alonso, J.L., S. Mascellaro, Y. Moreno, M.A. Ferrus, and J. Hernandez, **2002**, Double-staining method for differentiation of morphological changes and membrane integrity of Campylobacter coli cells. *Appl Environ Microbiol*. 68(10): p. 5151-4.
34. Valea, F.A., S. Haskill, D.H. Moore, and W.C. Fowler, Jr., **1995**, Immunohistochemical analysis of alpha 1-integrins in cervical cancer. *Am J Obstet Gynecol*. 173(3 Pt 1): p. 808-13.
35. Wan, C.P., C.S. Park, and B.H.S. Lau, **1993**, A Rapid and Simple Microfluorometric Phagocytosis Assay. *Journal of Immunological Methods*. 162(1): p. 1-7.
36. Du, H., R.C.A. Fuh, J.Z. Li, L.A. Corkan, and J.S. Lindsey, **1998**, PhotochemCAD: A computer-aided design and research tool in photochemistry. *Photochemistry and Photobiology*. 68(2): p. 141-142. http://omlc.ogi.edu/spectra/PhotochemCAD/html/dapi(H2O).html.
37. Green, T.R., J. Fisher, M. Stone, B.M. Wroblewski, and E. Ingham, **1998**, Polyethylene particles of a [`]critical size' are necessary for the induction of cytokines by macrophages in vitro. *Biomaterials*. 19(24): p. 2297-2302.
38. Olivier, V., C. Rivière, M. Hindié, J.L. Duval, G. Bomila-Koradjim, and M.D. Nagel, **2004**, Uptake of polystyrene beads bearing functional groups by macrophages and fibroblasts. *Colloids and Surfaces B: Biointerfaces*. 33(1): p. 23-31.
39. Zahr, A.S., C.A. Davis, and M.V. Pishko, **2006**, Macrophage uptake of core-shell nanoparticles surface modified with poly(ethylene glycol). *Langmuir*. 22(19): p. 8178-85.
40. **1992**, Biological evaluation for medical devices-part 5: tests for cytotoxicity: in vitro methods. *ISO 10993-5 (EN 30993-5),*.
41. UnitedStates Pharmacopoe XXIII, **1995**.
42. Jepson, M.A., **2005**, Advances in fluorescence imaging: opportunities for pharmaceutical science. *Advanced Drug Delivery Reviews*. 57(1): p. 1-4.

43. Huang, M., E. Khor, and L.Y. Lim, **2004**, Uptake and cytotoxicity of chitosan molecules and nanoparticles: effects of molecular weight and degree of deacetylation. *Pharm Res*. 21(2): p. 344-53.
44. Ma, Z.S.L.Y. Lim, **2003**, Uptake of chitosan and associated insulin in Caco-2 cell monolayers: a comparison between chitosan molecules and chitosan nanoparticles. *Pharm Res*. 20(11): p. 1812-9.
45. Harush-Frenkel, O., N. Debotton, S. Benita, and Y. Altschuler, **2007**, Targeting of nanoparticles to the clathrin-mediated endocytic pathway. *Biochem Biophys Res Commun*. 353(1): p. 26-32.
46. Ruponen, M., P. Honkakoski, M. Tammi, and A. Urtti, **2004**, Cell-surface glycosaminoglycans inhibit cation-mediated gene transfer. *J Gene Med*. 6(4): p. 405-14.
47. Lemarchand, C., R. Gref, C. Passirani, E. Garcion, B. Petri, R. Muller, D. Costantini, and P. Couvreur, **2006**, Influence of polysaccharide coating on the interactions of nanoparticles with biological systems. *Biomaterials*. 27(1): p. 108-18.
48. Peer, D.R. Margalit, **2004**, Loading mitomycin C inside long circulating hyaluronan targeted nano-liposomes increases its antitumor activity in three mice tumor models. *International Journal of Cancer*. 108(5): p. 780-789.
49. Lemarchand, C., R. Gref, and P. Couvreur, **2004**, Polysaccharide-decorated nanoparticles. *European Journal of Pharmaceutics and Biopharmaceutics*. 58(2): p. 327-341.

Chapter 3

Chitosan/TPP microparticles

3 Chitosan/TPP microparticles

3.1 Summary

The production of chitosan-based matrixes, or microparticles by ionotropic gelation with sodium triphosphate was abundantly studied[1-3]; the need for an efficient production of monodisperse micro-beads in a sterile condition, the possibility to have high percentage of loading without waste and the opportunity to scale up the production without use large amount of materials, makes of the Inotech® encapsulator one of the best device for the entrapment of biomolecules, cells, proteins and others actives for medical, cosmetic, agricultural or food purposes.

This work was focused on the use of this device combined with the ionotropic gelation technique, thereby the use of chitosan and its counterpart sodium triphosphate. Chemical parameters and instrumental constraints were optimized in order to obtain the best kinetic of complexation and the best physical conditions for the production of the microparticles. Solely one group[4] worked on the production of chitosan-based microparticles using the Inotech encapsulator, and however they fabricate these by simple precipitation without the use of complexant agent like sodium triphosphate. It is for this reason that is important to focus on the potentiality of chitosan in the immobilization of actives principles and investigate the main properties of the beads.

3.2 Introduction

The preference of a material for the microparticles formation is determined depending on the purposes. In medical application, the low toxicity of a substance is the most important parameter followed by the efficiency in the mechanical properties. Concerning the delivery of an active principle, the transport capacity and the shape are factors to optimize.

In the last twenty five years the production of chitosan-based microparticles has been a target in many fields, from the treatment and purification of the water waste to the food and medical applications. Focusing on this last function, the production of non toxic beads can be exploited and optimised for intestinal or topical drug delivery, these should have a satisfactory mechanical properties and an efficient loading and controlled release. A zero order release is the optimal trend for pharmacokinetics purposes, indeed

a constant concentration, compared to a sudden rise or fall of actives in the blood or in the tissues, is preferable in order to avoid side effects.

Factors influencing the diffusion of a solute in a polymer matrix are various: chain mobility, degree of entanglement, crosslinking density, degree of swelling, crystallinity, porosity, and interaction between the solutes and the matrix[5]. The diffusion depends on the solute size, on the mesh created by the polymer chains and the relaxational behaviour of the network. Modulating the degree of crosslinking of a polymer matrix, the release of an active principle with a fixed molecular size can be regulated.

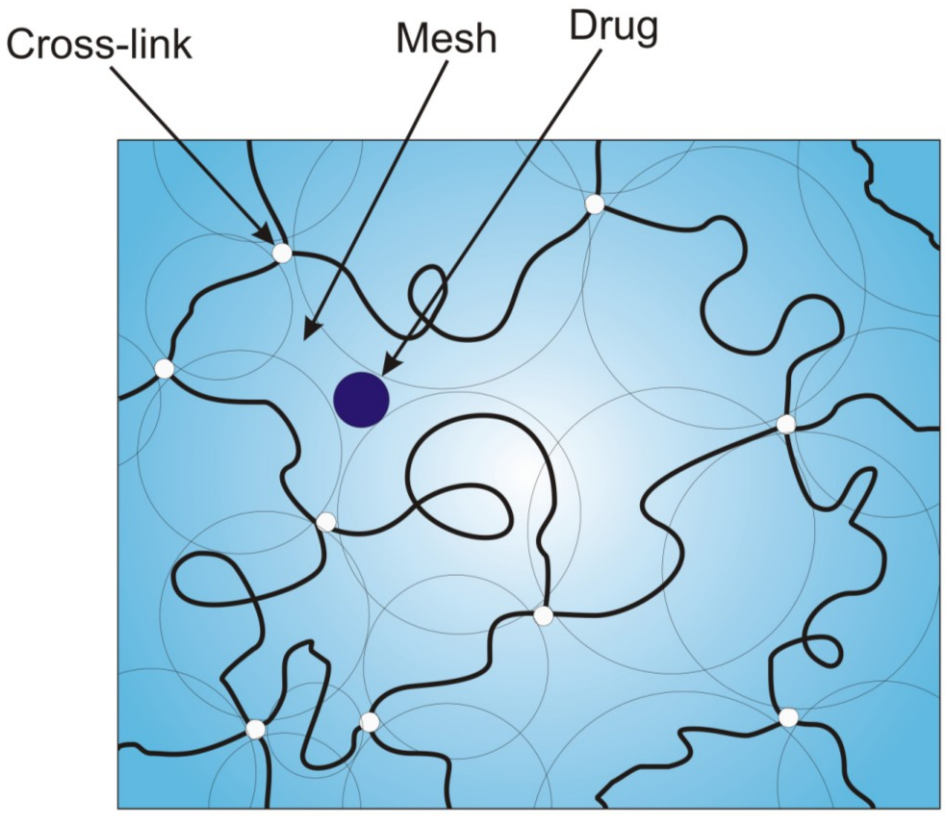

Figure 3-1. An example of crosslinked polymeric matrix; the circles are "blobs", a term coined by de Gennes[6], it is a concept used to explain the free movement of chain segment. The mesh size ξ is the empty parts not overlapped by the blobs (inspired by de Gennes *et al* [6]).

3.2.1 Chitosan-TPP microparticles

The chitosan can be used for microparticles production, the use of the biopolymer gives the prospect to modulate the pore size, the diffusional, the loading properties and the degree of swelling of the beads varying the concentrations, pH, ionic strength and dissolution medium[2, 7]. It is also known that the intermolecular linkages are in larger

numbers with the increase in molecular weight but the shrinking and the porosity of the microparticles depend deeply on the method of drying[2]. Moreover, the degree of linkages influences the release and diffusion of molecules[8] and the degree of hydration of the matrixes[5]. The diffusion of molecules, the ones that do not have interactions with the matrix network, is ruled by the Fick's law[9, 10]; the flux of molecules goes from a more concentrated area to a less concentrated, the magnitude is proportional to the concentration gradient:

$$J = -D\frac{\partial \varphi}{\partial x} \quad \text{(I);}$$

where J is the diffusion flux, D is the diffusion coefficient, φ is the concentration in moles/m^3 and x is the position of the molecules.

3.2.2 Techniques of production of microparticles

The production of microparticles chitosan-based can be processed by using several techniques:

- **physical gelation.** Molecules or polymer with opposite charges simply complex by ionotropic forces, the most used polyanions were sodium triphosphate (TPP)[11], alginate[12], pectin[13] and similar molecules;
- **complex coacervation** consists in the preparation of a solution with three immiscible phases, one with the core material, a coating material and a solvent. The coating will deposit around the core material in the moment when a change of parameter happen, that could be temperature, pH or ionic strength[14-16];
- **spray drying** is a technique which allow the production of dry powders or agglomerates from raw excipients and drugs in form of suspensions or solutions; this technique need the presence of a crosslinking agent like glutaraldehyde or formaldehyde[17];
- **emulsification/solvent evaporation** is a method that use a double emulsion in order to maintain monodisperse the particles and work at the same time with hydrophobic polymers[18].

The first two methods provide extremely mild and safe conditions; physical gelation is the chosen method to be used with the available equipment, the Inotech® encapsulator.

3.2.3 Jet break-up technology

The encapsulator IE-50 R can be used for the biopolymer encapsulation of microbial, animal, plant cells or other pharmaceuticals and biomolecules. The vibration technology is a powerful tool to obtain reproducible control of bead formation, sterile conditions of application and possibility to scale-up in production lines[19]. The bead formation technique is possible since a laminar liquid flow can be broken in uniform droplets and gelify in beads once they are in a hardening bath.

The instability of liquid jets was initially studied by Rayleigh[20]; he demonstrates that the frequency for the production of stable droplets was related with the jet velocity and to the nozzle diameter; then Weber[21] expanded the Rayleigh construct including a relation between an optimal wavelength for the jet break-up formation and the rheological characteristics of the extruded solution (II, III):

$$\lambda_{opt} = \pi\sqrt{2}d_N\sqrt{1+\frac{3\eta}{\sqrt{\rho\sigma d_N}}} \qquad \text{(II)}$$

$$\lambda = \frac{v_J}{f} \qquad \text{(III)},$$

moreover Branderberger and Widmer[22] showed the correlation between the droplet diameter d_D with wavelength and jet diameter (IV):

$$d_D = \sqrt[3]{1.5 d_J^2 \lambda_{opt}} \qquad \text{(IV)};$$

λ is the wavelength, v_J is the jet velocity, f the frequency, λ_{opt} is the optimal wavelength, d_N is the diameter of the nozzle, η is the dynamic viscosity, ρ is the density and σ is the surface tension.

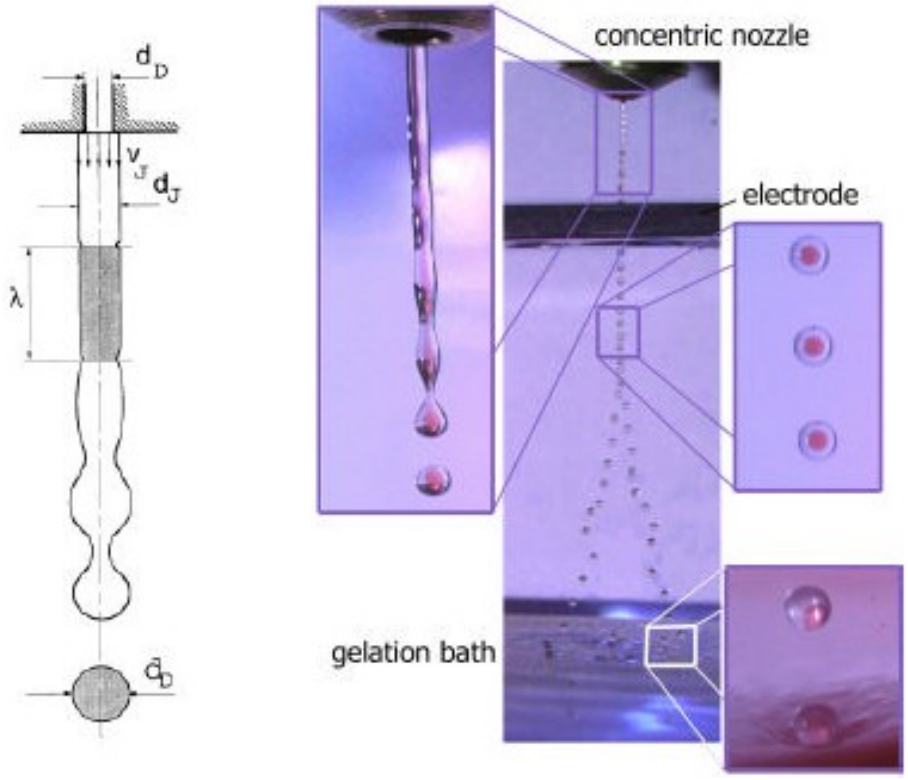

Figure 3-2. Droplet formation using a vibrating nozzle; the images on the right, precisely, are droplets formed by two immiscible solutions (adapted from Heinzen *et al* [19]).

3.3 Experimental section

3.3.1 Materials

Pentasodium triphosphate (Fluka), 1N hydrochloric acid, 1N sodium hydroxide (Aldrich), glacial acetic acid (VWR BDH Chemicals), sodium chloride (VWR BDH Chemicals), polysorbate 20 (Tween 20), fluorescein isothiocyanate-dextran 500000 (FITC-dextran) (Fluka) and, 98% sulfuric acid (Fisons Scientific Equipment) were used as received. Chitosan ("low MW": Cat. No. 448869, Aldrich) was used after purification as described in the paragraph 2.3.3. Chitosan, low molecular weight (Aldrich) was used after purification. Double distilled Milli-Q water was produced using in series an ELGA Docking Vessels DV35 and a Milli-Q Gradient A10 System.

3.3.2 Physicochemical characterisation

The chitosan microparticles were produced using an Inotech encapsulator IE-50 R (Fig. 3-1). It was equipped with a pulsation unit and a nozzle that allows the formation of the jet break-up, essential for the beads formation. The encapsulator could be equipped with two different nozzles, one with an overture of 300 and the other one of 200 micron.

Two microscopes were used to assess the shape and the dimension of the microparticles: the inverted microscope Olympus CKX41, equipped with a tilting and trinocular head options and a pre-aligned phase contrast slider that has an alternative annulus for 4x magnification, and a bright field position; the stereo-microscope Olympus SZ61, equipped with two separate eyepieces in order to observe the tridimensionality of the objects. The digital camera Olympus DP12-2 was used to record the images of the microparticles. ImageJ was the program used to process the images recorded with the digital camera. A Perkin Elmer LS55 luminescence spectrometer was used to detect fluorescence in the release tests.

Figure 3-3. Inotech® encapsulator IE-50 R.

3.3.3 Preparation of chitosan-TPP microparticles by ionotropic gelation

The purified chitosan was dissolved in a 0.1M HCl solution and left in stirring for 2 hours; several solutions were prepared at different concentrations. The pH was corrected with 1N NaOH to the wanted values. Separately, the TPP was dissolved in Milli-Q water and the pH corrected to the wanted values using 1N HCl. The ionic strength was buffered to 0.15M with NaCl, in both chitosan and TPP solutions, in all the experiments.

For all the tests, the chitosan solution was placed in a syringe connected with the encapsulator and the TPP solution was placed as a hardening bath under the vibrating nozzle. Chitosan solution was extruded through the nozzle (200 or 300 μm in diameter) and was broken down into homogeneous droplets that gel in contact with the stirred hardening bath (Fig. 3-2). The lateral amplitude of the nozzle was fixed to 7, in the apparatus the possible values range between 1 and 7. The electrostatic charge was applied in order to spread the drops and avoid drop coalescence after the ejection from the nozzle, in this way the jet-break up was improved. Additionally, the distance between the nozzle and the bath was an important parameter which was optimized. The parameters and their range are shown in table 3-1.

Once the microparticles were produced, they were drained and size and shape were evaluated with the microscopes.

Table 3-1. Parameters under investigation during the experiments

Parameter	Meaning	Range
Nozzle	Aperture size	200, 300 μm
Frequency	Frequency of the vibration of the nozzle	800-1200 Hz
Amplitude	Amplitude of lateral vibration of the nozzle	7
Pump	Polymer pumping rate	0.076-2.310 g/sec
Height	Distance between the nozzle and the hardening bath	29.5 cm
Charge	Electrostatic charge applied to the jet break-up	0.76-2.31 kV
[CS]	Chitosan concentrations	0.5, 1.0, 1.5, 2.0 %w/v
[TPP]	TPP concentrations	1.25, 2.50, 3.68, 5.00 %w/v
CS pH	Chitosan pH value	2, 4, 5, 5.5, 6
TPP pH	TPP pH value	4, 5, 5.5, 6, 7

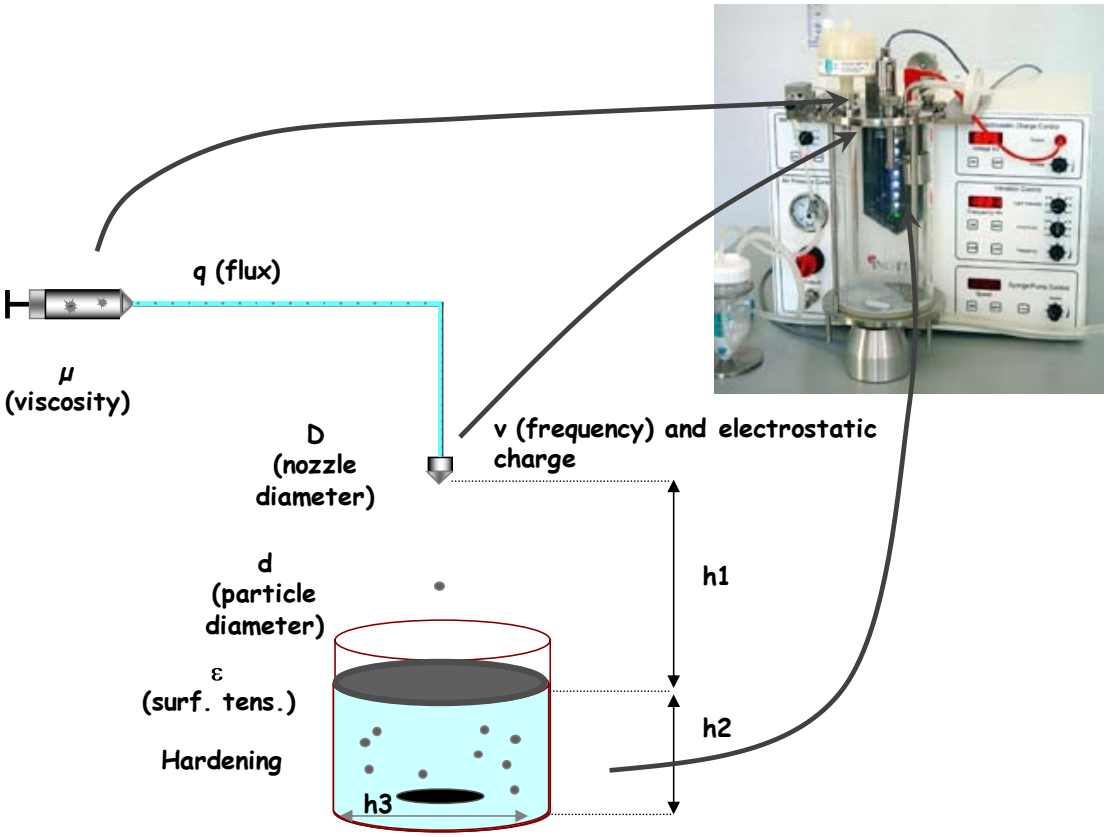

Figure 3-4. Parameters that influence the production of monodisperse microparticles.

3.3.4 Tests of release

Three types of microparticles with the best standard deviation were used for the tests of release. Dextran 500′000 Fluorescein isothiocyanate conjugate was used in the experiments; it was dissolved in the chitosan solution at a concentration of 90µg/mL prior the extrusion, the flow rate was fixed to 0.052g/sec. The beads did not show any type of physical change from the ones used as a blank without FITC-dextran. The releasing of FITC-dextran was monitored by using the luminescence spectrometer (λ_{ex}=492 nm; λ_{em}=518 nm) for a range of time of 24 hours.

3.3.5 Beads stability

Chitosan/TPP complexes are not resistant to strong acid conditions; these tend to swell in acidic solution and start to dissolve in a solution with a pH value below 2.5[23]. In order to evaluate the stability, one optimised system of microparticles were prepared and shared in five vials; these were centrifuged and the supernatant (TPP solution) was removed, the beads were weighed and placed in different solutions (40 mL) at different pH values (0.7, 2.1, 3.0, 4.2, 5.7); the correction of the pH in the new solutions was performed using 1M HCl; the beads were left on the mixer at speed of 72 rpm for 72 hours. The vials were centrifuged and the supernatant removed (with eventual chitosan/TPP in form of debris), the beads collected at the bottom of the vials were washed with distilled water until the pH of the solution was 7. The samples were freeze-dried and, soon after, the remnants microparticles weighed. The beads stability is quantified in degradation percentage using the following formula:

$$\text{Degradation}\,\% = \frac{\text{weight before exp.} - \text{weight after exp.}}{\text{weight before exp.}} \cdot 100$$

3.4 Result and discussion

3.4.1 Preparation

The encapsulation system produces beads based on laminar jet break-up induced by applying a sinusoidal frequency with defined amplitude to the nozzle. The top plate

contains a feed-line connected to a syringe or hydraulic polymer reservoir and a nozzle which can have a diameter in the range of 50-1000 μm. This nozzle is connected via steel or poly(tetrafluoroethylene) (PTFE) membrane to an insulated vibrating device containing rubber mounts which avoid the generation of resonance frequencies in the system.

The target was the production of chitosan monodisperse microparticles linked with TPP and the range accepted was 300-600 μm; several preliminary tests were executed in order to optimize the complexation.

Concentration and pH. For spherical and monodisperse beads, the gelation kinetics was a determinant factor; this property could be enhanced by increasing the concentration of the reagents, by modulating the temperature or, if this influence the number of charges, the pH values. Higher concentration of the two partners means higher concentrations of both negative and positive charges and therefore quicker reaction and higher cross-link density in the final material. Concentrations need therefore to be maximised. On the other hand, increasing concentration implies an increase in viscosity, which is detrimental to the process of drop formation (in the liquid that is extruded from the nozzle) or of bead dispersion (in the liquid that accepts the drops).

In preliminary experiments, with a simple dropping of chitosan in TPP at pH=5 for both the solutions, which provides a good charge density on both polycation and polyanion, several concentrations were used to qualitatively assess the optimum range.

Nozzle. For homogenous bead production the quality of the nozzle's drilled sapphire disc is the most important parameter. The diameter of the beads is double the nozzle aperture and the range can be modified by about ±20% by varying jet velocity, vibration frequency or applying an electrostatic charge[24]. The method used here was executed in an aqueous environment and under mild conditions.

3.4.2 Results and characterization

A first set of preliminary experiments were produced in order to choose the right parameter values and begin a more in deep research of the best type of microparticles. In table 3-2 there is a list of values used and the results obtained in terms of complexation and shape:

Table 3-2. Preliminary experiments, factors and responses; VS=very slow, S=slow, G=good, D=debris, Sp=spherical, I=irregular.

Factors									Responses	
Experiment number	Nozzle diameter (μm)	[CS] (wt.%)	[TPP] (wt%)	TPP pH	CS pH	Flow rate (g/sec)	Electrostatic charge (kV)	Range of frequency (Hz)	Complexation	Shape
1	300	0.5	3.68	5	5	0.100	0.84	1000-1200	VS	D
2	300	1	3.68	5	5	0.100	0.84	1000-1200	S	D
3	300	1.5	3.68	5	5	0.070	0.84	500-600	G	Sp
4	300	2	3.68	5	5	0.100	2.31	800-1000	G	Sp
5	300	1.5	3.68	4	4	0.139	0.92	500-600	G	Sp
6	300	1.5	3.68	5	5	0.139	0.92	500-600	G	Sp
7	300	1.5	3.68	5.5	5.5	0.139	0.92	500-600	G	Sp
8	300	1.5	3.68	6	6	0.139	0.92	500-600	G	Sp
9	200	1.5	3.68	4	4	0.077	0.76	1075	G	I
10	200	1.5	3.68	5	5	0.077	0.76	1075	G	Sp
11	200	1.5	3.68	6	6	0.077	0.76	1075	G	Sp
12	200	1.5	3.68	7	2	0.077	0.86	1075	G	Sp

In all the experiments the flow rate was kept lower than 0.140 g/sec, since a higher value gave always formation of non spherical shaped microparticles. Complexation in particulates always occurred, except for chitosan concentrations below 1% in weight.

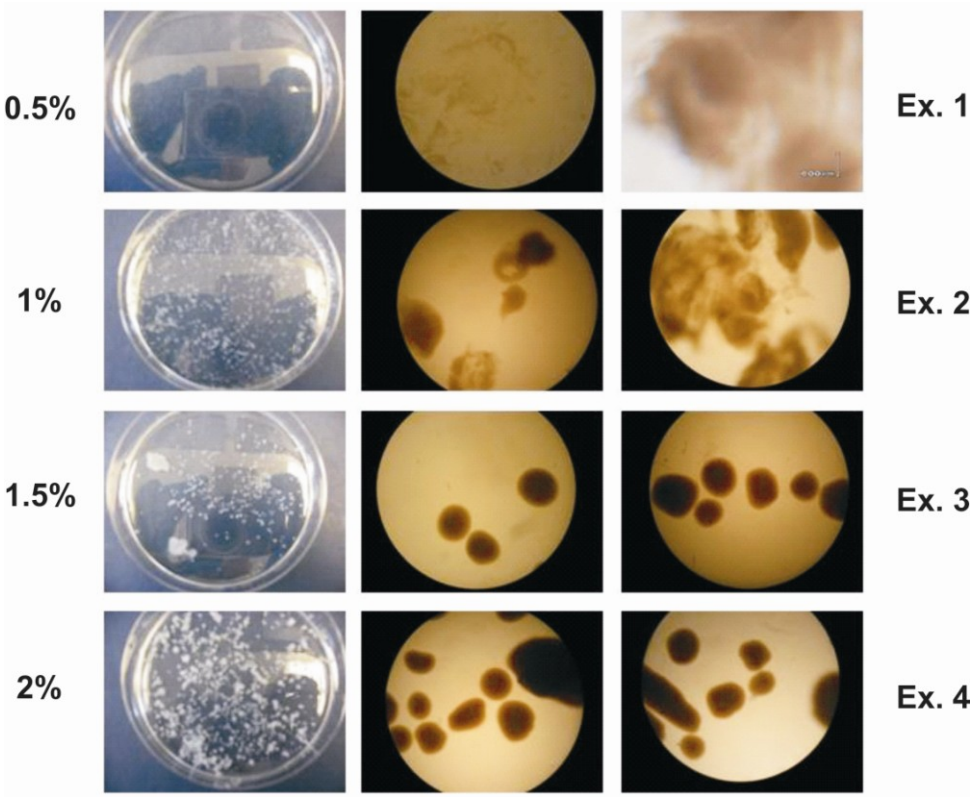

Figure 3-5. Experiments 1 to 4 (see table 3-2). In the first column there is no magnification, in the second and third column the magnification is 10X.

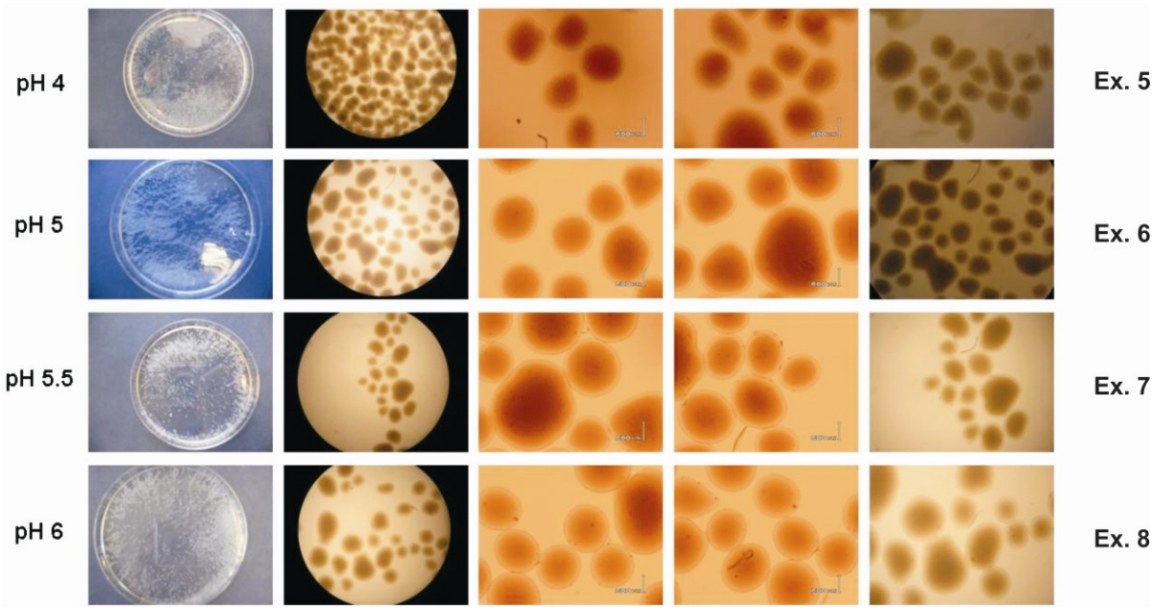

Figure 3-6. Experiments 5 to 8 (see table 3-2). There is no magnification in the first column, in the second column the magnification is 4X meanwhile in all the others is 10X.

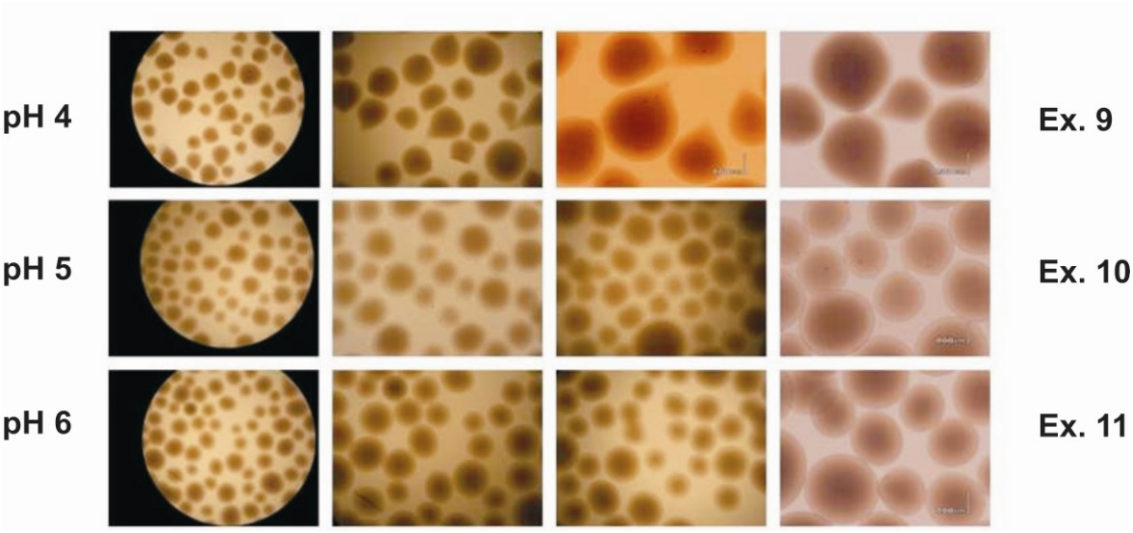

Figure 3-7. Experiments 9 to 11 (see table 3-2). In the first column the magnification is 4X, in the second and third columns the magnification is 10X, in the last column is 40X

The most monodisperse microparticles after the first sequence of experiments (Fig. 3-8) had a diameter between 400 and 750 μm; these substantial differences from the other samples were due to the change in nozzle diameter of the encapsulator and to the value of flow rate fixed to 0.077g/mol.

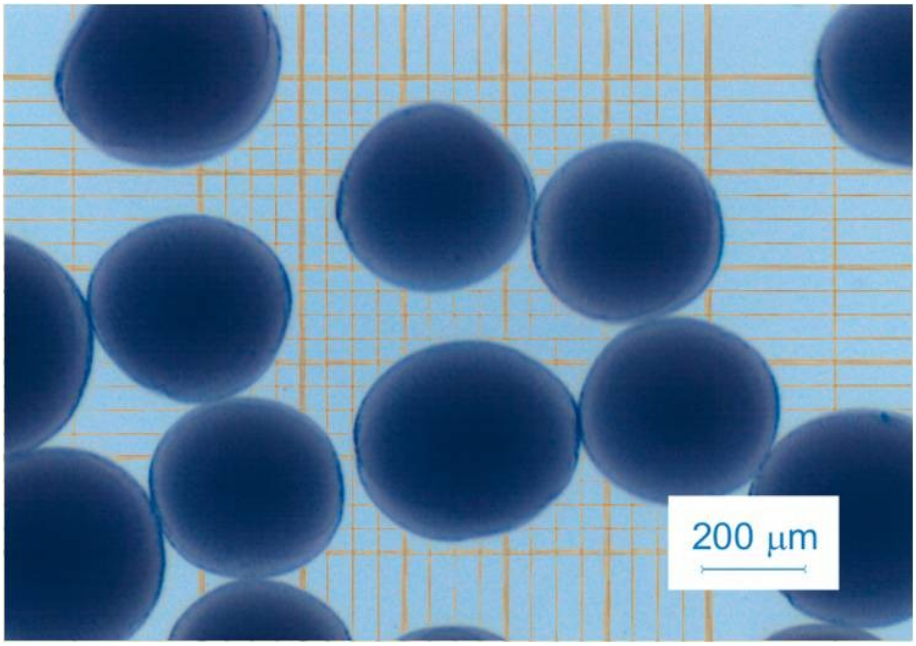

Figure 3-8. Experiment 12 (see table 3-2). The magnification is 40X. Here two photos are superimposed, one with the beads and the other one with the hemocytometer (device usually used to count the cells and evaluate the dimensions).

A second set of experiments were performed in order to decrease further the size of the microparticles. It was still focused on the optimization of concentrations and pH values; additionally the Tween 20 was used in some of these experiments as a wetting agent in order to lower the surface tension and to decrease the interfacial tension between the droplet of chitosan and the hardening bath. In the following table and graphs are exposed all the variables and the results obtained.

Table 3-3. Factors used in the second lot of experiments. The nozzle used has a diameter of 200 μm, charge voltage 0.86 kV, frequency 1075 Hz and flow rate 0.077 g/sec.

Factors							Responses	
Experiment number	[CS] (wt.%)	CS pH	[TPP] (wt%)	TPP pH	[Tween] (wt%)	n. of beads In the count	Size (μm)	±SD
1	1	4	2.5	4	0	80	668	165
2	1	4	2.5	4	1	80	635	148
3	1	5	2.5	5	0	80	653	147
4	1	5	2.5	5	1	80	586	117
5	1	5.5	2.5	5.5	0	80	563	135
6	1	5.5	2.5	5.5	1	80	682	103
7	1	6	2.5	6	0	80	620	102
8	1	6	2.5	6	1	80	632	121
9	1	4	2.5	7	0	80	526	55
10	1	4	2.5	8	0	80	479	85
11	1	5.5	2.5	7	1	80	662	145
12	1	5.5	2.5	8	1	80	684	117
13	0.5	4	1.25	7	0	--	--	--
14	0.5	4	2.5	7	0	--	--	--
15	0.5	4	5	7	0	--	--	--
16	1	4	1.25	7	0	80	413	79
17	1	4	2.5	7	0	80	281	44
18	1	4	5	7	0	80	402	51
19	1.5	4	1.25	7	0	80	522	131
20	1.5	4	2.5	7	0	80	555	150
21	1.5	4	5	7	0	80	497	85

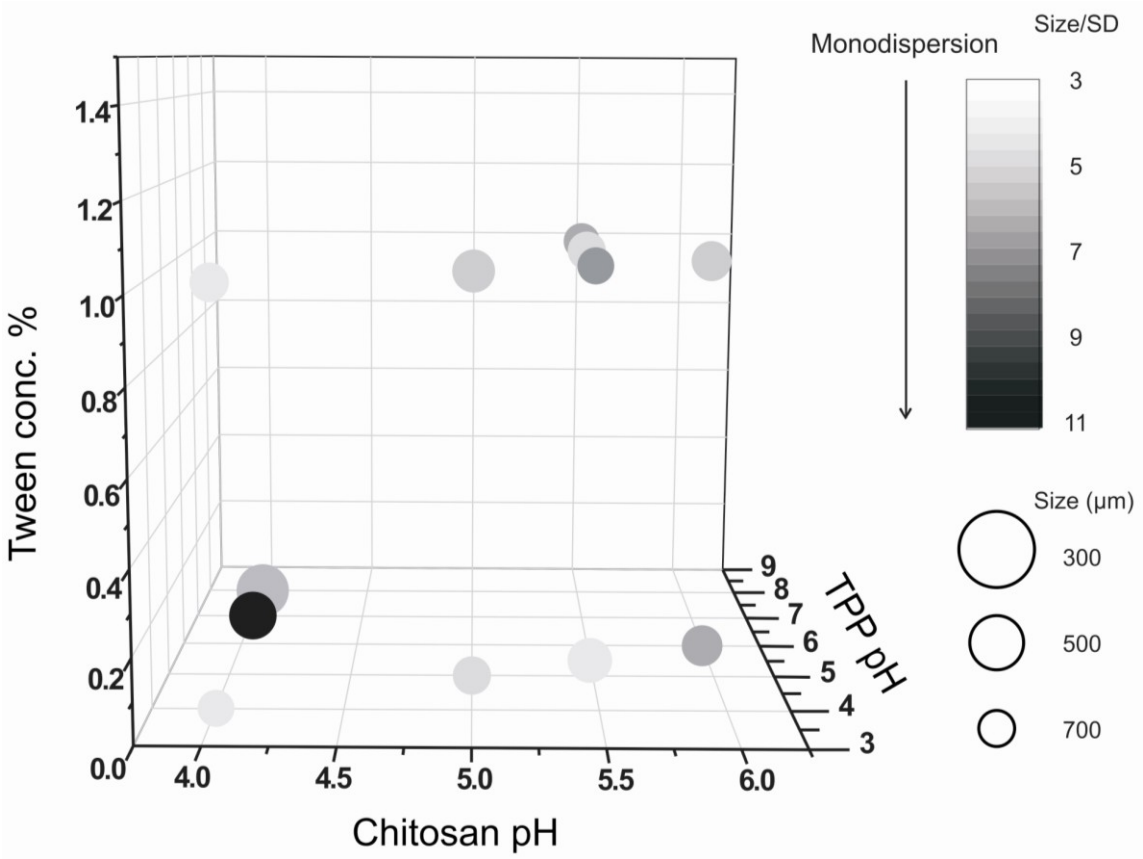

Figure 3-9. Experiments 1 to 12 (second set, see table 3-3). The dispersion of the microparticles is represented by colour, the darker appear circle the better is the dispersion; the larger will appear the size of the circles in the graph and the smaller correspond the microparticles produced; thereby the darker in colour and the larger in circle size are the best in the tests.

The use of the Tween 20 did not imply any difference in bead's formation, evidently the surface energy of the droplets and of the hardening bath did not change sufficiently with a concentration of the 1%wt (Fig. 3-9). The microparticles dispersion is satisfactory when the pH of the hardening bath is 6 or higher. During the beads formation the hydrochloric acid in the chitosan droplets is displaced by the TPP, which diffuse inside the droplets of chitosan and provoke the gelation, this process happen faster when the pH of the TPP solution is higher. A chitosan pH below 6 was necessary to obtain a uniform jet break-up, and the couple of pH 4(CS)-7(TPP) was the one gave better results.

Finally, in the set of experiments 13-21 (Fig.3-10), once fixed the pH of the solutions, the concentrations were optimized. At higher value of concentration of TPP in the hardening bath results a quicker gelation and a more monodisperse

microparticles. The best samples were obtained with a concentration of chitosan of 1%wt and concentrations of TPP higher than 2.5% in wt.

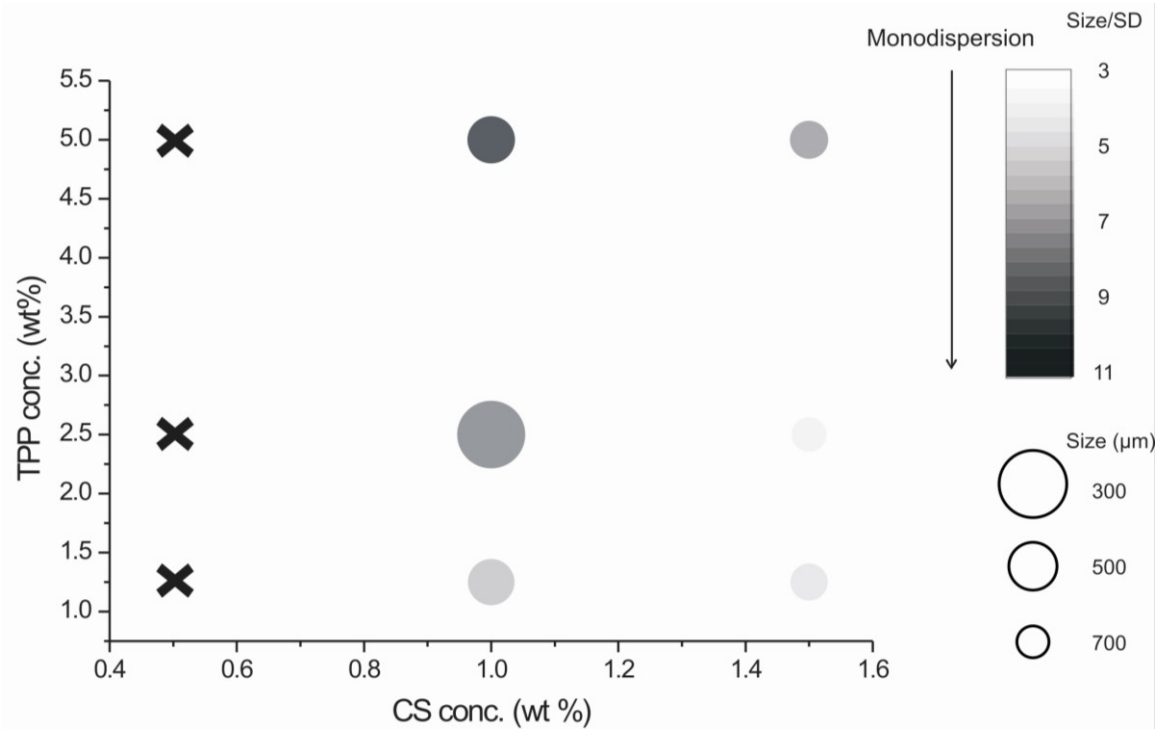

Figure 3-10. Experiment 13 to 21 (second set, see table 3-3). The dispersion of the microparticles is represented by colour, the darker appear circle the better is the dispersion; the larger will appear the size of the circles in the graph and the smaller correspond the microparticles produced; thereby the darker in colour and the larger in circle size are the best in the tests.

3.4.3 Tests of release

Three types of microparticles were chosen (ex. 9, 10, 18, see Table 3-3) since they were the least disperse in terms of size; a large, non-ionic fluorescently-labelled macromolecule, FITC-dextran, was used to qualitatively assess the mesh size of the chitosan matrices by the means of fluorimetry: dextran has no electrostatic interactions with either TPP or chitosan, and it is completely water-soluble, therefore its possible retarded release is solely due to the mesh size of the chitosan-TPP network. FITC-dextran was dissolved in the chitosan solution is therefore supposed to be 100% entrapped in the bead structure at the gelation. It is apparent (Figure 3-11) that the FITC-dextran is quickly released from all the beads. However, while particles 9 show a substantially quantitative release within the first minute (the drift in fluorescence

intensity is due to experimental problems, possibly evaporation of the solution), the release of particles "10" and even more particles "18" shows a first-order-like behaviour. One should take into account the sample "10" particles are prepared using a higher pH of the TPP solution, which may cause some chitosan-chitosan aggregation, which would increase the tortuosity of the matrix, while the increased concentration of TPP used in the preparation of sample "18" should increase the cross-link density of the matrix, thus decreasing its mesh size. We can therefore conclude that the effect of increased cross-link density of sample "18" seems to overwhelm that of increased tortuosity of sample "10".

Furthermore, since dextran of MW=500,000 g/mol has an hydrodynamic radius of about 16 nm[25], it is reasonable to think that sample "18" has a mesh size in the order of magnitude of tens of nm.

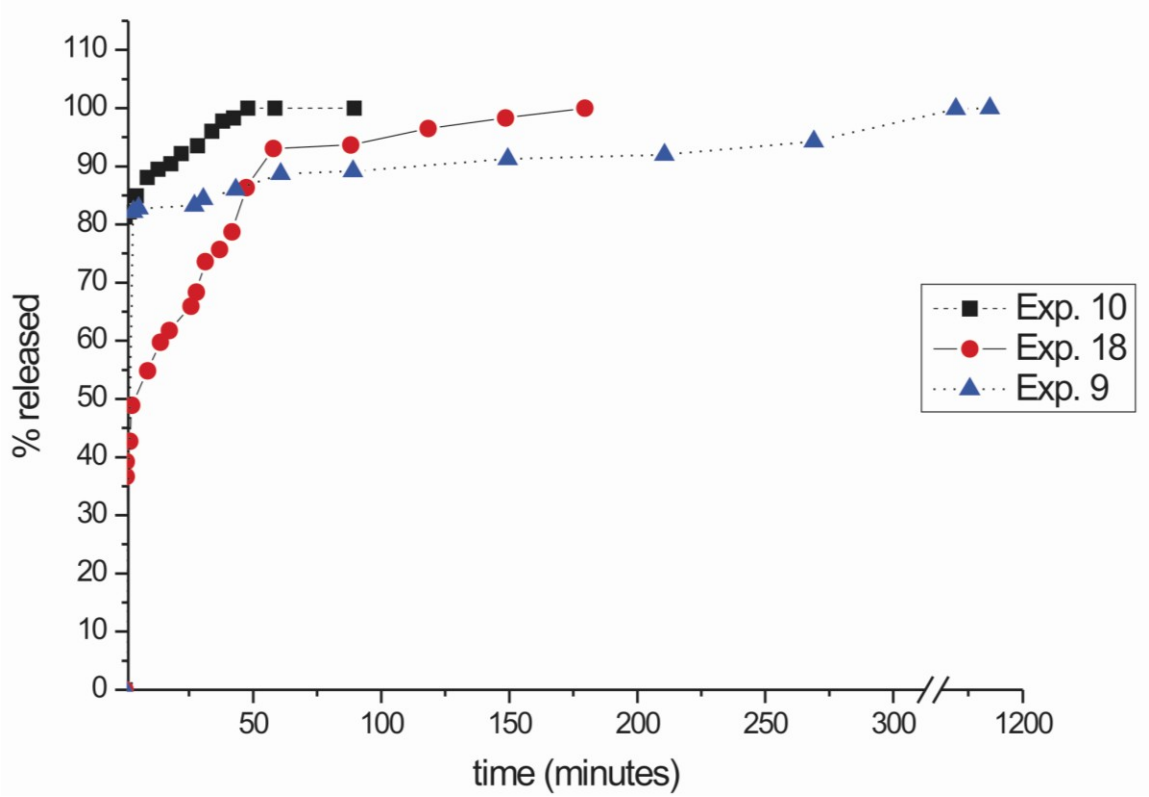

Figure 3-11. The best three samples (2nd set of experiment) were used in the experiment of release for a run of 24 hours. Within the first 50 minutes the 80% of FITC-dextran is released in the media.

3.4.4 Beads stability

The beads stability was performed suspending the optimised microparticles in different solutions, each of them having different pH values. The damaging of the microparticles depended on the penetration of the medium, successive hydration, and dissolution of the matrix. Swelling and then degradation is sensitive to the pH, in the following table the variables and percentage of degradation are expressed after the execution of the experiment:

Table 3-4. The table shows the parameters in the experiments of stability and the percentage of degradation. The experiment lasted 72 hours. The theoretical starting dry weight is calculable since the water content in the beads was the 74% of the total weight; this percentage value was confirmed in the preliminary experiment.

pH of the solutions	Starting wet weight (gr)	Theoretical starting dry weight (gr)	Final dry weight (gr)	Degradation (%)
0.7	0.420	0.109	0.000	100
2.1	0.233	0.060	0.025	58
3.0	0.463	0.120	0.118	2
4.2	0.491	0.128	0.127	0
5.7	0.557	0.145	0.134	7

From the results of the experiment was deducible that, when the microparticles were dipped in solutions with pH values lower than 3, these started to break themselves; the lower was the pH value and the higher was the degree of dissolution.

3.5 Conclusion

The results obtained were really promising, optimized and monodisperse beads were produced with the Inotech® encapsulator; the use of this device allows working in sterile conditions and the production of microparticles was performed using limited quantities of materials; several active principles can be loaded with a yield of entrapment of 100%, the single drawback to avoid is the rapid degree of release. Furthermore, tests on the mechanical properties must be executed and the degree of crosslinking has to be known, instruments like rheometer can be used for the first

purpose. In the next steps, the loading of hydrophobic molecules with different MWs could be tested and moreover the embedding of living cells could be a target to follow too. A method for drying and store the beads without damage them permanently can be studied, to maintain the structure intact could be the use of alcohol exchange and CO_2 supercritical drying[26], this process was already executed with alginate/chitosan microcapsules and gave good results.

References

1. Shu, X.K.J. Zhu, **2000**, A novel approach to prepare tripolyphosphate/chitosan complex beads for controlled release drug delivery. *International Journal of Pharmaceutics*. 201(1): p. 51-58.
2. Bodmeier, R., K.-H. Oh, and Y. Pramar, **1989**, Preparation and Evaluation Of Drug-Containing Chitosan Beads. 15(9): p. 1475 - 1494.
3. Ko, J.A., H.J. Park, S.J. Hwang, J.B. Park, and J.S. Lee, **2002**, Preparation and characterization of chitosan microparticles intended for controlled drug delivery. *International Journal of Pharmaceutics*. 249(1-2): p. 165-174.
4. Sorokin, A.B., F. Quignard, R. Valentin, and S. Mangematin, **2006**, Chitosan supported phthalocyanine complexes: Bifunctional catalysts with basic and oxidation active sites. *Applied Catalysis a-General*. 309(2): p. 162-168.
5. Korsmeyer, R.W.N.A. Peppas, **1981**, Effect of the Morphology of Hydrophilic Polymeric Matrices on the Diffusion and Release of Water-Soluble Drugs. *Journal of Membrane Science*. 9(3): p. 211-227.
6. de Gennes, P.-G., **1979**, Scaling Concepts in Polymer Physics*, ed. Cornell University Press. Ithaca, New York.*
7. Hwang, C., C.K. Rha, and A.J. Sinskey, **1986**, Encapsulation with chitosan: trans-membrane diffusion of proteins in capsules, pp. 389-396. In: R. Muzzarelli, C. Jeuniaux, and G.W. Gooday, Chitin in nature and technology. *Plenum Press, New York.*
8. Lee, S.-T., F.-L. Mi, Y.-J. Shen, and S.-S. Shyu, **2001**, Equilibrium and kinetic studies of copper(II) ion uptake by chitosan-tripolyphosphate chelating resin. *Polymer*. 42(5): p. 1879-1892.
9. Fick, A., **1855**, Poggendorff's Annalen der Physik und Chemie. (94,): p. 59−86.

10. Fick, A., **1995**, On liquid diffusion. *Journal of Membrane Science*. 100(1): p. 33-38.
11. Shiraishi, S., T. Imai, and M. Otagiri, **1993**, Controlled release of indomethacin by chitosan-polyelectrolyte complex: optimization and in vivo/in vitro evaluation. *Journal of Controlled Release*. 25(3): p. 217-225.
12. Vorlop, K.D.J. Klein, **1981**, Formation of Spherical Chitosan Biocatalysts by Ionotropic Gelation. *Biotechnology Letters*. 3(1): p. 9-14.
13. Meshali, M.M.K.E. Gabr, **1993**, Effect of interpolymer complex formation of chitosan with pectin or acacia on the release behaviour of chlorpromazine HCl. *International Journal of Pharmaceutics*. 89(3): p. 177-181.
14. Bungenberg de Jong, H.G.H.R. Kruyt, **1930**, Kolloid-Z. 50, 39.
15. Tay, L.F., L.K. Khoh, C.S. Loh, and E. Khor, **1993**, Alginate Chitosan Coacervation in Production of Artificial Seeds. *Biotechnology and Bioengineering*. 42(4): p. 449-454.
16. Berthold, A., K. Cremer, and J. Kreuter, **1996**, Preparation and characterization of chitosan microspheres as drug carrier for prednisolone sodium phosphate as model for anti-inflammatory drugs. *Journal of Controlled Release*. 39(1): p. 17-25.
17. He, P., S.S. Davis, and L. Illum, **1999**, Chitosan microspheres prepared by spray drying. *International Journal of Pharmaceutics*. 187(1): p. 53-65.
18. Alex, R.R. Bodmeier, **1990**, Encapsulation of Water-Soluble Drugs by a Modified Solvent Evaporation Method .1. Effect of Process and Formulation Variables on Drug Entrapment. *Journal of Microencapsulation*. 7(3): p. 347-355.
19. Heinzen, C., I. Marison, A. Berger, and U. von Stockar, **2002**, Use of vibration technology for jet break-up for encapsulation of cells, microbes and liquids in monodisperse microcapsules. In: U. Prusse and K.D. Vorlop, Practical Aspects of Encapsulation Technologies. *Bundesforschungsanstalt Landwirtschaft (Fal) Braunschweig.* p. 19-25.
20. Rayleigh, L., **1878**, On the stability of jets*: Proc. London Math. Soc. 10, 4 -13.*
21. Weber, C., **1931**, Zum Zerfall eines Flüssigkeitsstrahles. 11(2): p. 136-154.
22. Brandenberger, H.F. Widmer, **1998**, A new multinozzle encapsulation/immobilisation system to produce uniform beads of alginate. *Journal of Biotechnology*. 63(1): p. 73-80.

23. Fwu-Long Mi, S.-S. Shyu, C.-Y. Kuan, S.-T. Lee, K.-T. Lu, and S.-F. Jang, **1999**, Chitosan-Polyelectrolyte complexation for the preparation of gel beads and controlled release of anticancer drug. I. Effect of phosphorous polyelectrolyte complex and enzymatic hydrolysis of polymer, J.o.A.P. Science, Editor. p. 1868-1879.

24. Instruction Manual for the Inotech Encapsulator Research IE-50 R. *Inotech Encapsulation AG*.

25. Armstrong, J.K., R.B. Wenby, H.J. Meiselman, and T.C. Fisher, **2004**, The hydrodynamic radii of macromolecules and their effect on red blood cell aggregation. *Biophysical Journal*. 87(6): p. 4259-4270.

26. Valentin, R., K. Molvinger, F. Quignard, and D. Brunel, **2003**, Supercritical CO2 dried chitosan: an efficient intrinsic heterogeneous catalyst in fine chemistry. *New Journal of Chemistry*. 27(12): p. 1690-1692.

Chapter 4

Conclusion

4. Conclusion

The aim of the entire project was to use chitosan and sodium triphosphate for producing structures able to form matrixes of limited dimensions in a reproducible fashion. Nano- and micro-vehicles were fabricated by ionotropic gelation.

Efficient complexation in nanoparticles formation

The first achievement was the purification and the characterization of the chitosan, in terms of average molecular weight and degree of deacetylation had to be known in each step of the above mentioned process in order to produce reproducible materials.

The investigation regarding the complexation between chitosan and sodium triphosphate focused on optimizing the interplay between nucleation and growth of the nanoparticles in the two mixed solutions. When the mixing was executed with different pH (acid for chitosan and slightly basic for TPP) larger aggregates were produced. This confirmed that there was a kinetic control of the complexation, chitosan complexation with TPP happened faster than proton exchange or at least with a comparable kinetics. Moreover, analyzing the ageing of the colloidal suspensions, it was noticed that the systems evolved with a resultant increase in pH, this could be explained since a complexed chitosan possesses ammonium ions with different pK_a values respect to a non-complexed chain of polymer, consequently the nanoparticles during time sequestrate protons from the solution.

The coating procedure of the nanoparticles, based on the electrostatic interactions between the positively charged the chitosan nanoparticles and the polyanion hyaluronic acid (HA), had to be fast in order avoid flocculation of particles with negligible or zero zeta potential produced at intermediate stages during the complexation; having this in mind, a large excess of coating agent (HA) was used respect to the amount of nanoparticles,. The degree of swelling was highlighted being dependent from the ionic strength, and the feasibility of the encapsulation of nucleic acid oligomers was evaluated as well.

In in vitro cellular tests on macrophages, the nanoparticles, both coated and uncoated, showed principally a clathrin-mediated uptake, in support of this thesis several effectors were used; additionally the coated ones resulted much less toxic than the uncoated nanoparticles, this was due to the high compatibility of the hyaluronic acid.

Chitosan microparticles

The parameters related to the Inotech® encapsulator were influencing the shape and the dimensions of the beads but the optimization of the beads was reached subsequent to an exhaustive study on the kinetic of complexation between chitosan and TPP. The triphosphate had to be in condition to enter deeply in the chitosan droplets and bridge with the free primary ammines of the chitosan, additionally the complexation happens simultaneously with the pH equilibrium of the two phases. Once formed, the microparticles demonstrated to last for a long period of time; however more studies regarding the ageing and the degree of crosslinking must be conducted.

The main use of these microparticles could be the entrapment of cells with a consequent positioning in a biological environment. The control of the degree of crosslinking will be important in the facilitating the survival of the cells, protecting them from the immunosystem activation and allowing the permeation of nutrients and the clearance of waste materials of the cells. In conclusion the modulation of the bioerodibility of the beads *in situ* must be evaluated in order to avoid quick matrix degradation.

This is a simple technique for the embedding of active principles based on biodegradable and cost-effective raw materials, ready to be scaled up in mass production.